Tuesday, 25 May

0800–0945

Parallel Session 5: Image Cytometry I

Chair: Andreas O.H. Gerstner

98346

HIGH PERFORMANCE CCD IMAGING SYSTEM FOR MICROARRAYS AND OTHER LARGE FORMAT OBJECTS

Daniel Pinkel[1], Nils Brown[2], Vanessa Oseroff[2], Greg Hamilton[3], Jay Kumler[4], Mark Scheeff[5], Donna Albertson[6]

[1]University of California San Francisco, Laboratory Medicine, School of Medicine, San Francisco, California; [2]University of California San Francisco, San Francisco, California; [3]UCSF, Cancer Center, San Francisco, California; [4]Coastal Optical Systems Inc., West Palm Beach, Florida; [5]Lawrence Berkeley National Lab Berkeley, California; [6]University of California San Francisco, Cancer Research Institute, San Francisco, California

CCD imaging systems offer the potential acquiring data from microarrays that may be more quantitative than the more frequently used laser scanning systems. Among the potential advantages is the excellent photometric linearity over a wide dynamic range. Most CCD-based array imaging instruments use conventional microscope optics to sequentially obtain numerous images of small parts of the array, that are then stitched together to obtain the full data set. We have taken a different approach. Our system employs custom designed low magnification telecentric optics to image large areas in a single image. Three sets of lenses allow imaging a 12, 18, or 25 mm square area onto a ~ 25 mm square CCD chip (magnifications ~ 2X, ~1.5X and ~1X respectively). Light collection is ~ f/2, ~f/3 and ~f/4 for the three configurations. The lenses are chromatically corrected to allow acquisition of images over a wavelength range from 450 to 750 nm. Excitation light is supplied by a 200 watt Hg-Xe lamp. A well-corrected condenser lens is used to minimize excitation intensity variations over the object field. Filter wheels permit use of up to 9 fluorochromes. Our typical measurements employ DAPI to visualize the DNA in the microarray spots, and fluorescein, Cy3 and Cy5 in nucleic acid probes. Cross talk between these fluorochromes is less than 0.5%. The CCD camera contains 2K x 2K pixels, each with a well depth of about 105 electrons, allowing very high dynamic range imaging. In a typical array image, each spot is contained in a square of approximately 11 x 11 pixels, so that over images of over 36,000 spots can be obtained in a single frame. Measurements with test objects consisting of solutions known concentrations of fluorochromes in buffered glycerol indicate that the signal intensities are linear down to concentrations below 1 fluorochrome / mm2. Acquisition of 3-color images (DAPI, Cy3 and Cy5) of arrays used for comparative genomic hybridization (array CGH) typically takes less than 1 minute. Supported by grants RO1-CA 83040, UO1-CA84118 and Vysis -Abbott Inc.

96639

ONE AND TWO PHOTON EXCITATION OF CELLS AND MOLECULES LABELED WITH A EUROPIUM(III)-MACROCYCLE (QUANTUM DYE®) UNDER LANTHANIDE ENHANCED LUMINESCENCE (LEL)

Robert C. Leif[1], Margie C. Becker[2], Alfred J. Bromm[3], Nanguang Chen[4], Ann Cowan[5], Lidia M. Vallarino[3], Sean Yang[6], Robert M. Zucker[7]

[1]Newport Instruments, Research & Development, San Diego, California; [2]Phoenix Flow Systems, Development & Manufacturing, San Diego, California; [3]Virginia Commonwealth University, Chemistry, Richmond, Virginia; [4]University of Connecticut, Electrical & Computer Engineering Department, Storrs, Connecticut; [5]University of Connecticut, Health Center, Department of Biochemistry and Center for Biomedical Imaging Technology, Farmington, Connecticut; [6]Phoenix Flow Systems, Newport Instruments R&D, San Diego, California; [7]U.S. E.P.A. Research Triangle Park, Developmental Toxicology Division(MD-67), Research Triangle Park, North Carolina

Improvements in the Lanthanide Enhanced Luminescence (LEL) protocol have facilitated the use of the recently synthesized Eu (III)-macrocycle-mono-isothiocyanate, Quantum Dye®, as a label for direct staining of cells as well as for indirect staining as a Streptavidin conjugate to observe apoptotic and S phase cells. The ultraviolet light induced fading of the lanthanide macrocycle enhancers has been markedly reduced by mounting and then drying the cells in a conventional medium, Clearium, without use of a coverslip. Preliminary studies indicate that cells stained with the europium Quantum Dye can be observed both by conventional UV laser excitation and by infrared two photon confocal microscopy. The improvements in the LEL protocol have demonstrated that the streptavidin conjugate of the europium Quantum Dye can be employed in sensitive quantitative assays. An enhancer has been found that enables the observation of simultaneous emissions from both the europium and the terbium macrocycles. This abstract does not necessarily reflect EPA policy.

96909

ACCURATE ASSIGNMENT OF CYTOPLASMIC STRUCTURES TO INDIVIDUAL CELLS IN AUTOMATED, HIGH-VOLUME IMAGE CYTOMETRY

Kris Ver Donck[1], Peter Van Osta[2], Luc Bols[1], Bart Vanherck[1], Johan J.G.H. Geysen[1]

[1]Union Biometrica NV, Geel, Belgium; [2]Union Biometrica NV, Union Biometrica ESO, Geel, Belgium

In image cytometry, the ‘cytoplasmic area’ of cells is often identified by applying a polygonal or elliptical model around a central reference point, often the nucleus. This leads to biased measurement of cytoplasms and to assignment of objects or events at the cell perimeter to the nearest instead of the correct cell. Multimode reading allows tracking multiple structures in individual cells in e.g. monolayer cultures. Fluorescent and brightfield multimode microscopic images were captured and analyzed with MIAS-2 microscopy readers. Using the eaZYX-IMAGING software, we applied novel shape detection principles that lead to dynamic cell perimeter identification and to accurate assignment of cytoplasmic structures to individual cells. Examples will be given that show a robust performance in high and moderate intensity signals, but also in brightfield images of living cells acquired in highly variable background conditions resulting from air-liquid meniscus effects and in ‘high noise’ images resulting from extremely weak fluorescent signals acquired in real time with an intensified camera.

97233

HIGH CONTENT VS. HIGH THROUGHPUT: YOU CAN'T HAVE ONE WITHOUT THE OTHER

Raffi Manoukian[1], Laura Chiu[1], Gary Elliott[1]

[1]Amgen, Thousand Oaks, California

Small molecule chemistry and advances in therapeutic antibody production continue to dominate drug discovery where screening hundreds of thousands of compounds a year has become commonplace. However, once the "hit" has been made, the question remains, "is it functional in a relevant cell-based assay?" High content screening, can play an essential role in demonstrating the functionality of compounds by the sheer power of signal detection and localization that HTS cannot convey. Using the I-Cyte inverted platform laser scanning cytometer, HCS can rapidly produce multiplexed data that is quantitative, and that allows for visual confirmation of fluorescent events. For certain adherent cell or tissue-based assays, the validation of cytometric data with high-resolution imaging can prove invaluable. Here we demonstrate the efficacy of various Amgen compounds in their capacity to induce nuclear translocation of STAT5 transcription factor. Using mammalian cell lines expressing specific target receptors, we are able to measure effect in a dose response manner reflecting the amount of nuclear phosphorylated STAT 5; furthermore we can visually validate the data with laser-scanned imaging. In other assays, we demonstrate the detection of antibody-induced receptor clustering, a phenomenon that could not previously be measured in an accurate and quantitative manner; the extraction of apoptotic cells hidden in one dimensional DNA cell cycle histograms; and rapid scanning/mapping of fluorescently labeled tissue sections. High or informative content screening proves to be a powerful tool in the detection of subtle biological changes at a cellular level. At Amgen, such technologies are heavily used to provide specific answers to questions that cannot be otherwise addressed in research & discovery.

97132

A FLEXIBLE LARGE-SCALE BIOLOGY SOFTWARE MODULE FOR THE AUTOMATED QUANTITATIVE ANALYSIS OF CELL MORPHOLOGY

Richik N. Ghosh[1], Oleg Lapets[2], Linnette Grove[2], Everett Ramer[2], Jeffrey Peterson[2]

[1]Cellomics, Inc., Pittsburgh, Pennsylvania; [2]Cellomics, Inc., Assay Development, Pittsburgh, Pennsylvania

The ability to automatically quantify the morphology of individual or clusters of cells over many samples would assist efforts in a wide range of cell biological research, and in compound screening and characterization for drug discovery in different therapeutic areas. We have developed an automated cell-based fluorescence-imaging assay that detects, distinguishes and quantifies the morphology of individual or clusters of fluorescently labeled cells. Fluorescent images are analyzed by a dedicated software module that reports multiple quantitative measures of morphology over three different dimensional scales: subcellular morphology, whole cell morphology, and multicellular morphology. Features reported for whole cell morphology include cell shape, dimensions, orientation, and extent, as well as quantitation of cellular outgrowths. Features reported at the subcellular level include the intracellular location and amounts of macromolecules or discrete objects, their intracellular arrangement including a range of different texture measures, properties of intracellular spots or fibers, and the shape and dimensions of major intracellular compartments such as the nucleus or Golgi. Multicellular features reported include the shape and dimensions of multicellular assemblages such as colonies or multi-nucleated cells, the proximity and spacing of similar and dissimilar cells or colonies, and the number of cells in such assemblages. Use of this automated morphology application has been demonstrated on a range of different biological problems such as myotube formation, simultaneous measurement of F-actin and microtubule rearrangement in the same cells, colony formation and disassociation, cell spreading, location of discrete intracellular objects such as fluorescent endosomes, and the quantitation of cellular processes such as neurite outgrowth. This flexible tool realizes the promise of extracting quantitative multiparametric morphological information from microscopic images of cells married to the automated robust performance required for the processing of large-scale biology and large sample numbers.

Parallel Session 5: Microbeads

Chair: Francis F. Mandy
Co-Chair: Michèle Bergeron

95752

MULTIPLEX BEAD ARRAY ASSAYS AND ELISAS FOR DETECTION OF SOLUBLE CYTOKINES: COMPARISONS OF SENSITIVITY AND QUANTITATIVE VALUES AMONG KITS FROM MULTIPLE MANUFACTURERS

Sameena S. Khan[1], Meghan Smith[2], Anthony F. Suffredini[3], J. Philip McCoy Jr.[2]

[1]National Institutes of Health, Bethesda, Maryland; [2]National Institutes of Health, NHLBI, Bethesda, Maryland; [3]National Institutes of Health, Clinical Center, Critical Care Medicine Department, Bethesda, Maryland

This study was designed to compare the sensitivity and quantitative values of various manufacturers' cytokine detection kits using the Luminex 100 (Austin, TX). Intravenous endotoxin administration to humans induces the secretion of various cytokines in a reproducible dose and time dependent fashion. Seven subjects were given 4 ng/kg of *E. coli* O:113 endotoxin and blood was collected at 0, 3, 6, and 24 hours after injection. Serum was separated from the blood and used for cytokine determination. A total of 26 samples were analyzed in duplicate using the following human multiplex bead kits: LINCO Research, Inc., (St. Charles, MO), Bio-Rad Laboratories, Inc., (Hercules, CA), R&D Systems, Inc., (Minneapolis, MN), and BioSource International, Inc., (Camarillo, CA). Cytokines with each kit included IFNγ, IL-1β, IL-6, IL-8, and TNFα. Each multiplex assay was performed according to the manufacturers' specifications. Standard curves for each cytokine were generated through the use of reference cytokine concentrations supplied by each manufacturer. Raw data were analyzed by MasterPlex™ Quantitation Software (MiraiBio, Inc., Alameda, CA) to obtain concentration values. Each sample was run in duplicate on two different occasions. ELISAs for IL-8 were performed on all samples using kits from R&D and BioSource. The amount of cytokine detected among kits followed similar patterns although absolute concentrations differed. ELISA and Luminex values for IL-8 were similar in kits from the same manufacturer (R&D r=0.96, p=0.0004; BioSource r=0.92, p=0.0037). The range of detection in the samples among all kits extended from a low of 0.71 pg/ml by BioSource for IL-6, to a high of 7,011 pg/ml, also by BioSource for IL-6. All kits ran smoothly on the Luminex with the exception of the LINCO product which required frequent stopping and unclogging of the instrument. All kits exhibited similar patterns of rise and fall of the respective cytokine levels, but the absolute concentrations varied among the test kits, possibly reflecting different antibodies utilized by the various vendors. Since cytokine measurements are valuable in clinical research when performed serially, it may be possible to make interlab comparisons even if different suppliers' kits are used. When comparison of absolute cytokine values is crucial, it is recommended that they only be attempted if kits from the same supplier are used. In the latter instance, bead array and ELISA values are comparable in some kits.

96752

CELL STIMULATION USING HERCEPTIN®-COVERED MAGNETIC BEADS

Elza Friedlander[1], Diane Lidke[2], Donna Arndt-Jovin[3], Thomas M. Jovin[3], János Szöllõsi[4], György Vereb[4]

[1]University of Debrecen, Medical and Health Science Center, Department of Biophysics and Cell Biology, Debrecen, Hungary; [2]Max-Planck-Institute for Biophysical Chemistry, Department of Molecular Biology, Goettingen, Germany; [3]Max-Planck-Institute for Biophysical Chemistry, Goettingen, Germany; [4]University of Debrecen, Medical and Health Science Center, Debrecen, Hungary

Background: Magnetic beads covered with ligands or antibodies are widely used for separation of proteins and cells. Addtionally, this technique allows non invasive stimulation with precise timing. In our model system we stimulated with Herceptin® and EGF-covered paramagnetic beads some cell lines expressing ErbB1 (EGFR) and ErbB2 at different levels. **Methods:** 4 carcinoma cell lines with different levels of ErbB2 expression were used for our experiments: SKBR3, MCF-7, JIMT and A431-erbB2-YFP, the latter stably transfected with the ErbB2-YFP fusion gene. The cells were seeded onto coverslips 2 days before the experiment and used at a confluency of 30-50%. 24 hours before the stimulation the cultures were starved in DMEM without serum. For the stimulation carboxy-functionalized superparamagnetic 1µm beads (SERA-MAG, Seradyn, IN) were covered with Herceptin®. Before stimulation, the free reactive residues of the beads were blocked with BSA (Sigma). The beads were diluted in PBS so that the final density was 10-30 beads per cell. To accelerate the sedimentation of beads, coverslips were positioned on magnets. After 10 minutes, cells were rinsed with PBS and fixed with ice-cold methanol. We used EGF-covered magnetic beads and Herceptin® in solution as controls. Confocal laser scanning microscopy was done with a Zeiss LSM 510 system. **Results:** ErbB2 activation and tyrosine phosphorylation could be detected upon Herceptin® bead stimulation in all cases. ErbB1 was activated by the Herceptin® beads only in the case of high expression of this receptor (A431-derived line), whereas no ErbB1 activation could be seen using Herceptin® in solution. EGF-beads activated ErbB2 only in SKBR3 and A431-erbB2-YFP, which is in accordance with the high expression level of ErbB1 in these cells. In the case of applying Herceptin® in solution, we detected lower activation levels than with Herceptin® beads in all cell lines; this may be the result of the higher local concentration of the Herceptin® in the latter case. **Conclusions:** Interactions among members of the ErbB family are sensitively regulated by their cell surface expression levels and determine the palette of ligands that can efficiently activate signalling pathways originating form each kind of ErbB kinase.

96894

SUSPENSION ARRAY TECHNOLOGY: APPLICATION OF MICROPARTICLE-BASED FLOW CYTOMETRY FOR THE DETECTION AND QUANTIFICATION OF CYTOKINES IN PEDIATRY, OPHTHALMOLOGY, RHEUMATOLOGY AND HAEMATOLOGY

Gérard Lizard[1], Serge Monier[2], Jean-Bernard Gouyon[3], Marc Labenne[3], Catherine Creuzot-Garcher[4], Thomas Montange[2], Céline Prunet[2], Jean-Françis Maillefert[5], Marc Maynadié[6], Philippe Gambert[7]

[1]Inserm U498, Laboratoire de Biochimie Médiacle, Dijon Cedex, France; [2]Inserm, U498, Dijon, France; [3]CHU/Hôpital du Bocage, Service de Pédiatrie, Dijon, France; [4]CHU/Hôpital Général, Service d'Ophtalmologie, Dijon, France; [5]CHU/Hôpital Général, Service de Rhumatologie, Dijon, France; [6]Service d'Hématolologie Biologique, Dijon, France; [7]CHU/Hôpital du Bocage, Laboratoire de Biochimie Médicale/Inserm U498, Dijon, France

Suspension array technology based on the combined use of microbeads and flow cytometry constitutes a powerful multiplexed method to identify and simultaneously quantify some analytes in various biological fluids. This emerging technology is particularly well adapted when small volumes of biological samples are available and/or when it is necessary to simultaneously identify several analytes in the same sample. According to these considerations, the pro-inflammatory cytokines (IL-12, TNF-α, IL-6, IL-1 β, IL-8) and the anti-inflammatory cytokine (IL-10) were simultaneously quantified on 5 to 10 µl (or less) of tears obtained in patients one day after cataract surgery, on 10 to 50 µl of plasma or sera of newborns and early newborns, and on 50 µl of sera of polyarthritic patients, as well as of patients with lymphoid malignancies with the combined use of the Cytometric Bead Array (CBATM, BD Biosciences) and of a PARTEC flow cytometer. In those conditions, detection and quantification of cytokines were easily and rapidly (3 h) performed, and the following data were obtained: high levels of IL-6 and IL-8 were found in tears taken in patients one day after cataract surgery; in the plasma or sera of newborns and early newborns, high amounts of IL-1 β, IL-6, and IL-12 were detected; in polyarthritic patients, high levels of IL-8 were frequently identified, associated or not with high levels of IL-6, IL-12, and/or IL-1 β; in patients with lymphoid malignancies high levels of IL-8 were mainly observed. Noteworthy, in polyarthritic patients, IL-6 and C-Reactive Protein levels were strongly correlated ($R2=0.56$; $P<0.0001$). In conclusion, the microparticle-based flow cytometric method is an efficient and reliable method for simultaneously measuring multiple cytokines from a variety of biological samples, even when small volumes are available. Therefore, this technology opens numerous perspectives in clinical investigations.

96474

A MICROSPHERE-BASED BINDING ASSAY FOR ANALYSIS OF ESTROGEN RECEPTOR MODULATING COMPOUNDS

Marie Anne Iannone[1], Catherine A. Simmons[1], Sue H. Kadwell[1], Daniel L. Svoboda[2], Dana E. Vanderwall[1], Su-Jun Deng[1], Thomas G. Consler[1], Jean Shearin[1], John G. Gray[1], Kenneth H. Pearce[1]

[1]GlaxoSmithKline, Gene Expression and Protein Biochemistry, Research Triangle Park, North Carolina; [2]GlaxoSmithKline, Chemoinformatics, Research Triangle Park, North Carolina

Biochemical and structural studies have demonstrated that estrogen receptor α (ER α) protein conformation can be influenced by ligand binding. This conformational state can significantly effect the ability of the receptor to interact with a wide variety of protein accessory factors. We have applied a flow cytometric microsphere-based multiplexed binding assay to determine the simultaneous binding of ER α to over 50 different peptides. The peptide sequences were either from known cofactor proteins or were identified using random peptide phage display. Over 600 small molecule ligands were used to generate ER α peptide binding profiles. The ligand-induced binding patterns were then used to group the compounds into distinct shape-based clusters. Interestingly, we have observed that compounds within clusters exhibit similar cell-based activities (transcriptional regulation at an estrogen response element, MCF-7 breast cell proliferation, and Ishikawa endometrial cell stimulation). These *in vitro*:cellular correlations may in part explain tissue-specific activities of ER α-modulating compounds. These correlations support the use of this multiplexed peptide interaction assay to rapidly categorize ER α-modulating ligands and to assess nuclear receptor conformation.

97219

THE USE OF PTIR271 DYED MICROPARTICLES IN MULTIPLEXED FLOW CYTOMETRY

Mitch Gore[1], Robert L. Frescatore[2], Fernando Rubio[3], Rich Slawecki[3], Brian D. Gray[4], Katharine A. Muirhead[5], Betsy Ohlsson-Wilhelm[5]

[1]Polysciences, Inc., Warrington, Pennsylvania; [2]Polysciences, Inc., Malvern, Pennsylvania; [3]Abraxis, Particles, Warrington, Pennsylvania; [4]PTI Research, Inc., Exton, Pennsylvania; [5]SciGro, Inc., Malvern, Pennsylvania

PTIR271 is a long red emitting fluorochrome (em. max. ~650 nm) that can be excited, albeit suboptimally, at 488 nm as well at 635 nm. We hypothesized that PTIR271-dyed microparticles could be utilized for both single- and multi-analyte assays over a wide range of excitations ranging from 488 to 635 nm. To investigate this, microparticles were made that contained varying amounts of PTIR271 and analyzed on a FACSCalibur. Excitation of beads dyed with four different amounts of PTIR271 at 488 nm resulted in three distinct peaks in FL3 (670 nm LP). Excitation of the same bead set at 635 nm resulted in four distinct peaks in FL4 (661/16 nm). Negligible signal was observed in FL1 (530/30 nm) and FL2 (585/42 nm). To further demonstrate utility of these particles, competitive receptor binding assays for estrogen and corticosteroid receptors were developed. Dyed microparticles coated with protein-hormone conjugate were incubated with the relevant hormone receptor and rabbit anti-hormone antibody. The level of hormone receptor bound was quantified in FL1 after incubation with a sheep or goat anti-rabbit FITC labeled antibody. The results of these assays demonstrated that identification of bead populations in FL3 via 488 nm excitation and in FL4 via 635 nm excitation can be linked with hormone receptor levels via signal detection in FL1. Additional results will be presented that support the use of PTIR271-dyed microparticles over a wide range of excitation wavelengths (488 nm to 635 nm) and their potential to be used to create other single and multi-analyte detection systems.

Parallel Session 5: T/NK Cells III

Chair: Gregor Rothe
Co-Chair: Bruno Brando

98345

PERFORIN-CONTAINING CELLS IN HUMAN PERIPHERAL BLOOD: III. THE RELATIVE PROPORTIONS OF PERFORIN AND GRANZYME B VARY WIDELY AMONG HUMAN NATURAL KILLER AND T CELL SUBSETS

Doug Redelman[1], W. John Diamond[2], Dorothy Hudig[3], Ken Hunter[4]

[1]Sierra Cytometry/UNR Cytometry Center, Biology, University of Nevada, Reno, Nevada; [2]InteMedica, LLC., Nevada; [3]University of Nevada, Microbiology & Immunology, Medicine, Reno, Nevada; [4]University of Nevada, Microbiology & Immunology, Reno, Nevada

Perforin (Pf) and Granzyme B (GrzB) are among several components of natural killer (NK) and cytotoxic T lymphocytes (CTL) that may participate in mediating cytotoxic activities. For this reason, the intracellular expression of Pf and/or GrzB is considered one of the best markers of mature cytotoxic cells. Of the multiple cytotoxic mechanisms, CTL may trigger Fas (CD95) dependent apoptosis via their expression of Fas-ligand (CD178). In addition, both NK and CTL utilize products in their cytotoxic granules, including Pf and GrzB, to attack target cells. One widely accepted model is that cytotoxic cells produce a transmembrane pore by inserting Pf into the target cell membrane followed by the secretion of GrzB through this pore. GrzB in the target cell can then trigger apoptosis by direct activation of caspases. In order to explore cytotoxic mechanisms more fully, the Hudig laboratory, and others, have isolated granules from cytotoxic cells and examined the activities of those granules and/or components isolated from them. From those studies, it is clear that highly enriched Pf can directly damage membranes and rapidly lyse both erythrocytes and nucleated cells. In addition to these rapid lytic mechanisms, the Hudig laboratory has demonstrated that granules from some types of cells can cause growth arrest of tumor cells that is manifested by an accumulation of cells in late S phase and/or G2/M. Enriched Pf does not mediate this delayed growth arrest and the granules from highly active cells such as lectin and cytokine activated murine spleen cells also cause only rapid lytic effects. These data suggest that there may be differences in the composition of granules from various types of cytotoxic cells and the current results have confirmed that these differences do occur. As described in accompanying reports, we have shown that there may be six or more categories of Pf-containing T cells plus NK cells in the blood of healthy human subjects. We have now examined the expression of GrzB in these cells and first noted that Pf and GrzB were qualitatively co-expressed. However, whereas the amount of Pf expressed per cell could vary over nearly a 100 fold range in different cell populations in the same individual, the expression of GrzB was much more narrowly restricted. If these quantitative immunofluorescence measurements directly reflect the content of Pf and GrzB, then the relative amounts of these two lytic components can vary substantially among the various populations of Pf+ T and NK cells. Thus, NK cells and the various populations of Pf+ T cells we have identified may preferentially utilize different lytic mechanisms. Supported in part by the Office of Naval Research and Nevada BRIN RR16464 (DR) and NIH CA38942 (DH).

98215

FLOW CYTOMETRIC EVALUATION OF SURFACE AND INTRACELLULAR ANTIGENS DURING *IN VITRO* NK CELL DIFFERENTIATION

Loris Zamai[1], Barbara Canonico[2], Massimo Della Felice[2], Claudia Masoni[2], Chiara Felici[2], Francesca Luchetti[2], Stefano Papa[2]

[1]University of Urbino, Institute of Morphological Science/ Center of Cytometry and Cytomorphology, Urbino, Pesaro, Italy; [2]University of Urbino, Cytometry and Cytomorphology Center, Urbino, Pesaro, Italy

NK cell differentiation occurs in bone marrow, and IL-15 is believed to be responsible for bone marrow NK cell development *in vivo*. Human NK cells can be divided into two functionally and phenotypically distinct subsets based on their cell surface density of CD56: CD56bright and CD56dim (Cooper et al., Blood, 97:3146, 2001). CD56dim NK cells are more cytotoxic and express higher levels of KIR and CD16 molecules. By contrast, CD56bright NK cells are the primary source of NK cell-derived cytokines and express CD117 and CD25 molecules. It has been previously reported that IL-15 and IL-2 sustain the *in vitro* differentiation of hematopoietic progenitor cells into NK cells (Zamai et al., J Exp Med, 188:2375, 1998), but no report have distinguished the NK cells generated *in vitro* by CD56 surface density expression (i.e., CD56bright and CD56dim). To this aim, immunomagnetic purified human CD34+ peripheral blood cells were cultured *in vitro* in the presence of IL-15 or IL-2 plus Flt3 ligand. These culture conditions sustained the generation of both CD56bright and CD56dim NK cell subsets. Flow cytometric evaluation of surface and intracellular antigens revealed that a variable proportion of the CD56dim NK subset expressed CD158a,b and KIR3DL1 (DX-9) KIR molecules, CD94, CD161, CD16, CD8, and CD2 mature NK cell markers, CD18, CD11a, CD11b, and CD11c adhesion molecules and CD122, CD132, CD212 (IL-12Rβ1) receptor subunits. Unlike CD56dim cell population, CD56bright one expressed CD117, CD25 and produced IFN-γ, TNF-α and GM-CSF upon stimulation. IL-2Rα (CD25) and IL-15Rα receptor subunits were detectable on CD56dim NK cells generated in the presence of IL-15 or IL-2, respectively, instead CD135 and IL-12Rβ2 were undetectable on cells from both culture conditions. Altogether, the data indicate that IL-15 or IL-2 plus Flt3 ligand sustain *in vitro* differentiation of CD34+ hematopoietic progenitors into cells with distribution of surface and intracellular antigens similar to that present on mature NK cells from the corresponding peripheral blood samples. These culture conditions, recapitulating *in vivo* normal NK cell development, can be used to expand NK cells and to draw possible immunotherapeutic strategies based on NK cells.

98293

MEASURES OF PERTURBATION IN THE T-CELL RECEPTOR V-β (Vβ) REPERTOIRE

Sumita Ganguly[1], Erin McClelland[1], Vera Svobodova Donnenberg[1], Christopher Snow[2], Meryl Forman[2], Rose Kemp[2], Jesus Lemus[2], Charles R. Rinaldo[3], Albert D. Donnenberg[1]

[1]University of Pittsburgh, Medicine, School of Medicine, Pittsburgh, Pennsylvania; [2]Beckman Coulter, Inc., Miami, Florida; [3]University of Pittsburgh, Infectious Diseases and Microbiology, Graduate School of Public Health, Pittsburgh, Pennsylvania

We used 5-color flow cytometry (Beckman-Coulter FC500) to measure TCR V-β distribution across CD4 and CD8 T-cells, subsetted on the basis of CD45RA and CD27 expression. Peripheral blood samples from 39 HIV positive male subjects and 21 age and sex matched controls were analyzed using the Beta Mark reagents (Beckman-Coulter). We wished to evaluate subset-specific expansions and deletions of individual VB specificities, and also provide an indicator of skewness across the entire VB repertoire. Initially, we attempted to define perturbations in the VB repertoire based on our control data set, using a conventional mean plus and minus 1.96 standard deviations to identify expansions and deletions, respectively. In control subjects, the VB distribution was markedly skewed, resulting in a 4-fold overestimate of expansions and a commensurate underestimate of deletions, compared to the predictions of a normal model. After a simple log transformation of percent VB+, the data conformed excellently to a normal distribution, as confirmed using probability plots. Using log transformed data we used the mean values from our control dataset +/- 1.96 SD to define subset-specific cutoffs for VB expansions and deletions. For an individual subject, subset-specific skewness across the repertoire was measured by the sum of perturbations (expansions plus deletions). We defined an additional measure of skewness that is sensitive to the magnitude of perturbations as the skewness index (SI), using a "sum of squares" statistic similar to a SD defined by the formula: SI = SQRT((OBS–EXP)^2)/N-1 Where the sum of the squared differences between VB values observed in an individual (OBS) and the mean value observed in the control series (EXP) is divided by the number of VB specificities in our panel (24) minus 1. Analogous to a SD, the square root is taken. As above, log percent values are used in these calculations. Using these analyses, we concluded that HIV disease and age are significant factors for determining perturbations in the VB repertoire of CD8, but not CD4 T cells. In contrast to published results, no individual VB was expanded or deleted specifically in HIV disease, even at he level of naïve/memory/effector subsets. Age was positively correlated with perturbation number and SI in all of the CD8 subsets except effectors (CD45RA+/CD27-). HIV+ subjects had a greater number of perturbations in the total CD8 and effector/memory (CD45RA-/CD27-) subset, and a greater SI in the total CD8 population when compared to age-matched controls.

96303

MULTIPARAMETER PRECURSOR ANALYSIS OF T-CELL RESPONSES USING CELL-TRACKING DYES

P.K. Wallace[1], N. Bercovici[2], M.G. Waugh[3], J.L. Fisher[3], F. Vernel-Pauillac[2], Marc Ernstoff[4], J.P. Abastado[2], Alice Givan[5]

[1]Roswell Park Cancer Institute, Laboratory of Flow Cytometry, Buffalo, New York; [2]IDM (Immuno-Designed Molecules), Paris, France; [3]Dartmouth College, Department of Medicine, Lebanon, New Hampshire; [4]Dartmouth College, Lebanon, New Hampshire; [5]Norris Cotton Cancer Center, Lebanon, New Hampshire

We have used the PKH fluorescent dyes which stain cell membranes and then partition between daughter cells at division in conjunction with flow cytometry to measure cell proliferation. Described is an extension of this dye dilution methodology to calculate the precursor frequency of antigen-specific T-cells. With mathematical deconvolution of the fluorescence histograms, information can be derived about the precursor frequency of cells in the original population that responded to the specific stimulus. We estimate that this method can detect proliferation of cells, before addition of the stimulus, that represent approximately $1/10^5$ of the population. Next, we compared three individual methods for assaying the frequency of antigen-specific T cells: ELISPOT, tetramer-binding, and PKH dye dilution using human T cells cultured with influenza-peptide-loaded dendritic cells. The three methods yielded similar but not identical results. Using a multiparameter flow cytometric method, which permits simultaneous analysis of antigen-specific tetramer binding, T-cell proliferation, and cytokine production, we calculated the proportion of different precursor subsets in the original, resting population. We conclude that approximately half of the cells that bound specific tetramers actually proliferated and synthesized IFN(γ) in response to antigen. This method could be applied with additional markers of function and differentiation to describe the complex response potential of a T-cell pool.

98330

INDUCTION OF INTERLEUKIN-6 PRODUCTION BY HUMAN CD4+ OR CD8+ T LYMPHOCYTES: RELEVANCE FOR THE IMMUNEMODULATORY ROLE OF 1,25-DIHYDROXYVITAMIN D3

Martin Willheim[1], Peter Pietschmann[1], Ralf Thien[1], Katharina Wahl[1], Meinrad Peterlik[1]

[1]University of Vienna, Dept. of Pathophysiology, Vienna, Austria

There is evidence from epidemiological studies that prevention of rickets by vitamin D3 is associated with a lower prevalence of autoimmune diabetes mellitus in adolescence. This phenomenon has been traced to the potency of 1,25-dihydroxyvitamin D3 (1,25(OH)2D3) to reduce Th-1 lymphocyte activity, which in turn is believed to result in predominance of the Th-2 pathway. However, by the same token, vitamin D3 administration is believed to predispose to various allergic diseases in later life. We therefore conducted an extensive survey on the effect of 1,25(OH)2D3 on cytokine production by human cord blood as well as by adult T lymphocytes. By four-color flow cytometry we assessed the intracellular cytokine content (IL-2, Il-4, IL-6, IL-13 and IFN-g) of CD4+ Th and CD8+ Tc cells in peripheral blood mononuclear cell (PBMC) cultures. In cord blood as well as adult PBMC, addition of 10-8 M 1,25(OH)2D3 to the culture medium suppressed IL-12-mediated differentiation to Th/Tc-1 lymphocytes: Thereby, the steroid hormone had a major effect on IFN-g-positive cells, whereas IL-2 production was hardly affected. Interestingly, 1,25(OH)2D3 suppressed also IL-4 dependent maturation of Th/Tc-2 cells in cord blood-derived PBMC, whereas a significant positive effect on IL-4+ /IL-13+-positive T cells was observed in adults. Independently of age, and particularly in the presence of IL-4, 1,25(OH)2D3 caused the appearance of a large subpopulation of T cells, which produced mainly IL-6 but almost no IL-4 and IL-13, or IFN-g. Since IL-6 promotes proliferation and differentiation of B and T lymphocytes, it could well be that induction of IL-6-positive T lymphocytes plays an important role in the immunemodulatory action of 1,25(OH)2D3.

Parallel Session 5: Cancer Biology III

Chair: TBD

97064

ASSOCIATION OF ERBB2, β1 INTEGRIN AND LIPID RAFTS ON TUMOR CELLS

Maria Magdalena Tufeanu[1], Zsolt Fazekas[2], Miklós Petrás[3], Jorma Isola[4], György Vereb[3], János Szöllõsi[3]

[1]Carol Davila University of Medicine, Biophysics Department, Bucharest, Romania; [2]University of Debrecen, Medical and Health Science Center, Debrecen, Hungary; [3]University of Debrecen, Medical and Health Science Center, Biophysics and Cell Biology, Debrecen, Hungary; [4]University of Tampere, Finland, Institute of Medical Technology, Tampere, Finland

Background: The overexpression of ErbB2, a member of the EGF receptor tyrosin kinase family, can be observed in about 25 % of malignant breast tumors. The importance of ErbB2 expression pattern of tumor cells was greatly increased after the introduction of Herceptin® (Trastuzumab) therapy which is based on a monoclonal antibody against ErbB2. For better understanding the mechanisms of its anticancer efficacy and to find out factors leading to Herceptin® resistance, it is worth to consider the interaction of ErbB2 with other cell surface species. One of these is β1 integrin, which is involved in tumor progression, cell attachment and metastasis, another are the lipid rafts, which can be considered as signaling centers of cell surface receptors. **Methods:** A comparative investigation was performed on Herceptin® resistant (JIMT-1, MKN-7) and sensitive (SKBR-3, N87) tumor cells lines *in vitro*. The expression levels, colocalisation and association pattern of ErbB2 molecules, integrins, and lipid rafts were examined with flow cytometry and confocal laser scanning microscopy, including flow cytometric and imaging FRET (Fluorescence Resonance Energy Transfer) measurements. Colocalisation was determined by calculating the cross correlation value between each image pair of three colour confocal images of cells of interest. Changes of the above mentioned parameters induced by specific antibodies, epidermal growth factor (EGF), heregulin and cytochalazin-D have been also studied. **Results:** Herceptin® resistant cell lines showed higher expression level of β1 integrin compared to the sensitive ones according to flow cytometric measurements. The colocalisation of β1 integrin, ErbB2 and lipid rafts was found on all four cell lines. 4D5, EGF, and heregulin treatment slightly decreases the colocalization of erbB2 and β1 integrin. Cross-linking lipid rafts significantly decreased their colocalization with ErbB2 molecules and integrins on all cell lines, but had no effect on β1 integrin and ErbB2 colocalisation. β1 integrin crosslinking decreases the colocalization of this receptor and ErbB2 and also lipid rafts, but has no influence on the ErbB2-lipid rafts colocalization. Triple colocalization among β1 integrin, ErbB2 and lipid rafts on all four cell lines is maintained after cytochalazin-D treatment. **Conclusion:** Crosslinking lipid rafts with cholera toxin caused separation of the rafts and clusters of β1 integrin and ErbB2, while the later two stayed together. Colocalization of β1 integrin, ErbB2 and lipid rafts seems independent of cytoskeleton and probably can be dependent only on the relationship between membrane receptors and the lipid rafts.

97243

THE MITOCHONDRIAL CHARACTERISTICS OF CELL KILLING BY THE BCL-2 AND BCL-XL LIGAND HA14-1: A REAPPRAISAL OF THE BASIC MECHANISMS FOR ITS USE IN CANCER THERAPY AND APPLICATION TO CLINICAL SAMPLES

Patrice X. Petit[1], Francois Gonzalvez[1], Pauline Andreu[1], Dephine Fradin[1], Christian Slomianny[1]

[1]Instit Cochin, CNRS UMR 8104, Paris, France

Following the litterature report that the Bcl-2 ligand HA14-1 induces apoptosis via the mitochondrial pathway (1), we have investigated the mitochondrial and cellular effects of HA14-1. We show that HA14-1 has a clear dual effect on mitochondria: (i) it sensitizes the opening of the permeability transition pore (PTP); this is a potentially usefull effect because PTP opening in Bcl-2 or Bcl-XL overexpressing cells could lead to selective killing of tumor cells but apparently this effect is also obtained in control cells which do not overexpress Bcl-2 nor Bcl-XL; (ii) it both inhibits the ADP stimulated respiration and slightly uncouples respiration, representing a toxic side effects that may hamper the developpement and the use of such a drug in anticancer therapy. The sensitization of the pore opening (in uncoupled conditions) could be demonstrated in a concentration range that does not cause respiratory inhibition (up to 15 µM), while toxic effects became proeminent between 20 and 50 mM, we tested the mechanism underlaying the toxic side effects of HA14-1 at various concentration. We found that relatively low concentrations of HA14-1 cause PTP opening *in situ*, and that slightly higher concentrations causes PTP-independent depolarization and cell death. The characterization of this cell death has been realized by extensive flow cytometry analysis and at the mitochondrial level. Clearly, at 5 µM HA14-1 do not induce cell detah and can be associated to conventionnal anticancer drugs for evaluation. The consequences of the underlaying mechanisms depicted for the use of this compound in cancer therapy are evaluated.

95685

STUDY ON THE PATTERNS AND ROLES OF MAJOR CYCLINS EXPRESSED IN HUMAN CONTROLLED PROLIFERATION TISSUES

Jianping Gong[1], Weihua Li[2], Jinming Chen[2]

[1]Tongji Medical University, General Surgery, Tongji Medical College, Huazhong University of Science and Technology, Wuhan, Hubei, China; [2]Tongji Medical University, General Surgery, Wuhan, Hubei, China

Objective: To investgate the expression of human major cyclins in different regeneratable normal tissues, and to discover the laws and roles of cyclins expressed in the cell proliferation process Cas well as provide cues for research in the cell-cycle broken mechanism in clinical tumor. **Methods:** Major cyclins expressed in compound single cells detached from 19 jejunum or colon tissues, and 11 liver tissues were analyzed by FCM. The results were confirmed by confocal and Western blotting. **Results:** The expression of cyclin E, B1 was major and the expression of cyclin D1 or A was low or no in regeneratable normal tissue.The positive rates and the levels of cyclin E,B1 expressed were shown correlation with the activity of proliferation in different normal tissues.There were no cyclins expressed in the differentiated cell such as PBL. The positive rates and the levels of cyclins expressed, especially cyclin E, B1 expressed, were discrepant in different layers of jejunum or colon tissues, which attenuated gradually from crypt to luminal surface. The expression of cyclins, detected by confocal, is only located in crypt. **Conclusions:** The expression of major cyclins is related to the activity of cell proliferation, play a pivotal part in cell proliferation.The laws of major cyclins expression are that the level of cyclins expressed is declining gradually with the progression of cell regeneration. The laws of cyclins expression, especially cyclin E,B1 expression, were shown correlation with controlled proliferation and terminal differentiation of cell. Major cyclins play a pivotal role during the process of regeneration.

96646

CONTINUOUS EXPOSITION OF HUMAN BREAST AND BLADDER CANCER CELL LINES TO BROMODEOXYURIDINE (BRDU) DIFFERENTIALLY AFFECTS CELL CYCLE PROGRESSION

Gero Brockhoff[1], Manfred Kubbies[2], Elisabeth Schmidt-Bruecken[1], Leoni A. Kunz-Schughart[1], Simone Diermeier[1]

[1]University of Regensburg, Regensburg, Germany; [2]Roche Pharmaceutical Research, Penzberg, Germany

Background: The flow cytometric anti-BrdU and the BrdU/Hoechst quenching assay facilitate to analyze the regulation of cell proliferation in detail. Both techniques are based on the substitution of thymidine by bromodeoxyuridine. The BrdU/Hoechst method requires continuous BrdU treatment whereas the anti-BrdU method is based on a short term pulse. The evaluation of a potential inhibitory, cytostatic, or cytotoxic effect has to be evaluated in a continuous BrdU treatment setting even when cancer cells are the subject of investigation. **Methods:** We examined the impact of BrdU on the proliferation of four different tumor cells lines (bladder carcinoma: RT4, J82; breast carcinoma: BT474, SK-BR-3) when short-time or continuously applied. Both one- and two-parametric DNA measurements were performed to identify BrdU-induced alterations in the S-phase fraction and in cell cycle progression. An annexinV/propidium iodide (PI) assay was used to identify potential induction of apoptosis by BrdU. **Results:** Proliferative activity in BT474, SK-BR-3, and RT4 cultures is cell type specifically reduced due to continuous treatment with 60, 5.0, and 3.5 µM BrdU. The BrdU induced effect is exerted in different cell cycle phases of different consecutive cell cycles. The inhibition, which was not found in J82 cultures, is dependent on exposure time (96 h vs. 48 h) and is also dose-dependent for RT4 and SK-BR-3. A short-term exposure to BrdU of all cells investigated so far does not cause any inhibitory effect on proliferation. BrdU application does not induce apoptosis or necrosis as revealed with the annexinV/PI assay. **Conclusion:** Continuous BrdU treatment does not affect cell viability but essentially alters cell cycle progression in three out of four cancer cell lines tested. Cell-type specific validation of the feasibility of the powerful BrdU/Hoechst quenching technique due to a continuos BrdU treatment is essential and mandatory.

96914

TOPOISOMERASE II TRAPPING AGENTS INDUCING APOPTOSIS AND G2/M PHASES ARREST OF ORAL CARCINOMA CELLS

Wan-Tao Chen[1], Jinzhong Li[2]

[1]Shanghai Second Medical University Affiliated Ninth Hospital, Shanghai, China; [2]Affiliated Ninth People's Hospital, Oral Oncology Laboratory, Shanghai, China

Background: Teniposide is a kind of topoisomerase II trapping agents and has been used in lung cancer and nervous system malignant tumor, but there is few basic and clinical reseach for this drug in oral carcinoma treatment. Present study will investigate the effect and mechanism of teniposide on inhibiting oral carcinoma cells growth *in vitro*. **Material and Methods:** Teniposide was used as a topoisomerase II-trapping agent. Human tongue squamous cell carcinoma cell line (Tca8113) was used as subject in this study. MTT assay was used to assess the inhibition of teniposide on cell growth. Transmission electronic microscope (TEM), fluorescence staining and Annexin V-FITC and propodium iodide assay were employed for determining the apoptotic activity. Flow cytometer was used to examine the cell cycle arrest of Tca8113 cells. **Results:** The concentration of ID50 of teniposide on Tca8113 cells was 0.35µg/ml. Apoptosis rate of Tca8113 cells induced with 5µg/ml teniposide for 72hr was 92.85% and cell cycle appeared to be arrested at S phase. However, the G2/M phase of Tca8113 cells which were exposed to 0.15µg/ml teniposide for 72hr, increased from 10.75% to 75.18% in percentage while the apoptotic rate in this group was far below than that of cells treated with 5.0µg/ml teniposide. **Conclusion:** Teniposide could significantly induce apoptosis of oral carcinoma cells and inhibit cell growth. There may be another pathway inducing oral carcinoma cells apoptosis underlying G2/M phase arrest.

Parallel Session 5: Leukemia/Lymphoma III

Chair: Francesco Lanza

96755

CORRELATION OF ZAP-70 ANALYSED BY FLOW CYTOMETRY WITH IGVH MUTATIONAL STATUS IN B-CLL

Jan Jules Philippé[1], Barbara Leus[2], Ann Piette[2], Femke Van Bockstaele[2], Ann Janssens[2], Fritz Offner[3]

[1]Ghent University, Ghent, Belgium; [2]Ghent University Hospital, Ghent, Belgium; [3]Ghent University, Hematology, Ghent, Belgium

Introduction: Although generally regarded as an indolent disease, CLL has a considerable variability in clinical course. The prognostic significance of IgVH gene rearrangements is well established, those patients with unmutated IgVH genes having a worse prognosis than those with somatic mutations. Zap-70, a tyrosine kinase involved in T-cell receptor signalling, was found by gene expression profiling, to be expressed in the unmutated subgroup. The analysis by flow cytometry of the latter marker is much easier than the elaborate and costly sequencing technique. Therefore we evaluated the zap-70 expression by flow cytometry and compared these results with the mutational analysis. **Materials and Methods:** 23 B-CLL patients were included. In two patients analyses were

performed repeatedly. 5.105 cells were fixed and permeabilized with use of the Fix&Perm kit (Caltag) and 1.5 μg of anti-zap-70 antibody (clone 2F3-2, Upstate Biotechnology) was used and further stained with GAM-PE. Then cells were washed and incubated with normal mouse serum for 5 minutes and finally staining with CD19-FITC, CD3PerCP and CD56-APC/CD5-APC. For each sample a D-value was established as a result of the Kolmogorov-Smirnov statistics comparing the zap-70 expression of T-cells (CD3+) versus the zap-70 expression of the B-CLL cells (CD19+/CD5+, or all CD19+). Flow cytometric results were compared with the IgVH mutational status. **Results:** Seven patients had unmutated VH-genes (<2% mutations) and 16 patients showed a mutated profile. D-value was 0.81 ± 0.07 (mean ± SD) for the unmutated patients versus 0.89 ± 0.06 in the mutated patients (p=0.01). As cut-off for the D-value several options were possible: 0.855 with one patient with D=0.92 having an unmutated profile and 5 patients with D<0.855 showing a mutated profile, or 0.815 with 3 misclassifications for each group (3 false positives and 3 false negatives). Of the three unmutated patients with 'false high' D-values one patient (D=0.92) has a stable disease during more than 30 years, another (D=0.84) has a stable disease for 10 years, and one patient was recently diagnosed. **Discussion:** A cut-off value of 0.815 for D seems most promising. A prospective study is ongoing in order to further evaluate this flow cytometric assay.

96415

ROUTINE MONITORING OF MINIMAL RESIDUAL DISEASE BY FLOW CYTOMETRY IN ADULT ACUTE LYMPHOCYTIC LEUKEMIA

Yang Ok Huh[1], Jeong-Nyeo Lee[2], Danielle Cooper[1], Hagop Kantarjian[3], Sherry Pierce[3], Deborah Thomas[3]

[1]The University of Texas M.D. Anderson Cancer Center, Hematopathology, Houston, Texas; [2]Pusan Baik Hospital, Department of Clinical Pathology, Pusan, South Korea; [3]The University of Texas M. D. Anderson Cancer Center, Leukemia, Houston, Texas

Overall survival of adults with acute lymphocytic leukemia (ALL) remains poor despite achieving morphologic complete remission in the majority of patients. The patient in remission in conventional criteria may have as many as 10^{10} leukemic cells in bone marrow. Investgation of minimal residual disease (MRD) by immunophenotyping using multi-pararmeter flow cytometry has proven to be a powerful tool for disease monitoring in patients with ALL in mostly pediatric patients. We have tested bone marrow aspirate specimens form 92 adult patients with ALL (80 B-lineage and 12 T -lineage) in clinical and morphological (bone marrow blasts <5%) remission. Bone marrow aspirate specimen was submitted to clinical flow cytometry laboratory for routine acute leukemia study at various time points including at the end of remission induction (day21), and at 3 month interval thereafter. All specimens were evaluated by preliminary light scatter pattern using CD45 for detection of discrete blast population. Full acute leukemia work-up was performed when a discrete blast region was present. The flow cytometry protocol for MRD detection included 4-6 tubes of 4-color marker combinations that were individually customized for each patient based on the initial immunophenotype at the time of diagnosis. In over 90% of B-lineage cases, CD19/CD34/CD10 and CD19/CD34/TdT were included. Other combinations less frequently used were CD19/CD20/CD10, CD19/CD33/CD34, CD19/CD13/CD34 and CD19/CD38/CD34. For T-lineage ALL, CD3/CD34/TdT, CD4/CD8/TdT or CD3/CD33/CD34 were used most of the time. At least 2 x 10^6 cells were stained in each tube and 1 x 10^5 cells with positive marker were acquired within 6 hours of staining. MRD was defined as more than one cell with the same immunophenotype seen the original diagnosis in 1,000 cells (> 0.1%) in this study. In 33 of 80 patients (41%) with B-lineage ALL, we identified cells with leukemia-associated immunophenotype in a frequency of >0.1% of cells in the sample. Eight of these 33 patients had more than 1% of cells showing leukemia-associated immunophenotype. In 14 patients, more than 1 sample were collected at different time interval. MRD persisted in 9 patients and disappeared in subsequent samples in 4 patients. The clinical significance of MRD in this cohort of patients remains unknown at the present time since only a few patients relapsed. Correlation of MRD with the rate and the time interval to relapse is being monitored in these patients. Association of MRD with known clinical and laboratory parameters at diagnosis is being investigated. In summary, routine MRD monitoring by flow cytometry can be implemented in clinical laboratory, but the clinical usefulness remains unknown and will require a longer follow-up.

96981

ALTERED EXPRESSION OF NATURAL CYTOTOXIC RECEPTORS (NCRS) ON HAEMATOLOGICAL MALIGNANCIES

Cyril Fauriat[1], Christine Fornelli[2], Alessandro Moretta[3], Regis Costello[1], Daniel Olive[4]

[1]Institut Paoli-Calmettes, Marseille, Florida, France; [2]Beckman Coulter Immunotech, Marseille, France; [3]Universita di Genova, Histology, Genova, Italy; [4]Inserm U119, Immunologie, Marseille, France

Human natural killers (NK cells) are potent effector cells involved in destruction of virus infected cells or tumors. Fine tuning of NK activity involves the integration of negative signals provided by inhibitory receptors recognizing MHC class I molecules and positive signals provided by activating receptors. Among activating receptors, the natural cytotoxicity receptors (NCR) NKp44, NKp46 and NKp30, are potent activating NK-specific molecules. The 2B4/CD244 molecule is a co-activating receptor for NCR-mediated cytotoxicity. Interestingly, a correlation has been found between surface expression of NCRs which varies among normal individuals (with a common "NCR high or bright" expression) and cytolytic activity of NK cells. More recently Costello et al. have observed that the NCRdull NK phenotype (low NCR expression) is quite common in patients with acute myeloid leukaemia (AML) and correlates with poor NCR-driven cytotoxicity. These data point to an altered NK cell phenotype associated with a malignant hemopathy, a novel mechanism for tumors to evade innate immunity. In this work we have completed the previous study about AML-NK using direct analysis of these cells at the diagnosis and without *in vitro* culture. Moreover, we also extended AML observation to other haematological malignancies by the analysis of NCRs and 2B4 expression on NK cells in patients with B-cell lymphocytic leukemia (B-CLL), acute Lymphoblastic leukemia (ALL) and Multiple myeloma (MM). Direct analysis of AML-NKs confirmed the high prevalence of the NCRdull phenotype previously observed in cultured AML-NKs. In B-CLL and MM, abnormal NCR and 2B4/CD244 expression was observed, in sharp contrast with ALLs that displayed a normal phenotype for all tested molecules. This data suggest that an altered NK cell phenotype is common in haematological malignancies, except ALL, and may explain the reduced NK cytolytic activity observed in those pathologies and thus contribute to tumor escape and relapse.

98370

INDUCTION OF APOPTOSIS IN LEUKAEMIA CELLS—THE ROLE OF APOPTOSIS RELATED PROTEINS (ARP) AND MULTIDRUG RESISTANCE MOLECULE (P-GP)

Anna Pituch-Noworolska[1]

[1]Polish-American Children Hospital, Krakow, Poland

The apoptosis of leukaemia cells is a main tusk of induction therapy with steroids and cytotoxic drugs. The apoptosis related proteins (ARP) are involved in regulation of apoptosis induction and signalling pathway. The multidrug resistance molecule (p-gp) represens the main mechanism of resistance of leukaemia cells to cytostatics of natural origin and is associated with lowering of susceptibility of these cells to induction of apoptosis. The leukaemia cells from children in acute phase of disease before the induction therapy were isolated for diagnostic immunophenotype and for the study of induction of apoptosis *in vitro*. The apoptosis was induced after a short-time culture in the presence of dexamethasone, vincristine, cyclosporin, TNF and GM-CSF. The expression of p-gp and ARP and the percentage of apoptotic cells were assayed by flow cytometry before and after culture. The induction of apoptosis was noted in part of studied cases and was associated with changes in ARP levels. The expression of p-gp was associated

with expression of bcl-2 and decrease of susceptibility of leukaemia cells to induction of apoptosis. The expression of p-gp was independent of ARP expression and spontaneous apoptosis of leukaemia cells. The induction of apoptosis of leukaemia cells with dexamethasone, cyclosporin and vincristine was associated with decrease of bcl-2 level, changes of bcl-2—bax ratio. The level of bad, bak, bcl-x was unchanged under the induction of apoptosis. GM-CSF was protective for leukaemia cells against apoptosis. The atypic immunophenotype of leukaemia cells was associated with overexpression of p-gp and bcl-2 and lower inductive apoptosis. The susceptibility of leukaemia cells to induction of apoptosis is a complex process involving among other factors the expression and activity of p-gp, immunophenotype and expression of ARP.

96595

FLOW CYTOMETRIC DETERMINATION OF INDIVIDUAL BLOOD CELL RADIATION SENSITIVITY IN LEUKEMIA PATIENTS

Wolfgang Beisker[1], Michael Nuesse[1], Lucie Bauerschaper[2], Werner Grundler[1], Eberhard Fritz[2]

[1]GSF, Flow Cytometry Group, Neuherberg, Germany; [2]GSF, IMS, Neuherberg, Germany

Clinical Studies have shown that in individuals, even within a relatively homogeneous population, drastic variations in their responses to radiation exposure can be observed. The cause for this variability could be either of genetic or epigenetic origin. Identifying individuals with altered radiosensitivity may be an important factor for radiation protection as well as to improve regimens of tumor radiotherapy. The purpose of this study is to analyse multiple cellular parameters of radiosensitivity in human blood cells in order to establish a combination of *in vitro* assays that can predict individual radiosensitivity. To this end, blood cells of leukemia patients were isolated both before and after *in vivo* total body irradiation (administered as a conditioning regimen before bone marrow transplantation). Using dual laser flow cytometry, cells positive for CD3 as well as for CD19 (both labeled with antibody conjugated with APC) were analysed simultaneous for apoptosis by the Annexin/PI assay. Data were also analysed using the APO 2.7 assay. For comparison, the DNA repair capability was crosschecked using Comet assay. For all persons lymphocyte populations habe been measured with and without *in vitro* irradiation using doses of 0.4 and 0.8 Gy. For blood cells of healthy probands as well as for control cell lines, a similar reaction to radiation exposure could be determined without broad variations. The number of apoptotic cells either measured by Annexin or by APO 2.7 increases as expected with increasing irradiation. The scheme is in good agreement with the comet assay data. However, isolated blood cells from more than 50 leukemia patients show a significant broadening of the standard deviation, which could not be explained by experimental or logistic variations. Because we analyse only CD3 and CD19 positive cells (positive in APC fluorescence), any effects of other lymphocyte populations can be excluded. Individual populations have been found, which show a significant higher radiation sensitivity in their apoptotic behaviour as well as in the comet assay.

Parallel Session 5: Clinical Oncology I

Chair: TBD

95877

WHATEVER HAPPENED TO TPOT?

George D. Wilson[1], Nicolas Paschoud[2]

[1]Wayne State University, Radiation Oncology, School of Medicine, Detroit, Michigan; [2]Central Hospitalier Universitaire Vaudois, Lausanne, Switzerland

The flow cytometric measurement of potential doubling time (Tpot) was hailed as a major advance in human tumour cell kinetics with the first measurements being performed *in vivo* in 1985. Since that time, several thousand patients have been assessed with a variety of neoplasms and a wide range of treatments including surgery, chemotherapy and radiotherapy. Many of these studies were purely to increase biological knowledge and assess the prognostic significance of this different measure of proliferation. Perhaps, the most interesting and widely studied application of Tpot was its potential as a predictive test to identify patients, particularly head and neck cancer sufferers, who were likely to fail with conventional fractionation. There was a clear rational to believe that fast proliferating tumours would be at a disadvantage. The reality of Tpot has not lived up to its promise. The results from published studies are at best ambiguous with some centres reporting highly significant correlations with outcome and others failing to find any association with local control or survival. In addition, a meta-analysisof all the currently available data in head and neck cancer also failed to reveal any impact of Tpot although the simple labelling index (LI) did show a weak correlation with local control. Why should this be? Tpot is theoretically a better parameter of proliferation than LI or markers such as Ki-67. The answer is multifactorial and includes our inability to measure the parameter correctly, the problem of proliferative misclassification of diploid tumours, the problem of heterogeneity and the design of the clinical study. Each of these problems could be overcome or at least minimised and this can be achieved by understanding the areas of conflict in data analysis, combining flow cytometry and immunohistochemistry, taking multiple samples and undertaking larger scale studies. There is a trend to dismiss Tpot but this is premature, there is still one major studied to be completed, NCI T92-0045 trial in which 1000 patients are being studied. The criteria for this trial were that the tumour should be head and neck, cervix or rectum and be treated by what is considered to be conventional treatment in each centre and, most important, that a Tpot measurement should be made. The accrual to this trial has finished. There are several reasons why this trial will be the definitive Tpot study, these include the large number of patients and that that each Tpot measurement is critically reviewed and analysed by expert observers. In addition, where possible, more than one sample has been studied from the patients. This presentation will focus on the data being generated by this trial.

96558

SLIDE-BASED CYTOMETRY FOR THE DETECTION OF LARYNGEAL CANCER

Andreas O.H. Gerstner[1], Alexander Thiele[2], Friedrich Bootz[1], Andrea Tannapfel[3], Attila Tárnok[4]

[1]University of Bonn, Dept. of Otorhinolaryngology, Bonn, Germany; [2]University of Leipzig, Dept. of Otorhinolaryngology, Leipzig, Saxony, Germany; [3]University of Leipzig, Dept. of Pathology, Leipzig, Germany; [4]University of Leipzig, Leipzig, Saxony, Germany

Aim: The aim of this study was to test the applicability of a slide-based cytometric assay for the detection of laryngeal cancer in a clinical setting. **Material and Methods:** From patients presenting with clinical changes of their laryngeal mucosa swabs (n=51) were taken during routine diagnostic or therapeutic interventions in general anesthesia after written informed consent. At the same inter-

vention a specimen for histopathological examination was also obtained (e.g. excisional biopsy, laser resection, laryngectomy) which served as gold standard. Swabs were suspended in PBS and placed on a glass slide in two separated areas and fixed in ethanol after air-drying. The cells in the two areas were stained with anti-cytokeratin and control-antibody, respectively, by indirect immunolabeling with allophycocyanine and for DNA by propidium + RNase treatment. Slides were then analyzed in the laser scanning cytometer (LSC), and single cells were re-localized for documentation. Slides were then re-stained with hematoxilin-eosin and were re-localized in the LSC again. Data were analyzed with proprietary WinCyteÔ software. Applying a 5%-cut off set in the control staining, in the specific staining the DNA-diploid population of leukocytes was identified as cytokeratin-negative cells. Taking this peak as DNA-diploid the DNA-index (DI) of the cytokeratin-positive cells was determined. A specimen with 0.95<1.05 or 1.9<2.1 determined for the cytokeratin-positive population was classified as LSC-benign, a specimen with DI outside of these regions for the cytokeratin-positive populations was classified as LSC-malignant. Specimens with less than 2.500 cells were classified as LSC-insufficient. **Results:** Seven swabs were classified as LSC-insufficient. Of the remaining 44 swabs, 29 were from malignant lesions out of which 24 were recognized by LSC as "LSC-malignant". 15 swabs were from benign lesion out of which 13 were recognized by LSC as "LSC-benign". The 2 swabs from benign lesions mis-diagnosed as "LSC-malignant" were from parakeratotic squamous epithelium. The positive predictive value of the LSC-test was 0.92, and the p-value was 12 x 10-6 as determined by Fishers exact test. **Conclusion:** From a clinicians point of view the quantitative cytometric analysis of laryngeal swabs by LSC yields a high positive predictive value. Its sensitivity probably could further be improved by combining the LSC-analysis with subsequent conventional cytology on the same slide. The data have to be confirmed by a large-scale study on material obtained in local anesthesia in the out-patient department. If the data are validated this LSC-assay will be beneficial for the clinician and the patient in the decision making about the need and extent of a surgical intervention.

97577

FLOW CYTOMETRY AND P53 LOH IN COMBINATION ARE STRONG PREDICTORS OF PROGRESSION TO ESOPHAGEAL ADENOCARCINOMA IN BARRETT'S ESOPHAGUS

Peter S. Rabinovitch[1], Patricia C. Galipeau[2], Gary M. Longton[3], Carissa A. Sanchez[2], Xiaohong Li[3], Petra S. Kraemer[2], Heather D. Kissel[2], Kamran Ayub[4], Patricia L. Blount[5], Brian J. Reid[2]

[1]University of Washington, Pathology, School of Medicine, Seattle, Washington; [2]Fred Hutchinson Cancer Research Center, Human Biology, Seattle, Washington; [3]Fred Hutchinson Cancer Research Center, Seattle, Washington; [4]University of Washington, Medicine, School of Medicine, Seattle, Washington; [5]Fred Hutchinson Cancer Research Center, Human Biology, School of Medicine, Seattle, Washington

Barrett's esophagus (BE) is a neoplastic condition that predisposes to esophageal adenocarcinoma (EA). BE progresses to EA via pathways of genomic instability that include ploidy abnormalities and 17p (p53) loss of heterozygosity (LOH) and mutation. We hypothesized that a panel of biomarkers including p53 mutation, 17pLOH, aneuploidy, and tetraploidy would be a better predictor of progression to EA than any single biomarker. A cohort of 270 BE patients was surveyed for 1180 patient-years. Epithelial cells from endoscopic biopsies were purified by flow-cytometric sorting, analyzed by DNA content and cell cycle, assayed for p53 mutation by sequencing exons 5-9 and genotyped for LOH by microsatellites. Prevalences of p53 mutation, 17p (p53) LOH, and ploidy abnormalities were 15%, 20%, and 21%, respectively. The 5-year cumulative incidences of EA in patients with no ploidy abnormality at baseline, aneuploidy, tetraploidy, or both were 4%, 47%, 46%, and 59%, respectively. Aneuploidy (RR=10.9, CI:5.5-21.8) and tetraploidy (RR10.3, CI:5.2-20.5) are highly predictive of progression to cancer, and each abnormality adds to prediction of EA when stratified by the other [(aneuploidy RR=6.0, CI:2.8-12.9), (tetraploidy RR=5.2, CI:2.4-11.1)]. p53 mutation (RR=7.7, 95% CI:3.7-15.9) or 17p LOH (RR=17.7, CI:7.5-41.7) are also highly predictive of progression to cancer. We assessed the interdependence of these findings by evaluating the relationship between neither (aneuploidy or tetraploidy), one, and two ploidy lesions relative to p53 lesions. The contribution of mutation to EA outcome is not significant when stratified on ploidy status (RR=1.6, CI:0.7-3.8). However, after stratification, ploidy abnormalities (RR=6.9 for 1 vs. 0 abnormalities, RR=12 for 2 vs. 0; likelihood ratio test (LRT) p<<0.001) and 17pLOH (RR=6.4, LTR p<0.001) each still contribute to prediction of EA when accounting for the other. The highest 5-year cumulative EA incidence was 72% in patients with at least one ploidy abnormality and 17p LOH. Patients with 17p LOH, aneuploidy and/or tetraploidy had the highest risk of EA relative to all other patients (RR=24, CI:11-51) or relative to those with no lesions (RR=47, CI:16-137). The sensitivity and specificity of ploidy and 17p LOH measurements for the prediction of cancer 12, 36 and 60 months later was 94% and 94%, 92% and 92%, and 82 and 89%, respectively. A combination of flow cytometry and 17p LOH appears to identify the patients at highest risk of progression to EA. These measurements should prove useful in surveillance and management of patients with BE.

96954

IMMUNOPHENOTYPIC ANALYSIS OF BENIGN HUMAN MENINGIOMAS

Marek Sarissky[1], Maria Dolores Tabernero Redondo[2], Ana Belen Espinosa[3], Angel Maillo[4], Jose Maria Sayagues[2], Alberto Orfao[2]

[1]P.J. Safarik University, Kosice, Slovakia, Dept of Pharmacology, Kosice, Slovakia; [2]Universidad de Salamanca, Salamanca, Spain; [3]Centro de Investigacion del Cancer, Salamanca, Spain; [4]Hospital Universitario de Salamanca, Servicio de Neurocirugia, Salamanca, Spain

Introduction: Meningiomas are mostly slow-growing tumours which arise from arachnoidal cells. The large majority of these tumours are benign and can be cured by surgery. However, a proportion of up to 20-25% of all meningiomas has a tendency to recur. Attempts to define markers of recurrence are still inconclusive. In the present work, we sought to immunophenotypically characterize benign human meningioma cells by flow cytometry immunophenotyping. **Methods:** For three-colour flow cytometric analysis of the immunophenotype (DRAQ5 plus two immunophenotypical markers), we used tumour cell suspensions prepared from 22 benign (grade I) meningioma specimens. The cells were tested for expression of Bcl-2, CD38, CD52, Pgp, CD66b, CD39, CD45, Her2/neu, TACE and HLA DR. **Results:** Interestingly, the most frequent and highest positivity was detected for Her2/neu and HLA DR. The expression of CD52 and TACE was lower but was present in nearly all meningiomas. Pgp was expressed in half of the tumours while Bcl-2 and CD38 were detected only sporadicly. We observed no expression of CD39, CD45 and CD66b in meningioma tumor cells. CD45-positive cells were identified as infiltrating leukocytes. No significant differences in immunophenotype were observed in association with age, DNA ploidy status, alterations in chromosomes 17 and 22, and incidence of relapses. In contrast, we observed correlations between immunophenotype and gender, percent of S-phase tumour cells and chromosomal abnormalities in 1p36, chromosome 14 and the sex chromosomes. Female patients expressed significantly less Bcl-2 and CD38 than males. Alterations in chromosomes 1p36 or the sex chromosomes and chromosome 17 were associated with decreased expression of CD52 and Her2/neu, respectively. Interestingly, tumours having more than 1.4% of S-phase cells were virtually devoid of Pgp, Her2/neu and TACE. We also observed mutual positive correlations between the expression of Her2/neu, TACE and Pgp. **Conclusions:** In this work, for the first time immunophenotype of meningioma cells was studied by multiparameter flow cytometry. We observed heterogeneous expression of the selected antigens in different patients and found new associations between expression of cellular proteins and specific clinico-biological disease characteristics.

96640

COMBINING SIMULTANEOUSLY FISH AND IMMUNO-LABELING ON PARAFFIN-EMBEDDED TISSUE SECTIONS FOR THE STUDY OF HER2/NEU: THE DEVELOPMENT OF A NOVEL DIAGNOSTIC APPROACH

Christian Lottner[1], Rudolf Jung[1], Stephan Schwarz[1], Ruth Knuechel[2], Ferdinand Hofstaedter[1], Gero Brockhoff[1]

[1]University of Regensburg, Institute of Pathology, Regensburg, Germany; [2]RWTH Aachen, Institute of Pathology, Aachen, Germany

Background: HER2/neu is a protooncogene that encodes a transmembrane protein within the type I tyrosine kinase receptor family and is overexpressed in 25% to 30% of human breast cancers. The determination of the HER2/neu status in breast carcinomas has become essential for the selection of breast cancer patients for Trastuzumab (Herceptin) therapy. The humanized monoclonal antibody Herceptin is targeted to the HER2/neu receptor oncoprotein. Its efficacy in treating patients with metastatic breast carcinoma is determined by either HER2/neu protein overexpression—immunohistochemistry (IHC)—or gene amplification—fluorescence *in situ* hybridization (FISH). Evaluating the HER2/neu receptor immunohistochemically is supposed to be the most reliable approach to identify patients for Herceptin therapy, as the protein is the therapeutic target. However, a substantial difficulty of IHC is due to the lack of interlaboratory reproducibility and a mainly subjective evaluation of the staining intensity and pattern. In addition, numerous weak overexpressors on IHC testing show no gene amplification as identified by FISH analysis. These cases must be considered false-positives and patients with equivocal HER2/neu state should not be exposed to Herceptin treatment. In contrast to IHC, today's FISH testing is highly accurate and signal quantification is feasible. Aim: In order to increase the accuracy and to improve the reproducibility of the HER2/neu diagnostics we established a novel diagnostic approach based on the simultaneous detection of HER2/neu gene amplification via FISH and correlated protein expression via IHC. **Methods:** The HER2/neu oncogene, located at 17q21, was detected using the PathVysion HER2 DNA Probe Kit (VYSIS). The HER2/neu gene region was visualized with yellow fluorescence; the centromere 17 probe was green fluorescent. The HER2/neu protein expression (red fluorescence) was detected simultaneously using an epifluorescence microscope. Paraffin-embedded breast cancer cell lines were used as a reference for both gene amplification and protein expression. The diagnostic applicability was verified on primary breast cancer tissue sections. **Results:** The simultaneous detection of the HER2/neu receptor protein and gene copy number is reliably feasible in the multiparametric fluorescent approach. The immunohistochemical determination of the HER2/neu receptor status is in concordance with the FDA approved scoring, ranging from 0 to 3+ conventionally applied in the HercepTest (DAKO). With the novel approach gene copy number and protein content can be analyzed in the same cell. **Conclusion:** The combined fluorescent IHC and FISH on the same paraffin-embedded tissue section improves the diagnostic value of HER2/neu compared to the separated applications.

Plenary Session 2: 1045–1230

Measurement Approaches for Systems Biology

92689

MEASURING ENZYME ACTIVATION IN SINGLE CELLS

Nancy L. Allbritton[1]

[1]University of California, Irvine, Physiology & Biophysics, College of Medicine, Irvine, California

We have developed a novel assay system, the laser-micropipet system (LMS) to quantitatively measure the activation of multiple enzymes in the same single cell, portion of a cell, or group of cells. The method possesses an excellent temporal resolution (<33 ms) and sensitivity (zeptomoles). This strategy can be used to measure the activation of multiple different enzymes in a single cell and can be utilized with primary cells from patient samples.

92168

METABOLITE IMAGING USING FRET-BASED NANOSENSORS

Wolf B. Frommer[1], Marcus Fehr[1], Sylvie Lalonde[2], Ida Lager[1]

[1]Carnegie Institution of Washington, Plant Biology, Stanford, Plant Biology, Stanford, California; [2]University of Tübingen, Plant Physiology, Tübingen, Germany

A set of tools was developed for *in vivo* imaging of metabolites including maltose, glucose, ribiose and others. The nanosensors are based on bacterial periplasmic binding proteins coupled to two fluorescent proteins. Upon binding of their substrate, the binding proteins undergo a conformational change that can be detected by a change in FRET. The properties of the binding proteins were adjusted for measuring metabolites in living cells. Furthermore, signal sequences were added to target the nanosensors to subcellular compartments. Using FRET miscroscopy, dynamic changes in metabolites levels were measured in yeast, animal and plant cells with subcellular resolution. The myriad periplamic binding protein homologs in bacteria covers a wide spectrum of substrates permitting us to generate a box of tools for many important metabolites. The nanosensor-expressing cells can be used for pharmacogenomics, to study metabolism and transport and to identify and characterize physiological questions that were so far not amenable to *in vivo* analysis.

92637

MODELLING ANTICANCER DRUG ACTION IN REAL AND VIRTUAL TUMOUR CELLS

Paul J. Smith[1], Rachel J. Errington[1]

[1]University of Wales College of Medicine, Cardiff, Wales, United Kingdom

A major aim of systems biology is to gain an understanding of system dynamics for the purpose of prediction and modification—an approach that offers enormous potential for basic research and drug discovery. There is a demand for informative genetic, cytometric, pharmacological and mathematical analyses in modelling the systematic perturbations of tumour cell systems by cell cycle-targeting anticancer drugs. Aspects addressed in the presentation are: i) the prediction of single cell drug pharmacokinetics in fully-identifiable models, and ii) the accurate monitoring of the integrated responses to drug action at the level of genes, proteins and phenotypes using GFP-tagged stealth reporters, single cell-tracking flow cytometry and time-lapse imaging.

92618

ROLE OF LIPID RAFTS IN ORGANIZATION OF RECEPTOR COMPLEXES

János Szöllõsi[1], Peter Nagy[1], Maria Magdalena Tufeanu[1], György Vereb[1]
[1]University of Debrecen, Department of Biophysics and Cell Biology, Debrecen, Hungary

Lipid microdomains enriched in glycosphingolipids (GSL) and cholesterol, also named as "lipid rafts", may form in the plasma membrane. Definition of these lipid rafts highly depends upon the techniques (biochemical or biophysical) applied to detect them. According to the present status, GSLs form small, ordered microdomains, (so called "liquid ordered phase") which are further stabilized by cholesterol. Existence of such domains results in lateral phase separation which may promote compartmentation of raft-associated proteins and their spatial segregation from proteins excluded from rats. These properties suggest that lipid rafts existing in the plasma membrane may be critically important players in signal transductions processes by bringing together receptors with theirs signal transmitting/converting/amplifying molecules wile temporarily excluding others (e.g. negative regulator proteins) from these compartments. Biophysical techniques applied for detection and characterization of raft domains comprise atomic force microscopy, scanning near-field microscopy, single particle tracking, single dye tracing, optical trapping, confocal microscopy and various forms of fluorescence resonance energy transfer methods. Combined approaches can reveal biological and physicochemical factors controlling raft dynamics. Lipid rafts have crucial role in organizing receptor complexes and affecting their signal transduction processes, as an example the effect of rafts on signal transduction of tyrosine kinase receptors (e.g. epidermal growth factor receptor, ErbB2 and ErbB3) will be discussed in more detail. Clusters of ErbB2 colocalized with lipid rafts identified by the GM1-binding B subunit of cholera toxin. Pixel-by-pixel analysis of fluorescence resonance energy transfer between labeled antibodies indicated that the homoassociation (homodimerization) of ErbB2 was inversely proportional to the density of the raft-specific lipid GM1. Crosslinking lipid rafts with the B subunit of cholera toxin caused dissociation of the rafts and ErbB2 clusters, an effect that was independent of the cytoskeletal anchoring of ErbB2. Crosslinking also decreased ErbB2-ErbB3 heteroassociation and the EGF- and heregulin-induced tyrosine phosphorylation of Shc. When cells were treated with the anti-ErbB2 monoclonal antibody 4D5 (parent murine version of Trastuzumab used in the immunotherapy of breast cancer), internalization of the antibody was inhibited by crosslinking of lipid rafts, but the antiproliferative activity of 4D5 was retained and even enhanced. We conclude that local densities of ErbB2 and ErbB3, as well as the lipid environment profoundly influence the association properties and biological function of ErbB2.

1230–1400
Poster Presentations
(See abstracts beginning on page 111)

1615–1800
ISAC Business Meeting

Wednesday, 26 May

0800–0945

Parallel Session 6: Image Cytometry II

Chair: Laszlo Matyus

96967

THE SONIFICATION OF CYTOLOGIC IMAGES

Konradin Metze[1], Randall Luis Adam[1], Neucimar Jerônimo Leite[2]
[1]State University of Campinas (UNICAMP), Pathology, Campinas-SP, Brazil; [2]State University of Campinas (UNICAMP), Institute of Computing, Campinas, São Paulo, Brazil

Texture analysis is mainly based on mathematical principles which are sometimes rather difficult to transmit to students. Therefore we looked for a more intuitive way of teaching texture analysis applying principles of synesthesia. We tried to create various ways of sonifcations equivalent to different techniques of texture analysis. Two main forms of sonification can be differentiated and will be explained using cell nuclei of routine cytologic preparations: 1. Sound equivalent to 1D gray level signals obtained by peel-off scanning: This method consits of a transformation of the original digitalized 2-D gray-scale image into a 1-D signal (of about 5000 to 8000 pixels) by means of a spiral scan algorithm beginning at the periphery and finishing in the central part. This 1D-diagram can be transformed in sound by two different ways: 1 a .The gray levels represent the acoustic pressure while performing at high speed (8000 pixels/s). Variations of object size and texture create different sounds. 1 b. Frequencies are attributed to each pixel by multiplying its gray value with a factor while performing at low speed (about 2– 8 pixels/s). 2. Sound equivalent to the Fast Fourier (FFT)Image : Gray level transformed images were FFT-transformed and regional maxima extracted by geodesic reconstruction. In order to get the time dimension, a vector was defined which moves, like a pointer of a clock, from the zero to the six hour position of the FFT image. The sound is played when the vector strikes a pixel. Frequency is defined by the distance of the pixel from the center of the FFT image and the amplitude is equivalent to the gray value (moment of inertia). Thus each microscopic image is represented by a short sound clip. Normal bronchial mucosa and adenocarcinoma cells are easily discernible, because chromatin condensations in carcinoma cells create a spectrum with lower frequencies and high amplitudes both in the FFT image and in the sound. In summary different types of sound can be created from an image equivalent to the kind of texture analysis performed. The sonification of the chromatin texture can be regarded as an equivalent sound of the nucleus, with complete reproducibility. This method can be regarded as a synesthetic way for understanding both principles of texture analysis and microscopic structures, since the auditory system can be used for pattern recognition. Finally an interface between science and art is created, which can contribute to humanization of technology. Supported by FAPESP, CNPq.

96578

DOUBLE-SIDED FLUORESCENCE ENERGY TRANSFER: A NEW METHOD FOR THE *IN SITU* EXAMINATION OF THE ASSOCIATIONS OF ERBB RECEPTORS ON THE SURFACE OF TUMOR CELLS

Zsolt Fazekas[1], Miklós Petrás[1], György Vereb[1], János Szöllõsi[1]

[1]University of Debrecen, Medical and Health Science Center, Biophysics and Cell Biology, Debrecen, Hungary

Background: Members of the ErbB receptor family can form various homo- and heterodimers with integrins and each other. The ErbB2 protein plays an important role in the development breast cancers and other malignancies. The trigger of the signal transduction set off by the overexpressed ErbB2 in those tumors can often be the homo- and heteroassociation of ErbB2-ErbB2 and ErbB2-ErbB1 molecules respectively, as well as other ErbB heterooligomers. Signal transduction can also be modulated by other molecules—for example integrins—in the proximity of activated ErbB2 proteins. To find out the composition of such multi-molecular complexes, we have set out to implement a microscope-based FRET (Fluorescence Resonance Energy Transfer) method that gives information about the nm-level proximity of three molecules of interest in the same cell. **Methods:** Labeling of ErbB2 molecules on gastric and breast cancer cell lines (N-87, SKBR-3) was performed with 4D5 antibodies conjugated with Cy3 and Cy5 dyes. β1 integrin molecules of the same cells were marked with FITC-conjugated CD29 antibodies. In this three-colour system, the antibody labeled by the dye Cy3 serves as a donor to the Cy5 labeled antibodies and as an acceptor to the one labeled by FITC. The FRET efficiency characterising the homo- and heteroassociations of ErbB2 molecules can be determined by means of acceptor- and donor photobleaching techniques in a confocal laser scanning microscope. The method was tested on a model system comprising ErbB2 molecules labeled on three known epitopes with Cy5-4D5, Cy3-2C4 and FITC-7C2 antibodies. **Results:** In the case of the dye-pair Cy3-Cy5, the FRET efficiency can be assessed by using the acceptor photobleaching technique, while in the case of the dye pair FITC-Cy3 it can be evaluated by the use of the donor photobleaching procedure. In the model system the spatial distribution of the two epitope-pairs participating in the energy transfer process coincided with each other according to the measured intramolecular energy transfer efficiencies. The method was successfully applied to visualize the association of β1-integrin and ErbB2 together with the ErbB2 homoassociation on N87 gastric carcinoma cells. The energy transfer images showed low levels of energy transfer between β1 integrin and ErbB2 on the sites of high ErbB2 homoassociation and vice versa; sites displaying high β1 integrin-ErbB2 association showed low ErbB2 homotransfer. **Conclusion:** Double-sided fluorescence energy transfer is applicable to the examination of the concurrent spatial proximity of three molecules of interest on a pixel by pixel basis, as demonstrated on the ErbB2 three epitope model system and also on the ErbB2-ErbB2- β1 integrin system.

97130

THE USE OF POSITIONAL BIOSENSORS TO INVESTIGATE MECHANISMS OF CELLULAR APOPTOSIS

Megan Weiss[1], Amy M. Peters[1], Jeffrey R. Haskins[1]

[1]Cellomics, Inc., Assay Development, Pittsburgh, Pennsylvania

Apoptosis is integral to many normal developmental processes, but can lead to premature cell death when triggered by xenobiotics. There are several key criteria for determining whether a cell is undergoing apoptosis, including distinct changes in cellular morphology and alterations in specific biochemical and molecular markers. The general patterns of apoptotic signals are comparable, but mechanistic drivers can vary significantly depending on cell type and causative agent. Among key proteases that can trigger apoptosis are the caspases. We have developed two positional biosensors for *in vitro* monitoring of intracellular caspase 3 and 8 activity in living or fixed cells. Both biosensor designs are based on measuring the intracellular redistribution of fluorescent reporters from an initial subcellular compartment to a targeted compartment upon activation. These biosensors are composed of recombinant polypeptides containing several key components, including reporting, sensing and targeting elements. Following proteolytic cleavage of the sensing element by the activated caspase, the targeting and reporting elements are driven by a nuclear localization signal to the nucleus where they are easily detected using quantitative image analysis. To demonstrate applicability of this approach, a 240 compound library of known toxins was screened against HeLa cells stably expressing either the caspase 3 or 8 biosensor at concentrations of 1, 10 or 50 μM for up to 4 hours. By adding additional fluorescent probes for detecting changes in nuclear morphology, mitochondrial transmembrane potential and membrane permeability, further details were elucidated that allowed differentiation of apoptotic mechanisms. Individual cellular responses were quantitated using automated fluorescence microcopy. Results indicated the value of positional biosensors as a new generation of fluorescent protein reagents that function as temporal and spatial reporters of cellular processes *in vitro*.

95717

EASYCOUNT, A SIMPLE CELL ENUMERATION SYSTEM

Arjan G.J. Tibbe[1], Xiao Li[2], Alexander Van Der Kooi[1], Maria Koutroulis[3], Danesh Gohel[3], Erik Droog[2], Jan Greve[2], Leon W.M.M. Terstappen[3]

[1]Immunicon Europe Inc., Enschede, Netherlands; [2]University of Twente, Applied Physics / Biophysical Techniques, Enschede, Netherlands; [3]Immunicon Corporation, Huntingdon Valley, Pennsylvania

Introduction: We have developed EasyCount, a simple, whole blood, absolute cell counting device. The instrument is based on fluorescent labeling of nucleated cells and immuno-magnetic selection of cells of interest from whole blood to the optical transparent upper surface of an analysis chamber. Two Light Emitting Diodes (LED's) are used to excite the DNA / RNA dye Acridine Orange and a low magnification fluorescence image is captured by a "Smart Cam". This is a combination of a CCD and hardware to perform simple image analysis. The combination of cartridge and magnetic field are constructed such that the number of cells present at the upper surface can directly be converted to the number of cells per unit volume. The number of cells present in the image is determined by the Smart Cam and this number is converted to the number of cells per unit volume. The whole system runs on a 12 volt rechargeable battery and measures only 20 x 20 x 20 cm. **Results:** Blood was collected from 40 donors using EDTA as an anticoagulant. Absolute CD3 (T-lymphocytes), CD4 (monocytes / T-lymphocytes), CD19 (B-lymphocytes) and CD45 (leukocytes) count were obtained with EasyCount and by flow cytometry (TruCount, BDBiosciences). For the EasyCount immuno-magnetic particles labeled with antibodies against CD3, CD4, CD19 and CD45 antigens were used. Comparison with TruCount provided correlation coefficients (R2) of 0.97, 0.85, 0.95 and 0.91 and slopes of 0.9, 1.3, 1.1 and 0.9 respectively. **Discussion:** The correlation between TruCount and EasyCount is excellent for clear distinctive cell populations (CD3, CD19 and CD45). The simplicity of the system with a minimum of sample handling makes the system a suitable candidate for cell enumeration in poor resource settings. Capture of monocytes that express CD4 at a lower density gave rise to a lower correlation coefficient for CD4 T-lymphocytes as immuno-magnetically selected monocytes are counted on basis of their DNA fluorescence. Especially for T-lymphocyte counts below 300/μl, the presence of monocytes becomes significant, resulting in a poor correlation. For EasyCount to become a suitable candidate for CD4 T-cell enumeration in poor resource settings the monocytes will have to be eliminated from the CD4 count and various approaches are being investigated to accomplish that goal.

96529

CHARACTERISTICS AND APPLICATIONS OF IMAGESTREAM™ MULTISPECTRAL IMAGING FLOW CYTOMETRY

David Basiji[1], William E. Ortyn[1], Thaddeus C. George[1], James Brawley[1], Brian E. Hall[1], Philip Morrissey[1]

[1]Amnis Corporation, Seattle, Washington

The ImageStream 100 (IS100) is a high throughput multispectral imaging flow cytometer that combines the morphological capabilities of multiple forms of microscopy with the sample handling and quantitative power of flow cytometry. The IS100 produces up to six simultaneous high resolution images of each cell in flow at rates greater then 100 cells per second. Typical assays employ brightfield, darkfield, and up to four fluorescence images in different spectral bands. The system's broadband UV/visible excitation source and filter wheel arrangement, combined with a 488nm solid state laser, enables the use of a wide variety of analytes common to both flow cytometry and fluorescence microscopy. Post-acquisition data analysis with the IDEAS™ software package allows for automated spectral compensation and detailed quantitation of over 200 parameters for each cell. This comprehensive feature set gives the user tremendous power in distinguishing unique cell subsets based on fluorescence intensity and spatial distribution, as well as darkfield and brightfield morphometry. In addition to performing standard flow cytometric assays with enhanced results, Amnis has demonstrated the utility of the platform with a number of applications, including:

- enhanced apoptosis analysis incorporating darkfield (light scatter) morphometry, nuclear morphology, cell size, and caspase 3 expression
- nuclear translocation of cytoplasmic NFkB after ligand-mediated activation by TNF
- FISH in suspension with automated FISH spot enumeration
- cell classification by combined immunophenotyping and morphometry, as well as the analysis of probe co-localization
- cell cycle analysis using DNA content histograms to identify Go/G1, S and G2/M phases of the cell cycle, with mitotic cells identified and visualized based on detection of condensed chromosomes
- hematologic classification using a combination of fluorescent and chromogenic stains

Data illustrating the use of the ImageStream 100 platform in various applications will be presented. Development of ImageStream technology was partially supported by NIH grants 9 R44 CA01798-02 and 1 R43 GM58956-01.

Parallel Session 6: Data Analysis

Chair: Günter K. Valet

97420

DATA PATTERN ANALYSIS: A NON STATISTICAL BIOINFORMATIC STRATEGY FOR PREDICTIVE MEDICINE BY CYTOMICS

Günter K. Valet[1]

[1]Max-Planck-Institute for Biochemistry, Cell Biochemistry Group, Martinsried, Germany

Background: Predictive medicine by cytomics addresses the individualized prediction of patient's future disease course from multiparametric molecular measurements in cellular systems (cytomes) after exhaustive bioinformatic knowledge extraction. This promotes individualized patient therapy in stratified patient groups. **Material and Methods:** Data pattern analysis (CLASSIF1, http://www.biochem.mpg.de/valet/classif1.html) represents a new, fast computing, non statistical bioinformatic strategy for individualized predictions in medicine. An essential feature of the algorithm consists in the optimization of the diagonal sum of a confusion matrix between clinical and predicted patient future during the learning phase by iteratively recording classification improvement or deterioration upon temporary removal of single parameters or parameter pairs in all permutations. This is done following transformation of numerical parameter values into triple matrix characters: (-) = diminished, (0) = unchanged or (+) = increased according to their position below, in between or above the lower and upper percentile thresholds of the respective parameter value distribution in the reference patient group. Predictive disease classification masks are obtained at the end of the learning phase following removal of all parameters whose presence did not improve the classification (non parametric data sieving). The masks typically contain between 5 and 30 parameters. **Results:** Data pattern classification from up to 100.000 data columns is successfully used for individualized clinical predictions or diagnostic classifications from flow cytometric list mode, array data from Lymphochips, Affymetrix or proteomics chips or multiplex bead arrays, from spreadsheets (Excel), clinical or clinical chemistry data but also from high throughput image analysis parameter databases. Classifications are obtained as highest positional coincidence of a patient classification mask with any one of the learned disease classification masks. Random occurrence of data patterns is negligible and for example < 0.0017% or 0.0457% for 10 and 7 parameter patterns. The frequently observed partial deviation of patient classification masks from the selected disease classification mask indicates genotype and exposure influences. They represent a stimulating new approach to the understanding of disease formation on variable genotypic and exposure backgrounds. **Conclusion:** Algorithmic data pattern analysis provides standardized, interlaboratory exchangeable predictive classifiers with selected discriminatory parameters being useful for a bottom-up reverse engineering like investigation of molecular pathways in complex human diseases.

96811

"LOGICLE" FUNCTIONS PROVIDE IMPROVED DISPLAYS OF FACS DATA AND AVOID THE DECEPTIVE EFFECTS OF LOG SCALING FOR LOW SIGNALS

David Parks[1], Mario Roederer[2], Wayne A. Moore[3]

[1]Herzenberg Lab, Stanford, California; [2]National Institutes of Health, NIAID, Vaccine Research Center, Bethesda, Maryland; [3]Stanford University, Genetics, Stanford, California

We have developed a new data visualization method that scales the axes on histograms and two-dimensional contour (or dot) plots to provide good visualization of signals from all cells, including those that have minimal fluorescence values and are poorly represented with traditional logarithmic axes. This "Logicle" visualization method provides superior representations of compensated data and makes correctly compensated data look correct. It eliminates "picket fencing" and anomalous peaks introduced by log scaling. It should also make flow cytometry data more suitable for automated cluster analysis. Properly compensated data values for a cell population that is negative for a particular dye should be distributed symmetrically around a low value representing the autofluorescence of the cells in that dye dimension. Logarithmic displays, however, cannot accommodate zero or negative values and tend to show a peak above the actual mean of the population and pileup on the baseline. The "Logicle" method addresses these problems by plotting data on axes that are asymptotically linear in the region just above and below zero and asymptotically logarithmic at higher (positive and negative) values. Note that "Logicle" visualization does not change the data values or any statisitcs computed from them. "Logicle" scaling is a particular generalization of the hyperbolic sine function (sinh(x) = (e^x–e^-x)/2) in which a general biexponential function is constrained in ways that are appropriate for plotting cytometric data. "Logicle" functions thus have more adjustable variables than the hyperbolic sine but not as many as a fully general biexponential. To obtain an optimized display for a particular data set, a "Logicle" function must be chosen that provides sufficient linearization to suppress log-type artifacts in the cell populations. We have developed methods for selecting an appropriate "Logicle" scale automatically. "Logicle" displays with automatic scale selection are available in FlowJo software versions 4.3 and later.

97055

CLASSIFICATION OF CYTOMETRY DATA USING PRINCIPAL COMPONENT ANALYSIS

Murugesan Venkatapathi[1], Bartek Rajwa[2], Gérald J. Gregori[3], E. Daniel Hirleman[1], J. Paul Robinson[4]

[1]Purdue University, Mechanical Engineering, Engineering, West Lafayette, Indiana; [2]Purdue University, Basic Medical Sciences, Veterinary Medicine, West Lafayette, Indiana; [3]Purdue University, Biological Sciences, West Lafayette, Indiana; [4]Purdue University Cytometry Laboratories, Basic Medical Sciences & Biomedical Engineering, Purdue University, West Lafayette, Indiana

With the increase in fluorescent probes used and advances in instrumentation, the number of parameters measured in cytometric analysis has increased from a few to many. In order to study such cytometric data, typical scatter plots, while not yet obsolete, are not adequate to view the increasing the number of parameters and corresponding dimensionality of the parametric space. Data are usually viewed across three parameters because of our limited dimensionality of imagination (i.e.) 3D. Reducing the dimension of this parametric space to three by arbitrary parameter reduction does not facilitate effective discrimination of the constituent populations of the analyzed samples. Hence a more intelligent and consistent reduction of the dimension that takes into account the variations across all parameters is required. We demonstrate in this paper the use of principal component analysis of the cytometric data to determine the direction of maximum variation in the parametric space. Once the principal direction is computed in terms of all parameters, the three 'principal' components that contribute to the maximum variation in the sample are chosen. By then using a regular scatter plot across these three new parameters, there is a significantly improved ability to identify the populations within the sample. In addition, since the contribution of all the original parameters to these three new principal parameters is known, it does not reduce our ability to associate the significance of each original parameter with the populations. The consequence of such capability is that we can now identify biological processes that require multiple fluorophores simultaneously in action. In order to evaluate the utility of this analytic technique, a series of cytometric data sets were reduced to three principal parameters. The resulting distribution of particles identified more distinct populations that were not identifiable using any combination of three original parameters.

95921

RESEARCH DATA MANAGEMENT SYSTEM—AN OPEN SOURCE WEB-BASED APPROACH TO MANAGING CYTOMETRY DATA IN THE RESEARCH AND CLINICAL LABORATORIES

Martin Bigos[1], Antony Chiang[2], Larry Roberts[2], Elizabeth Sinclair[3], Barry Bredt[4], John Bennet[3], C. Poong[3], William Hyun[5]

[1]Gladstone Institute of Virology and Immunology, San Francisco, California; [2]BioTrue, Inc., San Francisco, California; [3] San Francisco General Hospital, University of California, San Francisco, California; [4]UCSF-GCRC, Gladstone CFAR, San Francisco, California; [5]University of California, Cancer Center, San Francisco, California

The managing of cytometric data, both for flow and imaging, is a challenge for many laboratories. The raw data is distributed across file servers, burned on CDs, and resides on desktops. Analyses based on these data usually reside on desktops and the sharing of data is usually done via large attachments to emails. We describe a web-based Research Data Management System (RDMS) which allows users to view their data by laboratories, projects (or users) and runs. After collection on any cytometer, data is uploaded to the RDMS through a drop-box interface. Using a web browser running on any platform, the end user can connect to the RDMS to add further annotations, download data for analysis, or give access permissions. The results of an analysis, as well as any other desired files, can be uploaded and stored as attachments to the particular project or run. We also describe further extensions to accommodate the specific needs of translational clinical research, which include uploading analyzed results from flow cytomotry data and viewing such results through a modifiable interface with search capabilities, matching assays (runs) with samples received, tracking status of dara processing and password controlled release of verified results to Investigators. The RDMS is based on open source technology, so commercialization costs will be significantly lower compared to other systems, and should be affordable to most academic and clinical research environments.

96535

TECHNIQUES TO COMPRESS THE SCALE OF FLOW CYTOMETRY DATA: BENEFITS, ARTIFACTS AND SOLUTIONS

James C.S. Wood[1]

[1]Consultant, Galax, Virginia

Logarithmic scaling of flow cytometry histograms has become a routine method for displaying and analyzing data when it is spread over a very wide data range, typically on the order of 3 or 4 decades. The benefits of logarithmic scaling of flow cytometry histogram data are well known. Researchers, however, are less familiar with the artifacts introduced by the logarithmic scaling. Logarithmic scaling tends to skew a normally distributed population toward the lower channels. This is most dramatic for the distributions in the lower decades of the histogram data. In this part of the histogram the observed mode of the distribution is far to the right of the mean. Because the mode is so far to the right there is a tendency to not include enough of the lower values of the distribution to accurately characterize the distribution. By varying the amount of compression, it is possible to see how the artifacts arise. It is possible to find the amount of compression at which the artifacts disappear. Increasing the compression causes the artifacts to become more pronounced. By analyzing data at different levels of compression, it is possible not only to become aware of the potential artifacts and their impact on analysis, but also to alter accordingly the statistical analysis to more accurately determine the distribution statistics.

Parallel Session 6: Inflammation & Autoimmunity

Chair: TBD

97294

FUNCTIONAL AND PHENOTYPIC CHARACTERIZATION OF ANERGIC B CELLS CIRCULATING IN THE PERIPHERY OF ACTIVE SLE PATIENTS

Randy Thomas Fischer[1], Rebecca Slota[1], Nancy S. Longo[1], Hae Won Sohn[2], Cheryl Yarboro[1], Gabor G. Illei[1], Susan Pierce[2], Peter E. Lipsky[3], Amrie C. Grammer[1]

[1]National Institutes of Health, National Institute of Arthritis and Musculoskeletal and Skin, Bethesda, Maryland; [2]National Institutes of Health, NAIAD, Rockville, Maryland; [3]National Institutes of Health, NIAMS, Bethesda, Maryland

A CD19lowIgD+ B cell population that was observed in the periphery of Systemic Lupus Erythematosus (SLE) patients, but not in non-autoimmune normal individuals, was examined to determine its functional and phenotypic characteristics. CD19lowIgD+ cells are small and in G0/G1 with very few cells in S/G2/M or undergoing apoptosis. In contrast, some of the CD19highIgD+ B cells were cycling or undergoing spontaneous apoptosis. In addition the CD19highIgD+ population expresses activation antigens, including CD69 and CD154, whereas CD19lowIgD+ B cells from active SLE patients do not express

activation antigens. CD19lowIgD+ cells remained resting even in short-term culture in medium without additional stimulation. Whereas CD19lowIgD- cells in the periphery of SLE patients are intracytoplasmic (IC) Ig+ plasma cells, CD19lowIgD+ cells are IC Ig-. Furthermore, fewer CD19lowIgD+ cells express CD38 when compared to CD19highIgD+ cells and those that do express CD38 do so at a lower density than CD19highIgD+ cells. Although similar percentages of CD19lowIgD+ cells and CD19highIgD+ cells express CD5 and CD27, the MFI of CD5 expressed on the surface of CD19lowIgD+ cells was significantly lower than that expressed on CD19highIgD+ cells. Whereas CD19highIgD+ cells were rescued from apoptosis and driven into S/G2/M following stimulation through sIg with a low amount of anti-IgM Fab'2 Ab or rCD154, CD19lowIgD+ cells required 100-fold more anti-IgM Fab'2 Ab or rCD154 to rescue them from apoptosis and drive them into cell cycle. Finally, sIgM was spontaneously in Raft or cytoskeletal associated membrane fractions of CD19lowIgD+ cells at a higher level compared to sIgM of CD19highIgD+ cells, suggesting that CD19lowIgD+ cells had recently been stimulated *in vivo* through the sIgM complex. Together, these results indicate that CD19lowIgD+ cells in the periphery of SLE patients may be a functionally anergic population of *in vivo* stimulated B cells that disappear when the disease becomes quiescent.

96955

ENUMERATION OF CSFE LABELLED LYMPHOCYTES ALLOWS THE STUDY OF BOTH PROAPOPTOTIC AND ANTIAPOPTOTIC EFFECTS OF IL-2

Alfredo Prieto[1], David Diaz[1], Hugo Barcenilla[2], Guillermo Revilla[1], Jorge Monserrat[1], Paz Prieto[1], Antonio De La Hera[1], Alberto Orfao[3], Melchor Álvarez-Mon[4]

[1]Alcala University, Immune System Diseases and Oncology Laboratory, CNB-CSIC R&D Associated Unit, Alcala de Henares, Madrid, Spain; [2]Alcala University, Alcala de Henares, Madrid, Spain; [3]Universidad de Salamanca, Salamanca, Spain; [4]University Hospital "Príncipe de Asturias", Immune System Diseases and Oncology Service, Alcala de Henares, Madrid, Spain

Background: The action of IL-2 on its receptors on T cells could lead T cells in different stages to outcomes so opposite as cell growth and apoptosis. These outcomes can be studied by the combination of methods of cell enumeration with cell tracking. **Methods:** We enumerated CSFE labelled T cells from phenotypically defined subsets, to monitorize the process of cell decision between growth and apoptosis and to study how exogenous IL-2 (eIL-2) affects such cell decisions subsequent to mitogen stimulation. We also studied how neutralizing antibodies against IL-2 can revert the processes induced by the action on IL-2 on cell receptors. **Results:** Survival rate measurements demonstrate that during the three first days of culture eIL-2 induces significant apoptosis which was observed in both resting cells and undivided blasts from CD3+CD4+ and CD3+CD8+ subsets. On the other side we observed that eIL-2 increased the number of T cells after 7 days of culture. We also performed studies on IL-2R expression and we found that expression of CD25 precedes both AICD and proliferation induced by mitogenic stimulation CD25 MFI of death T blasts was always higher than of viable T blasts. At 3 day, eIL-2 did not affect to CD25 MFI of CD8+ T blasts but increased two folds the CD25 MFI of CD4+ T blasts. CD25 MFI of CD8+ T viable blasts decreased 70% when blocking anti-IL-2 antibodies were added, while in the death blasts decreased 28%. In CD4+ T blasts the decrease was of 48% in viable blasts and only 7% in death blast. CD25 mean fluorescence intensity (MFI) of mitogen stimulated undivided CD8+ T blasts was 50 folds higher than their expression before stimulation while for undivided CD4+ T cells the MFI increment was only 15 folds. CD25 expression on CD8+ T cells decreased progressively along successive cell divisions, instead CD25 expression on CD4+ T cells remained constant until the fifth division. **Conclusions:** We have found that eIL-2 has opposed effects on mature resting T lymphocytes activated by mitogens before their first division and after it. Firstly it induces apoptosis on them and inhibits their transformation in blasts while later in the blasts inhibits their apoptosis decreasing the proportion of apoptotic cells and induces their growth increasing the number of divisions of the proliferating T cells. eIL-2 also presents different effects in the modulation of the expression of CD25 in both CD4 and CD8 stimulated T lymphocytes.

96452

INVOLVEMENT OF THE IMMUNE SYSTEM IN PROTEIN LOSING-ENTEROPATHY (PLE) OF CHILDREN WITH UNIVENTRICULAR HEART

Attila Tárnok[1], Dominik Lenz[1], Peter Schneider[1]

[1]University of Leipzig, Leipzig, Saxony, Germany

PLE is a fatal complication in children with univentricular and a Fontan type circulation. It is characterized by dramatic enteric protein loss. Its pathogenesis is not fully understood. In order to investigate the connection of PLE and immune system 35 patients who received a Fontan-type circulation were analyzed over a period of up to 7 years. One patient developed PLE about 9 months post-operatively. This case is the first where immunological changes were closely followed and documented before and after PLE. Her immunophenotype was compared to that of seven patients with a manifest PLE after Fontan. Acute and long standing PLE. At PLE onset in 7/8 patients had an acute inflammatory response, accompanied by acute infections mainly of gastric origin. The composition of cellular and humoral immune system changed dramatically with the selective loss of T-helper cells. Residual Th cells were memory cells and highly T-cell receptor (TCR)g,d positive (up to 40% of all T cells; PLE free <10%). TCRg,d cells are the major population of the gastric mucosal defense line. The normally very rare population of double negative T-cells (DNT: TCRa,b+CD3+4-8-), associated with autoimmune disease, made up to 15% of all T-cells. PLE and autoimmunity Changes after Fontan PLE were in agreement with Systemic Lupus erythematosus and/or celiac disease: decreased T-helper cell count, increased HLA-DR and CD45RA expression on T-cells and increased serum TNFa;, interleukin- (IL-)10, IL8, and C3d; decreased T4:T8 ratio; increase of serum IL2Ra. These similarities might indicate that Fontan PLE is associated with autoreactivity or is even an autoimmune response. Concurrently, 2/8 of the PLE patients had antibodies binding selectively to T-helper cells and 2/8 against myocardial structures (quantified by LSC). Predictive Medicine by Cytomics for PLE Increased systemic pressure is a risk factor for PLE. But also immunological differences are apparent between Fontan patients prior to PLE onset and patients without detectable PLE signs. The most discriminatory parameters between the three patient groups were increased NK and CD8+TCRab+, but decreased CD8+TCRg,d+ cell counts including L-selectin, IgE and Ca2+. Based on these data a predictor for PLE risk patients was constructed. Conclusion. PLE after Fontan surgery may be the common endpoint of multiple pathophysiological pathways. Infection could be an additional stimulus and could explain why PLE occurs with a very heterogeneous time delay after Fontan surgery. The autoimmunity observation and the predisposition hypothesis may explain why only a sub-population of the Fontan patients will develop PLE. Support: Herzkind eV

97003

DOSAGE OF CYTOKINES IN SEPSIS BY CYTOMETRIC BEAD ARRAY

Cristina Caraion[1], Claude Lambert[2], Christian Genin[1]

[1]Univ Hospital Saint Etienne, France, Immunology Lab, Saint Etienne, France; [2]Association Française Cytométrie, Saint Etienne, France

Sepsis, a dramatic event in intensive cares, is mediated by massive release of cytokines such as IL-1, IL-8 and TNF. Regulatory cytokines such as IL-6, IL-10 may have paradoxical effect by. Biological measuring of these cytokines should allow to monitor the pathologic process and status (susceptibility, gravity, progression) but the test must be precise, reproducible, cost effective and rapid response (i.e. : 8 hours). The aim of that study was to validate the cytometric bead array technic in the context of daily routine constrains for the monitoring of sep-

sis. **Materials and Methods:** 30 patients from intensive care unit were tested on CBA and compared with classical methods. Among them, 26 patients had raised serum procalcitonin (from 0.84 to 184), a marker of bacterial infection. The sera were frozen within 4 hours and tested within the same day in all methods. IL-6, IL-8, IL-1β, TNFα were measured by chemoluminescence method (Immulite DPC SAS). IL-10 and IL-12 p40 were tested using ELISA method (OptEIA, Pharmingen). Soluble TNFα receptor type 1 was analyzed using Quantikine R&D Systems. FCM analysis was performed using the BD Cytometric Bead Array (CBA) test for IL-1β, IL-6, IL-8, TNFα, IL-10 and IL-12. **Results:** The analysis was easily to settle in a routine lab with nice standard curves. The linear part of the curve was observed from 20 to 5000 ng/L for all cytokines tested except IL-1 (80-5000 ng/L). Most of the cytokines could be detected in the samples IL-1 : 0-484 ng/L; IL-8 : 10-5000; TNF : 0-265; IL-6 : 0-5000 and IL-10 : 0-5000 except IL-12 p70 that was never detected. The sample was out of the range in 5 and 4 patients for IL-6 and IL-8 dosages. The repeatability was correct for IL-8 (coefficient of variation) 4.6 to 5.3%; TNF : 4.1-19.8%; IL-6 : 2.1-5.5% and IL-10 : 5.2-9.1% but not for IL-1 : 6.1-19.8%. Reproducibility was also very good on two different dosages of 10 samples. The results were highly correlated to the classical results except. The results and technical point are discussed. **Conclusion:** CBA test was judged as a very convenient multiparametric, quantitative test, highly correlated with our usual techniques (Immulite ELISA) for most of parameters, being performed in 440 min and making CBA a unique method for a quick extended answer in clinical practice.

96377

PREDICTIVE MEDICINE: TOWARDS INDIVIDUALIZED THERAPY IN SYSTEMIC LUPUS ERYTHEMATOSUS (SLE)

Günter K. Valet[1], Annett M. Jacobi[2], Thomas Dörner[3]

[1]Max-Planck-Institute for Biochemistry, Martinsried, Germany; [2]Charité Hospital, Rheumatology & Clinical Immunology, Humboldt University, Berlin, Germany; [3]Charité Hospital, Rheumatology & Clinical Immunology, Berlin, Germany

Background: A substantial number of SLE patients benefit from the various available therapeutic options. Some suffer, however, from side effects or therapy resistance. The goal of this study was to determine whether therapy specific patterns of cellular, clinical or laboratory parameters exist which are useful for the pretherapeutic identification of susceptibility or resistance to therapy. This would permit the development of case adapted individualized therapies. **Material and Methods:** 11 flow cytometric, 15 clinical and clinical chemistry together with 11 serological parameters from 44 SLE patients were classified by a data sieving algorithm (http://www.biochem.mpg.de/valet/classif1.html, cytomics in predictive medicine). The algorithm selects the most discriminatory parameter patterns in an iterative way to pretherapeutically distinguish between various therapeutic schemes at the individual patient level. **Results:** Patients requiring high therapeutic intensity were pretherapeutically identified with a predictive value of 89.5% and patients with active disease who profited from therapy were distinguished with predictive values of 87.2%. Sensitivity and resistance to cyclophosphamide therapy was pretherapeutically predictable with 87.5% and 100% accuracy in a subgroup of 12 patients. Patients during Quensyl, Imurek and Sandimun therapy were discriminated by specific parameter patterns with predictive values of 83.3%, 90.0% and 100.0% while discrimination of low Prednison and CellCept therapies were more unreliable with predictive values of 55.5% and 75.0%. **Conclusion:** The present results suggest that specific patterns of cellular, clinical and serological data contain pretherapeutic information on therapy outcome and optimal therapy configuration for the individual patient. The findings are encouraging in the effort to provide individually optimized SLE therapy.

Parallel Session 6: Molecular Genetics

Chair: TBD

95011

A HIGH RESOLUTION GENE EXPRESSION MAP OF THE ARABIDOPSIS ROOT

David W. Galbraith[1], Kenneth D. Birnbaum[2], Philip Benfey[3], Georgina M. Lambert[1], Dennis E. Shasha[4], Jean Wang[3], Jee Jung[3]

[1]University of Arizona, Plant Sciences, Tucson, Arizona; [2]New York University, Biology, New York, New York; [3]Duke University, Biology, Durham, North Carolina; [4]New York University, Mathematical Sciences, New York, New York

The relationship between global gene activity, cell fate, and tissue specialization is of considerable interest to biologists. Here we describe a combination of technologies of Fluorescent Protein expression and targeting, fluorescence-activated sorting, and global analysis of gene expression to provide a global map of gene expression within the Arabidopsis root. We distinguish fifteen discrete zones of gene expression within the root, representing cell types and tissues at progressive stages of development. We relate the observed patterns of gene expression to the traditional anatomical boundaries, uncover previously unrecognized groups of genes having coordinated hormone responses, and identify novel chromosomal clustering of co-regulated genes. Together, these technologies provide unique approaches in biological research and, in principle, should be applicable to all multicellular organisms.

96665

MOLECULAR NATURE OF FETAL DNA IN MATERNAL PLASMA

Dorothy E. Lewis[1], Cassandra Horne[1], Jeffrey Scott[1], Dianne Dang[2], Joe Leigh Simpson[2], Farideh Z. Bischoff[2]

[1]Baylor College of Medicine, Immunology, Medicine, Houston, Texas; [2]Baylor College of Medicine, OB-GYN, Medicine, Houston, Texas

Most investigations of fetal genetic material in maternal blood have focused on the enrichment and detection of intact fetal cells for genetic diagnosis. However, such cells are rare, and can be apoptotic, rendering them more difficult to resolve Y sequences by fluorescence *in situ* hybridization. In addition, the target cell type likely changes during gestation. Recently, we have focused on detection and enrichment of cell-free fetal DNA in the maternal plasma. Surprisingly, by multiple methods, we find that the majority of this DNA exists in apoptotic bodies. Such particles are protected from metabolic breakdown, are refractile as measured by macrophage-like forward light scatter and can be labeled with DNA dyes like acridine orange (AO) or picogreen and sorted onto slides for microscopic analysis or studied for Y sequences by real-time PCR. A blinded analysis was recently conducted with 15 maternal plasma samples, 11 of which came from mothers with male fetuses, and 4 came from mothers of female fetuses. After centrifugation of maternal blood at 800g, the plasma was removed and 500 µl treated with 14 µg/ml proteinase K to minimize clumping and labeled with acridine orange (20 µg/ml). This procedure reduced forward scatter of the apoptotic bodies to lymphocyte-like and increased AO fluorescence by 2 fold. It was important to sort at room temperature to further minimize aggregation. The labeled apoptotic bodies were sorted onto slides for visible and fluorescence microscopy and about 1/3 of the sample sorted into tubes for PCR to quantify control GAPDH and FCY (male) sequences. Plasma pellets were also subjected to electron microscopy (EM) evaluation. Of the 11 male samples tested, eight were correctly identified as males, one was incorrect and two were inconclusive. For the four females, no Y sequences were detected in three and one was inconclusive. By fluorescence microscopy, the sorted AO stained material was seen as apoptotic bodies with

brightly stained DNA surrounded by a mesh of protein-like material. By EM, nucleosome structures and chromatin were detected. These results suggest that fetal DNA in maternal circulation is contained in apoptotic bodies, which can be enriched for subsequent genetic diagnosis.

95626

HIGH SPEED SORTING AS A TOOL TO IDENTIFY TOXOPLASMA GONDII PROTEINS EXPORTED INTO THE HOST CELL

Marc-Jan Gubbels[1], Julie Nelson[1], Boris Striepen[2]

[1]University of Georgia, Center for Tropical and Emerging Global Diseases, Athens, Georgia; [2]University of Georgia, Center for Tropical and Emerging Global Diseases & Department of Cellular Biology, Athens, Georgia

The obligate intracellular Apicomplexan parasite, *Toxoplasma gondii,* is a major opportunistic pathogen in immunosuppressed patients. *T. gondii* ensures its survival within the host cell by modulating the cell's pathways, most notably inhibiting host-cell apoptosis. How *T. gondii* achieves this is unknown but likely involves export of parasitic proteins beyond the vacuolar membrane into the host cell cytoplasm; no such proteins have yet been identified. In order to identify parasite components exported into the host cell, we designed a genetic screen employing Cre-Lox recombination technology. A murine erythroleukemia line was stably transfected with a reporter plasmid containing the CMV promoter and GFP separated by a LoxP-site flanked transcription termination sequence (GFP-STOP cells). A positive control using a mammalian Cre expression plasmid transfected into GFP-STOP cells showed induction of GFP expression by >500-fold indicating that this method would work as a very tight on/off switch upon presence of Cre. To screen for exported gene products in our system, the *T. gondii* genome was randomly tagged with a Cre encoding plasmid. Stably transfected parasites were allowed to infect the GFP-STOP cells (see Fig). Theoretically, when the Cre open reading frame fuses behind an exported protein, the exported Cre loops out the terminator so that GFP can be expressed. Indeed this was the case, and one mutant was identified in a very low initial percentage of infected cells (0.00019%). This positive population was sorted 24 hours post infection using a MoFlo high speed sorter. After propagation and further enrichment, the parasites from these green cells were cloned. Genetic analysis of the clone identified a Cre-fusion gene product encoding an unknown protein. To verify the export, the parasites were additionally transfected with P30-RFP, secreting RFP into the vacuolar space. Cytometric evaluation showed that only infected cells (red signal) turned green. Microscopy revealed that the secreted RFP protein stayed within the parasitophorous vacuole indicating the vacuolar membrane was intact. Currently we are verifying and characterizing this gene and the export process.

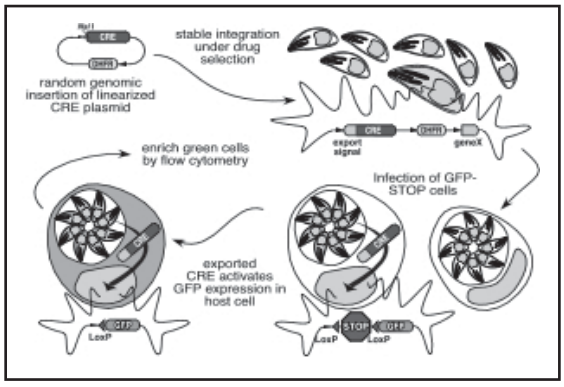

96949

TOPOGRAPHIC CHARACTERIZATION OF TELOMERES IN HEALTHY AND VARIOUS TUMOR CELL LINES DETERMINED *IN SITU* AND *IN VIVO*

Jana Amrichova[1], Emílie Lukasova[2], Miroslav Varecha[1], Stanislav Kozubek[2], Vladan Ondrej[2], Michal Kozubek[3]

[1]Faculty of Informatics, Masaryk University, Brno, Czech Republic; [2]Institute of Biophysics AS CR, Department of Cytology and Cytometry, Brno, Czech Republic; [3]Faculty of Informatics, Masaryk University, Laboratory of Optical Microscopy, Brno, Czech Republic

Nuclear and territorial positioning of p- and q- telomeres and centromeres of chromosomes 3, 8, 9, 13 and 19 were studied using repeated fluorescence *in situ* hybridization, high-resolution image cytometry and three-dimensional image analysis of human blood lymphocytes before and after stimulation (Amrichová et al., 2003). Our results suggest that in both G0- and stimulated lymphocytes, centromeres of HSA 3, 8, 9, and 13 are predominantly localized at the periphery of the cell nucleus; only centromere of HSA 19 in G0-lymphocytes is localized more centrally. Both p- and q-telomeres mostly adopt positions in the nuclear interior; q-telomeres are usually nearer to the center of the cell nucleus as compared to p-telomeres. Using repeated hybridization, tethering between telomeres of heterologous chromosomes 8, 9, and 19 was investigated. An attempt was made to find which particular telomeres are involved in telomere associations and whether any associations can be found also between homologous telomeres. We found no tethering of heterologous telomeres of chromosomes 8, 9, and 19. In contrary, both pairs of homologous telomeres of chromosome 19 (but not in other chromosomes) are tethered (associated) very frequently (Amrichová et al., 2003). Our interest was extended by investigation of topography of telomeres and incidence of telomere-association phenomenon in various types of tumor cells *in situ* and *in vivo*. Results of our observations will be discussed. This work was supported by the Ministry of Education (MSM 143300002 and ME 565), Ministry of Health (NC/6987-3), Academy of Sciences (S5004010 and A5004306) and by the Grant Agency of the Czech Republic (GA202/02/0804 and GA301/01/0186).

96604

GENETIC VARIATION IN ANTIGEN PROCESSING GENES AND SUSCEPTIBILITY TO HPV16-ASSOCIATED CERVICAL CANCER

Alina Deshpande[1], Cosette M. Wheeler[2], Hunt C. William[3], Norah Torrez-Martinez[4], P. Scott White[5], Yolanda E. Valdez[5], John P. Nolan[5]

[1]Los Alamos National Laboratory, Los Alamos, New Mexico; [2]University of New Mexico, Microbiology and Molecular Genetics and Obstetrics and Gynecology, Albuquerque, New Mexico; [3]University of New Mexico, Epidemiology and Cancer Control, Albuquerque, New Mexico; [4]University of New Mexico, Hope Clinic, Albuquerque, New Mexico; [5]Los Alamos National Laboratory, Bioscience Division, Los Alamos, New Mexico

Persistent infection with HPV16 is a primary etiological factor for the development of cervical cancer, and genes involved in antigen processing for HLA class I molecules influence the repertoire of antigens presented by HPV16 infected cells and the nature of HPV16-specific immune responses. Genetic variation in these genes may affect their structure and/or function, and consequently, the ability of an individual to clear an HPV infection. The role of 45 SNPs in 5 genes (LMP2, TAP1, LMP7, TAP2 and Tapasin) in susceptibility to HPV16-assocated cervical cancer was investigated in this study. Sequencing of selected regions of these genes, from 376 samples resulted in the discovery of 15 unreported SNPs. Genotyping of 805 samples that represented Hispanic and Non-Hispanic White ethnic groups, random controls, HPV16 positive controls, and HPV16 positive cases was conducted using microsphere arrays and flow cytometry. Association

analysis identified 10 SNPs that showed statistically significant differences in genotype distribution between cases and controls. Haplotype analysis, conducted for 3 haplotype blocks, further strengthened these associations. The LMP2-TAP1-LMP7 haplotype block showed statistically significant differences in distribution between HPV16 positive controls and cases of both ethnicities, suggesting an HPV16-specific association. Similarly, the TAP2 haplotype block showed HPV16-specific associations within each ethnic group, as well as statistically significant differences in distribution between the two ethnic groups. In case of the Tapasin block, statistically significant differences were observed between random controls and cases of Non-Hispanic Whites only suggesting a non-specific association with cervical cancer. These results indicate that the genes involved in antigen processing for HLA Class I may be susceptibility determinants for persistent HPV16 infection, and subsequent development of cervical cancer. Supported by RR01315 and RR14101.

Parallel Session 6: Cell Death III

Chair: Stefano Papa

96032

A NEW FUNCTION OF FADD IN CELL CYCLE PROGRESSION

Zichun Hua[1], Sue J. Sohn[2], Chulho Kang[2], Dragana Cado[2], Astar Winoto[2]

[1]Nanjing University, Biochemistry, Nanjing, Jiangsu, China; [2]University of California at Berkeley, Department of Molecular and Cell Biology, Bekerley, California

FADD is an adapter protein known to transmit apoptotic signals from death domain-containing members of the tumor necrosis factor receptor (TNF-R) family. However, characterization of FADD-deficient lymphocytes showed that FADD is also crucial for lymphocyte development and proliferation. Previous studies have shown that FADD-deficient T cells exhibit disarray of cell cycle machinery. Phosphorylation of FADD is G_2/M-specific but its significance is not clear. Here, we generated mice bearing a Ser→Ala or Ser→Asp mutation in the FADD phosphorylation site (serine 191) located outside the death effector- and death-domains to investigate the function of FADD phosphorylation *in vivo*. In these mice, Fas-mediated apoptosis is unimpaired. While FADD(S191A) mice exhibit no apparent defects, FADD(S191D) mice exhibit many immune developmental problems similar to FADD-deficiency. Thymocyte number of FADD(S191D) is on the average three fold less than the wild type counterparts while FADD (S191A) thymi contain normal number of cells. Flow cytometric analysis of CD4 and CD8 expression showed an arrest between the DN to DP ($CD4^+CD8^+$) transition in FADD(S191D) mice. FADD(S191D) thymocytes contain fewer L cells in DN3 stage than the wild-type counterparts. There are fewer mature T cells accumulated in FADD(S191D) peripheral organs. A decrease of $CD19^+$ B cells and an increase of Mac-1^+ cells can be seen in FADD(S191D) mice. The block in B cell is at the transition from $CD43^+$ to $CD43^-$ stage, suggesting a defective transition between pro-B and pre-B cell stage. In contrast to wild-type T cells, which undergo at least 4 cell divisions over the course of 4-day anti-CD3 plus ant-CD28 stimulation, FADD(S191D) T cells exhibit only one cell division. Cell cycle analysis also shows significantly fewer cells in S and G_2/M phases in the mutant FADD(S191D) T cells compared to the controls. Similar data were also obtained when cells were stimulated with ConA or a combination of PMA and ionomycin. Furthermore, FADD(S191D) mice are runted, anemic and exhibit splenomegaly but not T-cell autoimmunity. Alignment of FADD proteins shows a remarkable conservation of S191 among mammalian proteins but this region is absent in lower organisms. C-terminal region of the mammalian FADD may represent a domain distinct from its more conserved apoptotic region, and that this novel domain was acquired during evolution.

96969

SIVA: A NEW INTRACELLULAR LIGAND OF THE CD4 RECEPTOR MODULATING T LYMPHOCYTE APOPTOSIS VIA A CASPASE-DEPENDENT MITOCHONDRIAL PATHWAY

Patrice X. Petit[1], Benedicte Py[1], Dominique Mrugala[2], Martine Biard-Piechaczyk[3], Serge Benichou[1]

[1]Institut Cochin, INSERM U567, CNRS UMR8104, University of Paris 5, Paris, France; [2]CNRS UMR5121, University Montpellier, Biology Department, Montpellier, France; [3]CNRS UMR5121, University Montpellier, Institut de Biologies, Montpellier Cedex, France

Although the lymphocyte CD4 receptor has been involved in apoptosis processes related to T cell activation and HIV infection, the molecular pathways triggering those events are poorly understood. Here, we identified the death domain-containing protein Siva-1 as a new intracellular ligand of CD4. This interaction was revealed in a yeast two-hybrid screening of a T cell cDNA library using the cytoplasmic domain of CD4 as bait, and was then confirmed by biochemical approaches. Both Siva-1 and Siva-2, which is an alternative splice form lacking the death domain, associate with the membrane proximal region of CD4 cytoplasmic tail through their common C-terminus cystein-rich domain. Overexpression of Siva proteins triggers a typical apoptotic process manifested by cell shrinkage and surface exposure of phosphatidylserine, and confirmed by ultrastructural features. Siva-induced apoptosis results in activation of initiator and effector caspases and involves a mitochondrial pathway evidenced by activation of Bid, cytochrome c release, and its abrogation by Bcl-2 or Bcl-XL overexpression. Moreover Siva expression specifically sensitizes HPB-ALL cells to apoptosis induced both by anti-CD4 antibodies or co-culture with Hela expressing HIV-1 envelope at their cell surface. Altogether, these results demonstrate physical and functional relationships between these two molecules, indicating that Siva may modulate apoptosis of CD4-positive T lymphocytes through a caspase-dependent mitochondrial pathway.

96401

RETINOIDS (ATRA AND 4HPR) INDUCE CASPASE-INDEPENDENT DNA FRAGMENTATION AND CELL DEATH IN HUMAN B-LYMPHOMA CELLS

Gabor Barna[1], Anna Sebestyen[1], Rudolf Mihalik[1], Laszlo Kopper[1]

[1]Semmelweis University of Medicine, 1st Department of Pathology and Experimental Cancer Research, Budapest, Hungary

Retinoids are effective therapeautic agents in tumor therapy. In our study we investigated the effect of retinoids (all-trans retinoic acid, ATRA and fenretinide, 4HPR) on lymphoma cells. HT58 cell line (Non-Hodgkin lymphoma cells with B cell origin) was treated with ATRA (20-40 μM) and 4HPR (3-8 μM) for 2-24 hours. Most of the parameters were measured by flow cytometer. DNA fragmentation was detected by sub-G1 analysis, membrane integrity with propidium-iodide staining. We measured the depolarization of mitochondrial inner membrane by DiOC6, the elevation of ROS by H2DCF-DA and cardiolipin peroxidation by NAO. We inhibited the caspase activity with Z-VAD-fmk and measured DEVDase activity by fluorimeter. We determined the protein levels of Bcl-2 and Bax by western blot. Both of the agents induce cell death time and dose dependently in lymphoma cells, but at different concentrations and via different molecular mechanisms. 4HPR induce 60% cell death at 5 μM cocentration while ATRA only at 30 μM. Z-VAD-fmk at 100 uM decreased the DNA- fragmentation in ATRA treated cells but increased necrosis at the same time. Futher Z-VAD-fmk did not effect the DNA-fragmentation in 4HPR treated cells. We detected ROS elevation and cardiolipin peroxidation in 4HPR treated cells but not in ATRA treated cells. The depolarization of mitochondrial membrane occured earlier after ATRA than 4HPR treatment. The protein level of Bcl-2 was decreased by both

retinoids. We conclude that cell death induced by both retinoids is caspase independent although ATRA induced DNA fragmentation is partly caspase dependent. These results suggests that retinoids can be effective in tumors with defects in the caspase dependent apoptosis machinery.

95682

SUBCELLULAR LOCALIZATION AND VARIATIONS OF CASPASE 3 ACTIVITY CORRELATED WITH MORPHOLOGY CHANGES IN APOPTOTIC MOLT-4 CELLS INDUCED BY X-RAY

Jianping Gong[1], Yongdong Feng[2], Daxing Xie[2], Junbo Hu[1]

[1]Tongji Medical University, General Surgery, Tongji Medical College, Huazhong University of Science and Technology, Wuhan, Hubei, China; [2]Tongji Medical University, Tongji Cancer Research Institute, Wuhan, Hubei, China

Objectives to investigate the variations and sublocalization of Caspase 3 activity in apoptotic MOLT-4 cells induced by X-ray, and their relationship was determined. Materials and Methods MOLT-4 cells were induced by 10Gy X-ray, DNA fragmentation was assayed by agarose gel electrophoresis and subG1 flow cytometry, Annexin V/PI method determined the cell membrane diversity and fluorescence labeled inhibitor of Caspases (FLICA) was used to detect the Caspase 3 activity in apoptotic cells. Interesting cells were sorted by flowcytometer for observation with confocal microscope. Results MOLT-4 cells induced by X-ray were proved to undergo apoptosis by subG1 method and DNA fragmentation assay. Caspase 3 was activated at 2h after irradiated by X-ray and increased remarkably at 4h. And it was observed first at the membrane and then the cytoplasm and nucleolus area. Caspase 3 activity was detected 2 hours earlier than subG1 or Annexin V/PI method. Conclusion Caspase 3 was activated on the function of time in MOLT-4 cells induced by X-ray and its sublocalization correlated with the morphology changes. FLICA/PI method was more sensitive for detecting apoptosis.

95684

CASPASE3 AND CDK1 ACTIVATED BY X-RAY TRIGGER APOPTOSIS THROUGH THE PHOSPHORYLATION OF BCL-2 IN G1 MOLT-4 CELLS

Jianping Gong[1], Yongdong Feng[2], Jianhong Wu[2]

[1]Tongji Medical University, General Surgery, Tongji Medical College, Huazhong University of Science and Technology, Wuhan, Hubei, China; [2]Tongji Medical University, Tongji Cancer Research Institute, Wuhan, Hubei, China

The signaling pathway leading to X-ray induced apoptosis was investigated using a leukemia cell line, Molt-4. 10Gy X-ray induced a G1 phase specific apoptosis detecting by Annexin-V coupling with DNA analysis. Caspase3 activity increased progressively after X-ray, culminated in 4 hours, coincides with the phosphorylation of bcl-2 at the same time. More over, phosphorylation of bcl-2 was only detected in sorted G1 late cells, suggesting that bcl-2 phosphorylation play a critical role in X-ray induced apoptosis, and it takes place in G1 late phase exclusively. Inhibition of caspase3 activation could not abrogate bcl-2 phosphorylation in G1 phase, meaning that bcl-2 acted upstream of caspase3 activation. In conclusion, caspase3 activation triggers the apoptosis in Molt-4 cells induced by X-ray, and the apoptosis is G1 phase specific. Phosphoryaltion of bcl-2 in G1 late phase may be a target of X-ray, leading to apoptosis,

Parallel Session 6: Clinical Oncology II

Chair: Margit Balazs

96470

MOLECULAR INTERACTIONS OF ERBB2—IMPLICATIONS FOR CANCER THERAPY

György Vereb[1], Peter Nagy[1], Barbara Zsebik[1], Elza Friedlander[1], Jorma Isola[2], Thomas M. Jovin[3], John W. Park[4], János Szöllõsi[5]

[1]University of Debrecen, Medical and Health Science Center, Debrecen, Hungary; [2]University of Tampere, Finland, Institute of Medical Technology, Tampere, Finland; [3]Max Planck Institute for Molecular Biology, Department of Molecular Biology, Goettingen, Germany; [4]University of California, Medicine, San Francisco, California; [5]University of Debrecen, Medical and Health Science Center, Department of Biophysics and Cell Biology, Debrecen, Hungary

Background: The ErbB2 (HER2) protein is a member of the EGF receptor (ErbB) family of transmembrane receptor tyrosine kinases. Although no direct ligand has yet been assigned to ErbB2, recent biochemical and biophysical evidence suggests that this protein operates as a shared receptor subunit with other ErbB proteins. Its medical importance stems form its frequent overexpression in breast and other cancers, resulting in various tumorigenic phenotypic changes, including higher transforming activity, metastatic potential, angiogenesis and drug resistance. The multitude of possible small and large scale interactions among the ErbB proteins and other membrane antigens makes them especially diverse and important in initiating and directing signal transduction. Humanized antibodies against ErbB2 (i.e. Herceptin) have been introduced into clinical practice and were found to have cytostatic effect in ~30% of ErbB2 positive breast tumors. Our working hypothesis is expression levels of ErbB kinases, their interactions and activity within multimolecular complexes will determine the outcome of ErbB2 directed therapy. **Methods:** Imaging cytometric tools have been developed and applied to assess the interactions of ErbB2 molecules with each other and further potential partner molecules. Nanometer scale clustering and association was measured using acceptor or donor bleaching variants of FRET, as well as fluorescence correlation spectroscopy. Higher order aggregates were assessed with image correlation spectroscopy. **Results:** We have compared the Herceptin sensitive breast tumor line SKBR-3 to the resistant JIMT-1, the only line to our knowledge that can be grown in tissue culture. Herceptin binding in JIMT-1 was found to be much lower compared to SKBR-3, although expression measured with other antibodies was about 50%. Overall phosphorylation and its enhancement by EGF, Heregulin, or Herceptin was also considerably lower in the resistant line. ErbB2 homoassociation assessed with labeled Herceptin was relatively high in JIMT-1, but when using other antibodies for FRET, it was relatively low and did not increase upon Herceptin or EGF stimulus, contrary to the sensitive line. The association of ErbB2 with ErbB3 was measured by FRET in both cell lines. **Conclusions:** It is proposed that in the resistant cell line active ErbB2 homodimers that bind Herceptin with high affinity are scarce, and signaling that drives proliferation may originate from other ErbB kinase dimers such as the ErbB2-3 heterodimer. A candidate molecule that may be responsible for preventing ErbB2 homodimerization and Herceptin binding is MUC4, that is expressed at higher levels in the resistant line.

93710

DEVELOPMENT AND APPLICATION OF METHODS FOR INTRACELLULAR PHOSPHO-PROTEIN DETECTION FOR CLINICAL BIOMARKER ANALYSIS IN DRUG DEVELOPMENT

Lisa Green[1], Philip Marder[1], Chad Ray[1], Sue Jaken[1], Carolyn Cook[1], Robert Campbell[1], Ian Gourley[1], Donald Thornton[1]

[1]Eli Lilly & Co., Indianapolis, Indiana

Protein kinases regulate almost all cellular processes and may exhibit aberrant activity in disease states. They function by adding phosphate groups to substrate proteins within intricate cellular pathways. Kinases are particularly prominent in signal transduction and coordination of complex functions such as the cell cycle. Kinase activity has been routinely measured using phospho-specific antibodies in Western Blot analyses of cell lysates. Recently, investigators have used flow cytometry to study activity of kinases such as ERK and MEK in intact cells {Cytometry 46(2): 72}. Flow cytometric analysis of intracellular phospho-proteins provides an added benefit of studying the heterogeneity of response, both in terms of the percentages of cells that respond and the specific subsets of cells responding in mixed cell populations, such as contained in human peripheral blood mononuclear cells (PBMC). PBMC are a convenient sampling source for *ex vivo* biomarker assays. We have measured Protein Kinase C (PKC) activity *in vitro* in normal human PBMC by detecting intracellular phosphorylated PKC substrates (p-PKCsub) using a commercially available antibody (Cell Signaling Technology #2261) in an indirect immunofluorescent staining technique. We combined this with membrane surface staining to demonstrate that, among several common leukocyte subsets, monocytes have a robust PKC response to phorbol ester (PMA). *In vitro* addition of specific PKC inhibitors to whole blood or plasma reduced the signal in monocytes by 30–80%. We also performed *ex vivo* stimulation and p-PKCsub analysis on PBMC specimens obtained from patients before and during treatment with an investigational PKC inhibitor. Preliminary results indicated a decrease in PMA-induced PKC activity in five of six patients following dose. In addition, we have extended this technique to analyze activity of inhibitors of the p38 MAP Kinase pathway. With burgeoning interest in kinase-targeted therapies for cancer and other diseases, use of such flow cytometric assays is an important tool for clinical validation and for possible pharmacodynamic monitoring of treated patients.

96896

THE DYNAMICS OF THE P53 RESPONSE TO MITOMYCIN C *IN VIVO*

John McKnight[1], Hilary Russell[2], Neil H. Anderson[3], Robin Johnston[4], Perry Maxwell[5], Kate Williamson[6]

[1]Queen's University Belfast, Pathology, Medicine, Belfast, United Kingdom; [2]Queen's University Belfast, Oncology, Medicine, Belfast, United Kingdom; [3]Royal Hospitals Trust, Pathology, Medicine, Belfast, United Kingdom; [4]Belfast City Hospital, Urology, Belfast, United Kingdom; [5]Royal Hospitals Trust, Institute of Pathology, Belfast, United Kingdom; [6]Queen's University Belfast Uro-oncology Group, Pathology, Medicine, Belfast, Northern Ireland, United Kingdom

Intravesical administration of mitomycin-C chemotherapy reduces the post-surgical recurrence rate in patients with superficial bladder cancer by between 30 and 50%. How mitomycin C exerts its effects is poorly understood and at present, as there is no way to predict which patients will respond to mitomycin C therapy, many patients receive ineffective unnecessary treatment. To clarify the role of p53 *in vivo* in the differential response to mitomycin C in bladder cancer patients we designed an observational trial. Bladder washings provide an opportunity, unique amongst solid human tumours, to retrieve tumour cells at multiple time-points following the administration of chemotherapy. Fifteen TCCB patients received three intravesical mitomycin C instillations, one week apart, before tumour resection. On each occasion, tumour cells retrieved from the bladder washings taken pre and at 90 minutes, four hours and six hours post intravesical instillations of MMC were examined for evidence of apoptosis and inflammation and p53 protein expression up-regulation. The degree of apoptosis was scored as—for no evidence of apoptosis, + for <5 apoptotic cells per high power field (HPF), ++ for 5-10 apoptotic cells per HPF, and +++ for 10+ apoptotic cells per HPF. The percentage of inflammatory cells was scored as—for no evidence of inflammatory cells, +/- for <5%, + for 5-25%, ++ for 25-50% and +++ for greater than 50%. p53 protein expression was measured by established flow cytometry techniques. p53 mutational status for each patient was determined on pre- treatment tumour cells using single strand conformation polymorphism. After consideration of all the accumulated data, each patient was categorised as either a "responder" or "non-responder" with respect to apoptosis, inflammation and p53. Venn charts were plotted. Eight patients were classified as apoptotic responders and five of these exhibited evidence of up-regulated p53. Only five of the nine patients in whom p53 was up-regulated in response to mitomycin C chemotherapy had concomitant apoptosis. In two patients, apoptosis occurred in the absence of functional p53, but in the presence of a mitomycin C induced inflammatory response. One of these patients had a six base pair deletion in exon 5 corresponding to removal of amino acids cysteine and arginine. These results indicate that although p53 is involved in the *in vivo* response to mitomycin C, it is likely that another apoptotic pathway, such as that triggered by Fas plays a significant role in the response to chemotherapy in TCCB.

97053

FLOW CYTOMETRIC ANALYSIS AND MODELING OF GPCR ASSEMBLIES AND THEIR POTENTIAL APPLICATION IN DRUG DISCOVERY

Larry A. Sklar[1], Peter Simons[1], Anna Waller[1], Sean Biggs[1], Tione Buranda[1], Terry Foutz[1], Bruce S. Edwards[1], Eric R. Prossnitz[1]

[1]University of New Mexico, Cancer Center, Health Sciences Center, Albuquerque, New Mexico

G protein coupled receptors (GPCR) form a ternary complex of ligand (L), receptor ®, and G protein heterotrimer (G) during signal transduction. We developed a homogeneous, small volume bead-based approach for GPCR molecular assemblies. Dextran beads were derivatized with chelated nickel to bind his-tagged G proteins. Ternary complexes were assembled on these beads using fluorescent ligand with wild type formyl peptide receptor (FPR) or FPR-Giα2 fusion protein, and with a nonfluorescent ligand and FPR-GFP fusion protein. Assemblies were validated by showing time and concentration dependence of ternary complex formation. Affinity measurements of LR and LRG on beads and FPR-Giα2 fusion protein for G$\beta\gamma$ were consistent with comparable assemblies in detergent. Performance was assessed by showing: 1) the relationship between LR affinity and LRG affinity; 2) the use of the bead assembly as a sensor to report GPCR in solution; and 3) the observation of GTPγS-induced ternary complex disassembly, in which the activation step due to RG disassembly was fast and heterotrimer disassembly was slow. We next solubilized a fusion protein of β2-adrenergic receptor with green fluorescent protein (β2AR-GFP). β2AR-GFP bound to dihydroalprenolol-conjugated beads providing, by competition, Kds for β2AR ligands. Beads displaying chelated nickel bound ternary complex. The dose-response curves of LRG formation revealed maximal assembly for ligands previously classified as full agonists, and reduced assembly for ligands previously classified as partial agonists. When performed simultaneously, the two assemblies discriminated between agonist, antagonist, or inactive molecule in a manner appropriate for high throughput drug discovery. GTPγS-induced dissociation rates of the ternary complex were the same for full and partial agonists, apparently reflecting rapid RG disassembly. Mathematical models for ternary complex formation are cyclic. While simulations based on these models can account for ternary complex behavior, the affinity of the complexes normally formed in planar membranes (R to RG and LR to LRG) are difficult to measure. Solubilized formyl peptide receptor and β2AR retain physiological ligand binding in flow cytometric bead-based assays. Direct measurements of soluble LR to LRG formation provide dissociation constants >0.1 μM. Simulations based on these findings resulted in dissocia-

tion constants of soluble R to RG >1 μM, a previously unmeasurable quantity. Given the data that are now available, we anticipate that it may be possible to explicitly model the thermodynamics of full and partial agonists for wild type receptors and constitutively active mutants.

96917

THE ANTITUMOR EFFECT OF TENIPOSIDE COMPARED WITH CISPLATIN ON ORAL CARCINOMA XENOGRAFTS IN ATHYMIC NUDE MICE

Wan-Tao Chen[1]

[1]Shanghai Second Medical University Affiliated Ninth Hospital, Shanghai, China

Background: The purpose of this study was to explore the chemotherapeutic effect of teniposide (VM-26) compared with cisplatin(CDDP) on human oral squamous cell carcinoma cell line(Tca8113) xenograft in athymic nude mice and that of human salivary adenoid cystic carcinoma (ACC-M). Material and **Methods:** 18 athymic nude mice were inoculated with 2x106 Tca8113 cells at the right buttocks and another 18 mice were inoculated with 2x106 ACC-M cells. After seven days, each 18 animals implanted with the same cells were divided randomly into three groups: control group, teniposide group and cisplatin group, each group included 6 mice. Mice in each group were injected intraperitoneally with normal saline, teniposide and cisplatin, respectively. Teniposide and cisplatin were used with doses of 10mg/kg/d and 5mg/kg/d, once every 3 days and total 3 times. The sizes of tumors were measured every 3 days. **Results:** At the end of the treatment, the average volumes of tumors in control group, teniposide group, cisplatin group were 3146.50mm3, 315.08mm3 and 1225.43mm3 respectively in Tca8113 cells burdened mice, and were 4731.17mm3, 1184.13mm3 and 2688.35mm3 respectively in ACC-M cell burdened mice. The growth inhibition rates for teniposide and cisplatin group in Tca8113 cell burdened mice were 75.24% and 55.59%, and in ACC-M cells burdened were 72.45% and 39.65%. There was no severe side effect observed in this experiment. **Conclusion:** The inhibition rate of teniposide on tumor growth was higher than that of cisplatin ($P<0.01$). Teniposide was a promising drug for treatment of oral carcinomas included squamous cell carcinoma and adenoid cystic carcinoma.

Wednesday, 26 May

Plenary Session 3: 1045–1230

Stem Cell Plasticity

99048

CARDIAC STEM CELLS AND THE INJURED HEART

Pierro Anversa[1]

[1]New York Medical College, Cardiovascular Research Institute, Valhalla, New York

The notion of the adult heart as a terminally differentiated organ without self-renewal potential has been undermined by the existence of a subpopulation of replicating myocytes in normal and pathological states. The origin and significance of these replicating cells has remained obscure for lack of a proper biological context. This report documents the existence of Lin- c-kitPOS cells with all the properties of cardiac stem cells. They are self-renewing, clonogenic and multipotent giving rise to myocytes, smooth muscle and endothelial cells. When injected into an ischemic heart, these cells or their clonal progeny reconstitute a well-differentiated myocardium, constituted by blood-carrying new vessels and myocytes with the characteristics of young cells, encompassing ~70 percent of the ventricle. Thus, the adult heart, like the brain, is mainly composed of terminally differentiated cells, but is not a terminally differentiated organ because it contains stem cells supporting its regeneration. The existence of these cells opens new opportunities for myocardial repair.

92345

TELOMERE LENGTH REGULATION IN STEM CELLS

Peter M. Lansdorp[1]

[1]BC Cancer Agency, Terry Fox Laboratory, Medicine, University of BC, Vancouver, British Columbia, Canada

The ends of chromosomes in all vertebrates contain T_2AG_3 repeats and associated proteins. A minimum number of repeats is required to form a proper end structure and to prevent activation of DNA damage responses. The length of telomere repeats in human nucleated blood cells is correlated with mortality possibly because telomere shorting provides strong selective pressure for cells with altered DNA damage responses (e.g. loss of p53). Various *in situ* hybridization methods using flow and image cytometry will be discussed that are used to study the role of various genes in telomere length regulation.

99057

THE STEM CELL CONTINUUM

Peter J. Quesenberry[1]

[1]Roger Williams Medical Center, Providence, Rhode Island

The phenotype of bone marrow stem cells is extraordinarily plastic. We have shown that within the hematopoietic system, the phenotype fluctuates with cell-cycle transit. There are hotspots for differentiation into various lineages when cells are exposed to the same inductive cytokine combination, and both progenitors and engraftable stem cells show a reciprocal relationship with progress through cell cycle. These data have indicated that the regulation of hematopoiesis is based upon a fluctuating reversible continuum rather than a hierarchy. Further studies have shown that the marrow is also extraordinarily plastic with regard to its ability to produce cells in multiple other tissues.

1230–1400 Poster Presentations

(See abstracts beginning on page 111)

1615–1800

New Investigator/Student Symposium

Chair: Nicholas Terry

See abstracts, pages 96–98.

Exceptional Student Award candidates

95716

MINIATURIZATION OF ENZYMATIC ASSAYS

Heidelinde R.C. Dietrich[1], Ian T. Young[2], Gijs W.K. Van Dedem[3], Rob Moerman[3], Richard L. Van Den Doel[4], Pascale Daran-Lapujade[3], Johan Knoll[3]

[1]Delft University of Technology, Imaging Science and Technology, Delft, Netherlands; [2]Delft University of Technology, Delft, Netherlands; [3]Delft University of Technology, Biotechnology, Delft, Netherlands; [4]Delft University of Technology, Imaging Science & Technology, Applied Sciences, Delft, Netherlands

The miniaturization of bioanalytical assays and the development of new intelligent analysis systems represent a major development in cytomics. The aim of our research program has been to develop an intelligent molecular diagnostic system that measures different metabolic compounds simultaneously, in a very short time, using minimal amounts of reagents and samples. We have previously described a new technique for the deposition of pico- and nano-liter volumes of reagent solutions by means of an electrospray dispensing system. This technique allows the deposition of various reagents in well-defined dry spots onto a solid support such as a nanoarray. We spray components required for enzymatic reaction in wells of nanoarray chips. Thus, it is possible to develop chips suitable for rapid analysis of certain analytes, for example, those used for the determination of a hemogram. Substrates, co-enzymes, activator metals, and other essential reagents can be sprayed into the wells of the array and immediately frozen to guarantee the stability of the various ingredients. Enzymatic assays for alcohol dehydrogenase, enolase and pyruvate kinase have been used as a model system for the miniaturization procedure. Components necessary for certain enzymatic reactions are dispensed into the wells of the nanoarray using our electrospray system. These chips are then filled with sufficient enzyme solution to determine the enzymatic activity. We have compared enzymatic assays performed in our nanoliter arrays with measurements performed in microliter volumes and pre-sprayed arrays that use commercially available enzymes and enzymes derived from cell-free extracts.

95971

MONITORING CELL CYCLE DISTRIBUTIONS AND APOPTOSIS IN LIVING LYMPHOBLASTOID CELLS BY VIDEOMICROFLUOROMETRY AND DISCRIMINANT FACTORIAL ANALYSIS

Julien Savatier[1], Jean Vigo[1], Jean Marie Salmon[1]

[1]Universite de Perpignan, Biophysique et Dynamique des Systemes Integres, Perpignan, France

Single living cells are labelled with three fluorescent markers : Hoechst 33342 for nuclear DNA, Rhodamine 123 for mitochondria and Nile Red for plasma membrane. Numerical image analysis allows us to obtain, for each cell, morphological parameters (cell and nuclear sizes, nucleo-cytoplasmic ratio, shape factor) and functionnal information by fluorescence intensity (nuclear DNA content, level of mitochondria energetic state, amount and properties of plasma membrane) with total value, mean and standard error. These parameters are used in a typological analysis (dendrogram method) which separate control cells into four groups. A discriminant factorial analysis confirms these groups: G0-G1, S, G2+M and polyploid cells called Gn. Discriminant factorial analysis indicates which parameters are the most discriminant. It gives the mean value of each parameter for each group and the cell probability to belong to each phase. These control cells, from 4 different samples, define a learning population. Populations of treated cells (with several concentrations and times of incubation with adriamycin) are analysed as supplementary individuals in a discriminant factorial analysis using control cells as learning population. They are classified into G0-G1, S, G2+M and Gn groups. After 3 days, when the concentration of adriamycin increases to 200 ng.ml-1, the cell proportion in Gn goes from 1% to 70% and the cell proportion in G2+M increases too. Between 200 and 1000 ng.ml-1 the phenomenon is inverted and the proportions of the cells in each phase tend to return to their normal values. Furthermore such an approach allows to accurately evidence, after 5 days treatment, the changes of some cellular parameters values such as those induced during apoptosis. Are included shape factor and size of the nucleus, total and standard error of Hoechst 33342 fluorescence intensity (DNA amount and DNA clusterisation, respectively), as well as a decrease of the Rhodamine 123 fluorescence intensity. Apoptotic cells make up new groups that do not exist in standard conditions and allow to follow the apoptotic process induced by adriamycin treatment.

96601

WILMS' TUMOR (WT1) ANTIGEN LOADING OF DENDRITIC CELLS USING MRNA ELECTROPORATION FOR PRECLINICAL LEUKEMIA VACCINE DEVELOPMENT

Ann Van Driessche[1], Peter Ponsaerts[1], Griet Nijs[1], Marc Lenjou[1], Liquan Gao[2], Hans J. Stauss[2], Zwi Berneman[1], Dirk R. Van Bockstaele[1], Viggo Van Tendeloo[1]

[1]University Hospital Antwerp, Laboratory of Experimental Hematology, Edegem, Belgium; [2]Imperial College of Science, Technology and Medicine, University of London, Medicine, London, United Kingdom

In various types of cancer, in particular in acute leukemia, there is an overexpression of the Wilms' tumor gene WT1. Because WT1 plays an important role in leukemogenesis, it can serve as an antigenic target for dendritic cell (DC)-based immunotherapy. We chose for a genetic "whole protein" approach for loading of DC with WT1, using electroporation of WT1-encoding *in vitro* transcribed (IVT) mRNA. This strategy allows the presentation of multiple WT1 epitopes by MHC class I molecules, irrespective of the HLA-haplotype of the patient. First we constructed a transcription vector containing the WT1 cDNA under the control of a T7 bacteriophage promoter for production of *in vitro* transcribed WT1 mRNA. Following electroporation of monocyte-derived DC (Mo-DC) with WT1 mRNA, RT-PCR analysis using WT1-specific primers was performed to verify RNA transfection of Mo-DC and mRNA stability was studied in function of time. While WT1 mRNA could not be detected in non-electroporated Mo-DC, it was clearly present in electroporated Mo-DC up to 5 days following electroporation. Using western blot analysis, we tested whether WT1 mRNA could be translated into protein. WT1 protein was clearly detectable after *in vitro* translation and, more interestingly, in cell lysates of WT1 mRNA-electroporated Mo-DC, indicating efficient translation of WT1 mRNA in transfected Mo-DC. Next, we wanted to prove that the WT1 protein was correctly processed into peptide epitopes and presented by MHC class I molecules on the membrane of DC following WT1 mRNA electroporation. Using a cytotoxic T lymphocyte (CTL) clone 77, that specifically recognizes the HLA-A2 immunodominant WT1126-134 epitope, we showed that WT1 mRNA-electroporated Mo-DC were able to stimulate the CTL clone for IFN-γ production in an HLA- and antigen-specific manner. Based on these results, we are currently focusing on the priming of autologous WT1-specific cytotoxic T lymphocytes (CTL) using WT1 mRNA-electroporated Mo-DC. The ultimate goal of this study is to prove that WT1 mRNA-electroporated DC can induce an effective immune response against WT1-positive leukemia cells *in vitro*.

President's Award for Excellence candidates

95811

3D NUCLEAR ORGANIZATION OF TELOMERES IN NORMAL AND CANCEROUS MAMMALIAN CELLS

Bart J. Vermolen[1], Tony Chuang[2], Richard L. Van Den Doel[1], Alice Chuang[2], Ian T. Young[1], Sabine Mai[2], Yuval Garini[1]

[1]Delft University of Technology, Delft, Netherlands; [2]University of Manitoba, Physiology, Faculty of Medicine, Winnipeg, Manitoba, Canada

We present the high resolution 3D imaging and analyses of all the FISH-stained telomeres in mammalian nuclei. By using either confocal microscopy or 3D high-resolution microscopy measurements followed by an adequate 3D analysis that we have developed, we analyzed the space-filling properties of all the telomeres in the nucleus. The method was applied to normal, cancerous and c-myc disrupted cells. In normal cells we have found that telomeres occupy distinct and non-overlapping telomere territories (TTs), they localize in the middle of the nucleus during G0/G1 and S phases and assemble into a central telomeric disk (TD) during G2 phase. In tumors we have found that telomeres form aggregates and do not align in a telomere disk. 3D telomere order therefore forms an important tool for cancer research and possibly diagnostics. To analyze the data, a 3D image analysis program was developed. It segments the nucleus volume, counts the spots that are found and for each spot various parameters are calculated (volume, intensity and center of gravity). Then, the 3D distribution is determined by analyzing the shape of the volume occupying the telomeres. We have found that this volume can be described as a spheroid (i.e. an ellipsoid having two axes of equal length, a=b and a third different one c) and it's variation from a perfect sphere is described by the ratio a/c. This parameter provides objective criteria for analyzing the telomeres distribution and forms the basis for the study and the conclusions mentioned above. Other future analysis may include measuring the anueploidy of the genome, using the number of telomeres together with an analysis of the DAPI stained chromosomes. Typical distribution of telomeres in a mouse Pre-B lymphocyte cell line is shown in the figures. Figure 1 shows the distribution of telomeres in a normal cell and figure 2 shows the distribution in a cell upon a transient activation of MycER with 4-hydroxy-tamoxifen and exhibit alterations of its telomere organization. A large aggregate is clearly observed. The 3D shape of the DAPI counter stain clearly indicates that we are not looking at a flat nucleus, where it would be trivial that the telomeres are assembled in a disk. The fixation technique used preserves the full 3D nature of the nucleus. We will describe the experimental and analysis methods and discuss about some of our results.

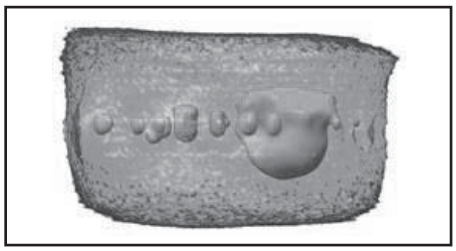

Figure 1

Figure 2

96381

DIFFERENT GLUCOCORTICOID RECEPTOR (GCR) EXPRESSION OF BALB/C MOUSE THYMOCYTE SUBPOPULATIONS

Ferenc Boldizsar[1], Tamas Czompoly[1], Laszlo Palinkas[1], Domokos Bartis[1], Peter Nemeth[1], Timea Berki[1]

[1]University of Pécs, Faculty of Medicine, Hungary, Department of Immunology and Biotechnology, Pécs, Hungary

Glucocorticosteroids (GCs) exert an important paracrine regulatory role on thymocyte survival and apoptosis during positive selection by modifying the T cell receptor (TcR) derived signals. Although the exact molecular mechanism is still unclear, several findings indicate the non-genomic (direct membrane or membrane receptor mediated) GC effects in addition to the classical genomic GC action. The aim of our present study was to characterise the GCR levels of thymocyte subgroups both at the mRNA and cytoplasmic protein levels and to investigate the effect of DX treatment on the GCR expression. 4 week old Balb/c mice were treated with high (20mg/kg) or low (2mg/kg) doses of DX ip. once. We used untreated animals as controls. After 24 hours thymi were isolated and homogenized. Samples were labeled with monoclonal anti-CD4-PE and anti-CD8-CyC antibodies. The thymocyte subgroups were identified and/or sorted according to their FL2-FL3 fluorescence. From the pure thymocyte populations we isolated RNA, then reverse transcription was performed followed by real-time PCR. Cytoplasmic GCR was determined after anti-GCR-FITC labelling and triple colour flow cytometric analysis. We also examined the time course of GCR mRNA expression after 30 min, 1, 2, 4, 8, 12, 16, 20, 24 h of a single high dose DX treatment. CD4-CD8- double negative (DN) thymocytes expressed the highest level of GCR mRNA followed by CD8 single positive (SP), CD4 single positive (SP) and CD4+CD8+ double positive (DP) thymocytes. Cytoplasmic GCR levels were highest in DN thymocytes followed by the CD4 SP or CD8 SP mature cells and DP cells. After 24 hours of high or low dose DX treatment DN, CD4 SP and CD8 SP cells showed significant decrease of GCR mRNA expression (75%, 66% and 80% decrease respectively). DP thymocytes, on the other hand, showed no significant alteration in GCR mRNA expression after either dose DX treatment. Interestingly, there was a transient, significant increase in the GCR mRNA level of thymocytes after a single high dose DX treatment at 8h, followed by a significant decrease at 24h. mRNA levels changes were followed by the cytoplasmic GCR levels approximately after 8 hours. The different GCR mRNA expression of thymocyte subgroups could explain the different cytoplasmic GCR protein levels. The down regulation of GCR expression seems to be a common mechanism in DN, CD4 SP and CD8 SP cells, but not in DP thymocytes. This could explain at least partly the different sensitivity of thymocyte subgroups to GC treatment. DP cells are unable to down regulate GCR levels in the presence of GC hormone, thus they are more sensitive to GC induced apoptosis. The low GCR expression of DP thymocytes together with the high sensitivity also raises the possibility of non genomic GC action.

97172

SHAPING OF GENOMES BY INSTABILITY AND SELECTION

Antoine Snijders[1], Jane Fridlyand[1], Pavla Gajduskova[1], Joshua Baughman[1], Dorus Mans[1], Richard Segraves[2], Ajay Jain[1], Daniel Pinkel[2], Donna Albertson[1]

[1]University of California San Francisco, Cancer Research Institute, San Francisco, California; [2]University of California, San Francisco, Laboratory Medicine, Medicine, San Francisco, California

Tumors result from the accumulation of genetic changes. Cytogenetic studies and genome-wide array based comparative genomic hybridization (array CGH) have shown that there is a wide spectrum in the types and numbers of copy number aberrations present in tumors. This is likely due to defects in mechanisms that normally maintain and/or control the integrity of the genome coupled with selection for growth advantage and increased survival. To investigate the role of spe-

cific gene dysfunctions on the types and numbers of DNA copy number aberrations, we have selected for methotrexate (MTX) resistance in the mismatch repair deficient cell line HCT116 (MLH1 -/-) and its mismatch repair proficient counterpart HCT116 +chr3, which carries a wild type copy of MLH1. We also included a third HCT116 derivative in which the Ku86 locus on one allele was disrupted (HCT116 Ku +/-). Ku86 is involved in the non-homologous end-joining (NHEJ) branch of the double strand break repair pathway. We analyzed the types and numbers of copy number aberrations in the MTX resistant cell pools by genome-wide array CGH. The resistant cells arising from mismatch repair deficient cell line HCT116 most frequently showed no DNA copy number aberrations (16/29 resistant cell pools). In contrast, the mismatch repair proficient cell line HCT116+chr3 resistant to MTX always showed aberrations involving chromosome 5, on which the target gene DHFR of MTX is located. Amplifications centering on DHFR or a more proximal region were detected in 7/13 resistant cell pools. FISH analysis using a DHFR specific probe on metaphase spreads of three cell lines with amplifications showed complex rearrangements involving chromosome 5 and other chromosomes. The chromosome containing the amplified sequence is unstable. MTX resistant colonies of the HCT116 Ku +/- cell line frequently showed copy number aberrations involving parts of chromosomes. A gain of chromosome 5q was observed in 8/22. An interstitial gain of part of chromosome 5q, including the DHFR locus, was observed in 6/22 colonies, while gain of a whole chromosome 5 was observed in 3/22 colonies. Since it is likely that distinct defects in mechanisms that normally maintain genome stability result in altered response to therapy, identification of these defects is important for not only choice or design of therapy but it might also avoid treatments of tumors already resistant to the therapy caused by the dysfunctional gene.

98255

QUANTITATIVE AND KINETIC ANALYSIS OF P-GP ACTIVITY IN T-CELL SUBSETS

Vera Svobodova Donnenberg[1], James Luketich[2], Albert D. Donnenberg[3]

[1]University of Pittsburgh, Surgery, Medicine, Pittsburgh, Pennsylvania; [2]University of Pittsburgh, Thoracic Surgery, Medicine, Pittsburgh, Pennsylvania; [3]University of Pittsburgh, Medicine, School of Medicine, Pittsburgh, Pennsylvania

P-gp actively eliminates substrate drugs from the cells. The majority of immunosuppressive drugs are P-gp substrates and T cells display P-gp activity. Dye efflux assays using fluorescent P-gp substrates have been successfully used to measure P-gp function. The objective of this study was to perform real-time measurement of R123 uptake and efflux in four circulating T-cell subsets. We measured P-gp activity in CD4 and CD8 T-cells subsetted according to CD45RA and CD27 expression (naïve/memory/effector). After surface staining, cells were maintained at 37°C and fluorescence was acquired on a flow cytometer for 2 minutes, after which they were loaded with R123 (0.0165-0.13 microM) and acquired continuously for 15 min. Cells were washed at 4°C and returned to the cytometer for continuous measurement of R123 efflux for additional 30 min. Kinetics of dye uptake and efflux were estimated for each T-cell subset and optimal loading and efflux times were determined. During uptake, linearized R123 fluorescence increased rapidly and approached plateau by 10 minutes. The rate of uptake increased linearly with R123 concentration. All cells tested achieved similar plateau levels. R123 efflux exhibited a biphasic profile. The initial slope over a 5-minute interval (log-fluorescence channels/min) differed markedly among T-cell subsets with CD8+ memory cells > CD8+ naive > CD4+ naive > CD4+ memory (30.55 +/- 0.93, 16.96 +/- 0.56, 12.71 +/- 0.39, 9.91 +/- 0.48, mean +/- SE respectively). The efflux is markedly decreased during the second phase, which is consistent with two-compartment distribution of R123 within the cell, but theoretical considerations and the work of others have led us to hypothesize a four-compartment model in which cationic substrates can be sequestered in the cytosol/mitochondia. From this data we conclude that: 1) R123 very rapidly diffuses into the cell (maximal loading achieved in 10 minutes) such that 15 minute incubation period is sufficient for maximal R123 loading; 2) The initial efflux of R123 (<10 minutes) is very rapid and differs among different T-cell subsets with a subset of CD8 memory cells exhibiting the greatest efflux; 3) The rapid initial efflux is followed by a second phase, where R123 transport into the extracellular medium is greatly decreased. Real-time measurement of dye uptake and efflux kinetic data has permitted for the first time a detailed quantitative analysis of P-gp activity in different T-cell subsets, revealing heterogeneity within these subsets. These results extend our previous static observations that the CD8 memory subset exhibits the greatest P-gp activity, which may have important pharmacological implications during cell-specific immune responses.

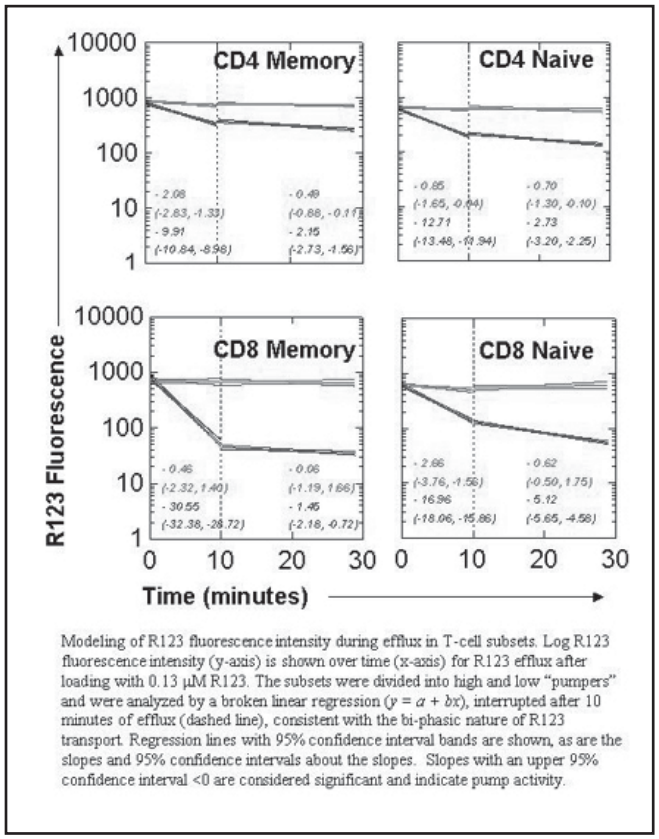

Modeling of R123 fluorescence intensity during efflux in T-cell subsets. Log R123 fluorescence intensity (y-axis) is shown over time (x-axis) for R123 efflux after loading with 0.13 μM R123. The subsets were divided into high and low "pumpers" and were analyzed by a broken linear regression ($y = a + bx$), interrupted after 10 minutes of efflux (dashed line), consistent with the bi-phasic nature of R123 transport. Regression lines with 95% confidence interval bands are shown, as are the slopes and 95% confidence intervals about the slopes. Slopes with an upper 95% confidence interval <0 are considered significant and indicate pump activity.

Thursday, 27 May

0800–0945

Parallel Session 7: Multicolor Fluorescence

Chair: Dirk R. Van Bockstaele

96591

NEW ADVANCES IN FLOW CYTOMETRY: HOW TO DO SUCCESSFUL POLYCHROMATIC FLOW CYTOMETRY

Stephen P. Perfetto[1], Mario Roederer[2]

[1]National Institutes of Health, Vaccine Research Center, Bethesda, Maryland; [2]National Institutes of Health, NIAID, Vaccine Research Center, Bethesda, Maryland

Advances in instrumentation and software allow the detection of more than 14 distinct cell parameters reveals the immense heterogeneity of the immune system. For example, it was recently reported that as many as 100 functionally distinct cell phenotypes can be identified in the peripheral blood of humans. In addition, the evolution of computer technology brings to light the ability to analyze very large sample sets using sophisticated algorithms and increasing the power of analysis of low frequency cell populations. We describe here the objectives, pro-

cedures, analysis and instrumentation needed to perform successful polychromatic flow cytometry (PFC). Quality assurance was developed in critical areas for successful PFC. These areas include: monoclonal antibody reagent titration, instrument alignment, specimen controls, instrument configuration and data analysis. Using fluorescent beads and fluorescently stained cells quality assurance procedures were optimized to detect more than 14 separate cell parameters on an LRSII flow cytometer. Data analysis and off-line compensation was performed using the FlowJo software program. For successful PFC all areas within quality assurance as outlined in this report must be maintained and monitored. Monoclonal antibody titration and the use of proper specimen controls are the most important factors in this process. While important to monitor, established instrument alignment checks and proper instrument configuration were found to be least problematic. Appropriate selection and validation of compensation control samples was the most important aspect of ensuring appropriate data; subtle problems in alignment, reagent mismatch, or experimental procedures were most evident in significant under- or over-compensation. The most challenging and time consuming aspect remains data analysis and presentation; new techniques for succinctly presenting and publishing this data are still needed.

96670

VISUALISATION OF PEPTIDE PRESENTATION FOLLOWING ORAL ANTIGEN APPLICATION

Dennis Kirchhoff[1], Desiree Kunkel[2], Andreas Radbruch[3], Alexander Scheffold[2]

[1]German Rheumatism Research Center, Berlin, Germany; [2]DRFZ, Cytometry Group, Berlin, Germany; [3]German Rheumatism Research Center, Berlin, Newfoundland, Germany

High doses of orally applied antigens are known to induce systemic hyporesponsiveness by induction of anergy and deletion of specific T cells, while administration of low doses leads to the generation of regulatory T cells. However, little is known about the involved antigen-presenting cell (APC) and the site of antigen presentation/T cell activation. To directly identify cells presenting orally applied antigens *in vivo* we use high sensitivity flow-cytometry to visualize APC which present a hapten-labelled peptide, even at a very low level (<100 peptides cell). Peyers Patches (PP) are regarded as a major entry site for intestinal antigens and the most important organ for specific T cell priming to orally applied antigens. We show that after feeding of Ova-peptide presentation is maximal on DC of the PP followed by DC in the mesenteric lymph nodes (mLN). At low doses (<1 mg) presentation is restricted to DC of PP whereas only at higher doses peptide presentation occurs in peripheral lymph nodes and spleen. Similarly Ova-specific T cells proliferate mainly in PP and to a lower extent in mLN depending on the peptide dose fed. In contrast, after feeding of limiting doses of ovalbumin protein, T cell activation preferentially occurs in mLN but only at higher doses also in PP. We conclude, that PP DC are the main APC presenting orally applied peptides *in vivo*. Nevertheless, at limiting doses of ovalbumin protein, T cell activation in the GALT occurs preferentially in the mLN. Taken together these data highlight the importance of mLN for low dose oral tolerance against proteins and may suggest a defect in protein uptake or processing by APC of the PP.

95630

TO DIGITIZE, OR NOT TO DIGITIZE, IS NOT THE QUESTION. THE QUESTION IS WHEN TO DIGITIZE

Christopher Snow[1], John Riley[1]

[1]Beckman Coulter, Inc., Miami, Florida

Digitization of raw pulses, more or less directly after the detectors, is still a hot topic on the Purdue Cytometry website, despite the fact that Leon Wheeless pioneered this aspect of instrument design over thirty years ago. The first commercial instrument to utilize this approach, Rick Thomas' RATCOM, appeared in 1990. Since then other manufacturers have introduced digital pulse processing instruments. Why is it that Beckman-Coulter, and others, continue to offer only instruments whose design follows the 'hybrid' approach, where detectors are followed by extensive analog electronics, including baseline restorers, peak detectors, integrators and sample-and-hold circuits, before finally digitizing the data? It is because the ADCs used to directly digitize pulses are currently too slow to do the job with adequate resolution. It is the quality of the data produced that should drive instrument design. When data known to obey a gaussian distribution (such as the negative population in a fluorescence histogram) are presented as discontinuous 'spikes', elsewhere referred to as resembling a picket fence, the accuracy of measures of the central tendency of that population, such as the mean, is diminished. Having gaps in the data make it difficult to do quantitative immunofluorescence, in which means of 'positive' populations are compared to the mean of a 'negative' population. Data based upon mathematical modeling of gaussian distributions will be presented, predicting the error to be expected as a function of insufficient ADC sampling frequency and resolution.

96826

A VERSATILE INSTRUMENT SETUP SYSTEM FOR A 6 COLOR FLOW CYTOMETER

Michael Lock[1], James Bishop[1], Zhenxiang Gong[1], Torbjorn Berglund[1], Eric J. Crowther[1], Neha S. Pathak[1]

[1]BD Biosciences, San Jose, California

We describe a system comprised of a set of fluorescent beads and associated algorithms used to automatically set up a multiparameter flow cytometer for a range of cellular analyses. Besides determining an initial, default setup for lyse-wash assays, the algorithms automatically calculate the detector voltages and compensation values needed for other setups (e.g., lyse-no-wash setup, or user-specified setups) without the need to reacquire beads or single-stained controls. The foundation of the system is a collection of standard curves that relate fluorescence intensity to detector voltage. More specifically, we determine standard curves to describe the relationship between the fluorescence intensity of each different color bead in the bead set and the voltage of each detector. In our system there are 7 different color beads and 6 different detectors, leading to a total of 42 standard curves. Each curve is estimated by fitting a straight line between log fluorescence intensity of a given bead and log detector voltage over a range of voltages. The resulting set of standard curves provides a complete description of the fluorescence intensity of the beads and the spectral overlap of the beads in every detector at all voltages. We show how the standard curves can be used to automatically calculate the voltage needed to place a particle at any fluorescence intensity target, for example, to change from a lyse-wash setup to a lyse-no-wash setup. In addition, since there is a standard curve for every fluorophore in every detector, the curves contain the information needed to automatically recalculate compensation for any specified brightness. We also describe a simple algorithm that uses the ratio of spectral overlap of stained cells to that of beads to adjust set-ups for differences in spectral overlap between beads and cells.

96522

FLUORESCENCE STANDARDIZATION: THE USE OF FLOW CYTOMETERS TO MEASURE THE FLUORESCENCE OF SOLUTIONS AND DETERMINE THE SPECIFIC FLUORESCENCE OF LABELED ANTIBODIES

Doug Redelman[1]

[1]Sierra Cytometry, Reno, Nevada

The goal of quantitative immunofluorescence flow cytometry is to estimate the number of cellular molecules by determining the intensity after labeling with a fluorescent antibody. In order to make such measurements, there are several relationships that must be determined including the number of antibodies bound per antigen and the specific fluorescence of the antibody, i.e., the fluorescence intensity per antibody molecule. The system that is most widely used to make these measurements is based on beads with specified numbers of fluorochromes that are expressed as "molecules of equivalent soluble fluorochrome" (MESF). The shortcomings of this approach are that MESF beads are not available for some fluorochromes and that the specific fluorescence of the labeled antibody is never directly determined. The current studies have developed procedures to measure the fluorescence of solutions with a standard flow cytometer and use this information to determine specific fluorescence. Knowing the specific fluorescence of labeled antibodies is the most critical information one needs in order to determine the number of antibodies bound per cell. In the case of fluoresceinated antibodies, one can determine the number of fluoresceins per Ig (F:P ratio) by measuring the absorbance at 280 and 495nm. However, the F:P ratio, while it may accurately reflect the number of fluoresceins per Ig, does not provide the information needed to determine specific fluorescence since it takes no account of fluorescent losses due to resonance energy transfer. Therefore, one needs to measure the fluorescence per Ig molecule directly. In order to obviate the need for assumptions concerning the equivalence of the optics in fluorometers and flow cytometers, a conventional and unmodified flow cytometer (Beckman-Colulter XL/MCL) has been used to measure the fluorescence of known solutions of fluorescein and fluoresceinated mouse IgG (FITC-MIgG). By adding non-fluorescent beads of 6-10um diameter to these solutions, triggering on light scatter and collecting integral fluorescence signals it was possible to measure fluorescence signals from fluorescein solutions of 10-10,000nM or from FITC-MIgG solutions from 1-100ug/ml (~6.7-667nM). From these measurements, one can directly determine the specific fluorescence of the FITC-MIgG. Using this FITC-MIgG with known specific fluorescence along with commercially available fluorescein MESF standard beads and beads with anti-MIg antibody, it was possible to determine Ig binding capacity. These beads could then be used with Ig's labeled with other fluorochromes in order to estimate their specific fluorescence. Supported in part by NIH SBIR RR16376.

Parallel Session 7: Advanced Microscopy

Chair: Jozsef Bocsi

97039

AN AOTF BASED MULTISPECTRAL IMAGING SYSTEM FOR MICROSCOPY

Wamiq Ahmed[1], Bartek Rajwa[2], Murugesan Venkatapathi[3], Gérald J. Gregori[4], Sudhir Trivedi[5], Jolanta Soos[5], E. Daniel Hirleman[3], J. Paul Robinson[6]

[1]Purdue University, Electrical and Computing Engineering, West Lafayette, Indiana; [2]Purdue University, Basic Medical Sciences, Veterinary Medicine, West Lafayette, Indiana; [3]Purdue University, Mechanical Engineering, West Lafayette, Indiana; [4]Purdue University, Biological Sciences, West Lafayette, Indiana; [5]Brimrose Corporation of America, Baltimore, Maryland; [6]Purdue University Cytomery Laboratories, Basic Medical Sciences & Biomedical Engineering, Purdue University, West Lafayette, Indiana

Multispectral classification techniques have become of significant interest to biologists because of the increase in the availability of broad-range fluorescent probes, the need to separate overlapping spectra, and, as always, a need to identify cellular autofluorescence. If multispectral imaging is used, the color spread or overlap can be modeled as a linear transformation y = Ax+b, where matrix A denotes the color spread among the channels and y is a vector of gray-scale images. Each element of A specifies the share of the intensity from a given fluorophore that appears in a one channel of a multispectral image. A solution for the above equation exists as long as number of channels (m) is larger than or equal to the number of fluorophores (n); it is unique if m = n or can be optimized for best fit if m > n. The case of m > n is preferred, as it helps us in eliminating the effects of any noise in the system that is independent of the wavelength measured. We have been developing an AOTF (Acousto-Optic Tunable Filter)-based imaging system that will operate on standard microscopes.

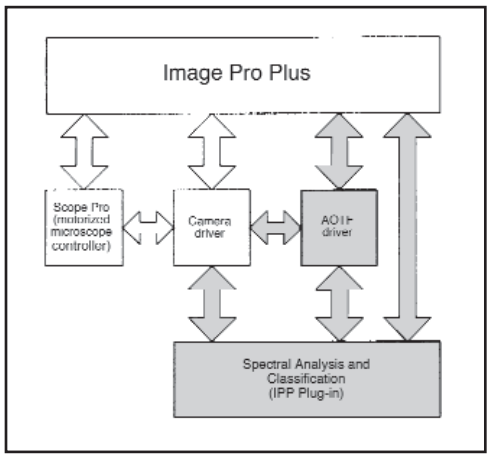

A schematic of the AOTF-based system

The AOTF has been designed with the goal of reducing dependency on traditional optical filters. The value of an AOTF is that it can scan a large spectral range, providing input for each frequency if necessary. We devised specific software that controls a Brimrose AOTF within the environment of a popular and well-established image-processing package. The advantage of the system we describe is that it allows the use of spectral separation techniques to discriminate certain cellular or subcellular components that are normally very difficult to distinguish. Further, there appears to be a significant advantage in using spectral patterns, as opposed to intensity profiles, for the discrimination of specific molecules. This presentation describes the hardware and software that we have developed as applied to

biological imaging. Our system operates using a PC-based computer, AOTF, and a set of custom-designed plugins written specifically for the Image Pro Plus package. This means that we can utilize off-the-shelf software which already has sophisticated image-processing capabilities.

94881

ANALYSIS OF FLUORESCENT MRI CONTRAST AGENT BEHAVIOR IN THE LIVER AND BLOOD VESSELS OF MICE

Edmond Kahn[1], Gérard Lizard[2], Dominique Dumas[3], Frédérique Frouin[4], François Ménétrier[5], Andrew Todd-Pokropek[4]

[1]INSERM U.494, Paris Cedex 13, France; [2]INSERM U.498 IFR 100, Dijon, France; [3]CNRS UMR 7563 IFR 111, Vandoeuvre les Nancy, France; [4]INSERM U.494, Paris, France; [5]INSERM U.498, Dijon, France

The usual magnetic resonance imagery (MRI) contrast agents contain Gadolinium (Gd) or Iron (Fe). Usually, these products are used to examine the biodistribution process *in vivo* and when they are fluorescent, it is possible to analyze their access to cells by means of confocal microscopy. The purpose of this work is to characterize the fate of magneto-fluorescent products injected *in vivo* in small animals intravenously. To simulate the conditions of ultra small particle iron oxide (USPIO) contrast agent imaging we used a product which combines nanoparticles of Fe and Texas Red (Institute für Diagnostik Forschung, Berlin) and to avoid the need to use molecules bearing fluorochromes we used a MRI contrast agent in which Gd can be replaced by Europium (Eu) (Bracco, Lugano). In this regard, Gd-BOPTA (Multihance) has been modified into Eu-BOPTA. To confirm the presence of Gd, Eu or Fe when products are administered to small animals (Kahn E et al, Cytometry 51A:97-106 (2003)) characterization studies were carried out by means of secondary ion mass spectrometry (SIMS) microscopy to map these chemical elements. Electron energy loss spectrometry (EELS) microscopy was also used to map the same chemical elements at a larger magnification and better resolution. Here in this presentation, bi-photon confocal microscopy was used to assess the presence of compounds containing Eu in the liver and blood vessels of injected mice in similar experimental conditions. To this end, the cell nuclei of samples were counterstained with Syto 13. To characterize Eu-BOPTA and Fe-Texas Red at the cellular level, confocal and bi-photon microscopes were used, and image analysis was performed on spectral sequences of images to get specific co-localized images of Eu or Fe and nuclei. Sequences of images were investigated by Factor Analysis of Medical Image Sequences (FAMIS). This method uses physical properties of fluorochromes (emission spectra and decay rates), and provides the images corresponding to each fluorochrome. Therefore, detection of Eu and Texas Red of injected compounds in tissues was made possible in samples of livers and blood vessels of mice after administration of these compounds. The characterization of the presence of Eu or Fe in tissues can be performed on the basis of a direct fluorescence microscopy analysis but we have made it much more specific and reliable by using spectral bi-photon confocal microscopy and FAMIS image processing. Our investigation also determines the interest to use fluorescent MRI contrast agents as *in vivo* staining tools of cellular sites.

96279

WHY 16.7 MILLION COLORS AREN'T ENOUGH: THE CASE FOR SPECTRAL IMAGING

Richard Levenson[1]

[1]CRI, Inc., Biomedical Systems, Woburn, Massachusetts

Spectroscopic imaging can generate a series of images at multiple wavelengths, yielding optical spectra at every pixel. In combination with appropriate mathematical tools, this technique reveals the presence of complex and useful spectral information in common biological and pathological samples and can be used to greatly increase molecularly based multiplexing capabilities. Applications exist in surgical pathology, immunohistochemistry, multicolor fluorescence and in-vivo imaging. Spectrally enabled microscopy can be accomplished using a variety of technologies, including tunable filters, Fourier-transform interferometry, line-scanning prism or gratings-based devices, computed tomography, and others. A novel approach for brightfield (non-fluorescence-based) microscopy utilizes a CRI-developed spectrally agile light source. The SpectraLamp™ system, which replaces the standard halogen lamp at the rear of most microscopes, can deliver any combination or intensity of wavelengths from 420 to 700 nm, including white light. This capability provides a number of advantages over previous techniques, enabling increased acquisition speed and faster analysis. CRI has also released a liquid-crystal-tunable-filter-based spectral imaging system (sensor plus software) that is suitable for fluorescence as well as for brightfield analyses. It has proved particularly useful for multicolor fluorescence in-situ hybridization (FISH), for resolving multiple species of green fluorescent proteins (GFPs) with overlapping emission spectra, and particularly for the identification and elimination of interfering autofluorescence. The system is also well-suited for use with quantum-dot-based fluorescent labeling, and can simplify the approach to FRET-based assays. It is also provides spectra of fluorescent reagents in-situ, which can differ markedly from those measured in cuvettes, and can monitor spectroscopic shifts due to a dye's sensitivity to changing intracellular environments. Standard histopathology can also benefit from spectral imaging. Routine stains can have sufficient spectral content to allow the classification of cells of different lineage or to separate normal from neoplastic cells. Advanced analysis techniques can be usefully applied; these include automated clustering algorithms, principal or independent component analysis, and machine-learning systems. The latter, which can combine spectral and spatial information for classification purposes, are particularly promising.

97090

HIGH RESOLUTION MICROSCOPY IMPLEMENTED BY PHOTON-PLASMON INTERACTION

Yuval Garini[1], Vladimir G. Kutchoukov[2], Paul F.A. Alkemade[1], Ian T. Young[3]

[1]Delft University of Technology, Applied Sciences, Delft, Netherlands; [2]Delft University of Technology, Faculty of Information Technology and Systems, Delft, Netherlands; [3]Delft University of Technology, Delft, Netherlands

By using a novel photon-plasmon interaction principle, we are developing and studying the optical properties of a method that will allow to achieve high-resolution three-dimensional microscopy. The method is based on a metallic thin-film with an array of holes that transmit light with unusual diffraction patterns. When combined with far-field collection optics, it is to measure high resolution objects. When compared to near-field microscopy (that can only measure few nanometer of the surface), our method provides the option to measure thick samples, and the measurement is also much faster. Both these advantages are important for biological samples. We will describe the physical principles of the method, the practical sapects and present preliminary results that we have.

96343

RECOGNITION OF INFLAMMATORY CELL TYPES DIRECTLY FROM COLOUR IMAGES

Bruce Milthorpe[1], Qing Zheng[1], Allan Jones[2]

[1]University of New South Wales, Biomedical Engineering, Sydney, New South Wales, Australia; [2]University of Sydney, Sydney, New South Wales, Australia

Automation of cell recognition is a complex problem especially with solid tissue histology. Traditionally, the image is segmented by methods chosen to suit the image type, the objects are measured and then a classifier is used to determine cell type from each object's parameters. There is a potential to reduce complexity and time by direct input of image data into a neural network. This project examines the application of direct input of image data and the structure of the neural network on automated recognition of inflammation-related cells. **Methods:** Images of inflammatory regions around biomaterial implants in the paravertebral muscle of rabbits were captured (Nikon E800 microscope, PCO Sensicam). Images of individual cells were cut from the main image, reduced to a common 32 by 32 pixel format and input directly into the neural network. Several neural networks were assessed with a variety of images of cells for accuracy and classification behaviour. Networks were trained with 75 cell images (25 of each type) and tested with an independent set of images comprising 205 cell images (26 heterophils, 94 lymphocytes an 85 monocytes). **Results:** The simple three-layer fully connected back-propagation neural network and a four-layer, with two layers of shared-weights, neural network were most successful at classifying the cells from the images, with 97% and 98% correct recognition rate respectively. The outputs of the neural networks include estimates of how well the images fitted to the specified cell types (Figure 1). Examination of the wrongly classified and unclassifiable images gives information on the reliability of classified cells. Heterophils had the most errors, followed by monocytes. Overlap of an adjoining cell, low colouration and poor image quality were some of the factors responsible for misclassification or inability to classify, although different neural networks had errors on different cells. The images were not rotated prior to submission of the images to the neural networks. Therefore, these neural network results would appear to be fairly orientation independent. **Conclusion:** The high accuracy recognition rate shows the potential for direct classification of visual image pixel data by neural networks. However, further work on using the trained networks on whole histological slides is required to demonstrate universal applicability.

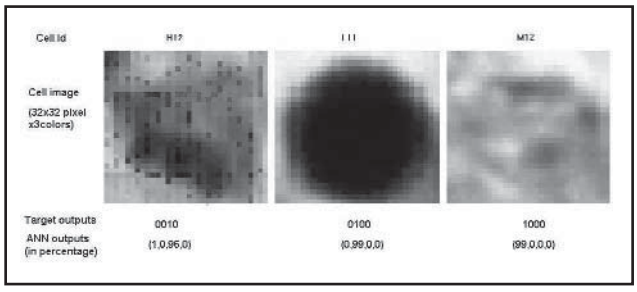

Figure 1

Parallel Session 7: Hematology/Oncology

Chair: Claudio Ortolani

96400

IS HUMAN PML GENE INVOLVED IN THE REGULATION OF MHC CLASS I ANTIGEN PRESENTATION?

Silvia Bruno[1], Fabio Ghiotto[1], Franco Fais[1], Carlo Enrico Grossi[1], Ermanno Ciccone[1]

[1]University of Genoa–Dept. Experimental Medicine–Human Anatomy Section, Dept. Experimental Medicine–Human Anatomy Section, Genova, Italy

The promyelocytic leukemia (PML) gene has been first identified in patients with acute promyelocytic leukemia (APL), in which it is fused to the retinoic acid receptor α (RAR α) as a result of the t (15;17) chromosomal translocation. In normal cells PML is localized in the nucleus within discrete nuclear structures termed nuclear bodies (PML-NB). When PML is aberrant, such as in APL, PML-NB are disrupted. PML is a tumor suppressor and exerts its anti-proliferative functions by interacting with cell cycle- and apoptosis-regulatory proteins. A novel additional mechanism of tumor suppression for PML has been proposed recently, based on the observation that murine PML regulates the expression of MHC class I molecules (Zheng, Nature 396: 373, 1998). A murine PML mutant (F12dG), found in a MHC class I-negative murine tumor, acting as a dominant-negative regulator of wt murine PML, was shown to be responsible for an antigen-processing defect that caused a decreased MHC class I expression. According to these results, it was proposed that PML controls genes devoted to MHC class I antigen presentation. If proven also in the human cell system, this mechanism would account for evasion from host immunity of tumors bearing malfunctioning PML, such as APL. In the present study we address the relationship between PML and MHC class I in human cells. We investigate the cell surface expression of MHC class I molecules in human cell lines subjected to PML impairment. PML function is impaired in different ways, i.e. by inducing expression of PML/RARa, that acts as a dominant negative regulator of PML, or by PML gene silencing through RNA interference. Third, a human homolog of F12dG, the murine PML mutant shown to down-regulate murine MHC class I, is transfected in human cell lines where it acts as a dominant-negative regulator of wt PML. In none of the three cases we observe down-regulated MHC class I expression. Also, the ability of γ-interferon to up-regulate the expression of MHC class I remains unaffected by the three above PML-impairing conditions. According to these results, PML does not seem to directly regulate the whole surface expression of MHC class I molecules in human cells. However, recent studies suggest an involvement of PML-NB in the proteasomal degradation of nuclear proteins. Thus, though not being a direct modulator of the bulk MHC class I expression, PML could be still involved in the endogenous pathway of nuclear antigen presentation. Thus, we are evaluating whether PML silencing by RNA interference affects the recognition of a nuclear antigen (i.e. EBNA4 of Epstein Barr Virus, that is expressed by B-EBV cells or by EBV-infected HLA-A11+ HeLa cells) by, respectively, autologous or HLA-A11-restricted specific cytolytic T lymphocytes.

96616

CHROMOSOME 6P AMPLIFICATION IN B-CELL NON-HODGKIN'S LYMPHOMA

Trond Stokke[1], Eivind Galteland[1], Einar Andreas Sivertsen[2], Paula M. De Angelis[3]

[1]The Norwegian Radium Hospital, of Biophysics, Oslo 3 N-0310, Norway; [2]The Norwegian Radium Hospital, of Immunology, Oslo 3 N-0310, Norway; [3]Norwegian National Hospital, Oslo, Norway

Comparative genomic hybridization has revealed that amplification of parts of chromosome 6p occurs in 11% of B-NHL cases; this aberration is mostly found in DLCL and MCL. As the 6p gain has independent prognostic value (together with p53 and ATM aberrations: Br J Cancer, 85:1900, 2001), we wanted to further define possible target genes. The copy number of PIM1, IRF4, CCND3, E2F2, and BMP6 at 6p was assessed by fluorescent *in situ* hybridization (FISH). These genes are either oncogenes or candidate oncogenes in B-NHL based on microarray expression studies, PIM1 was also found in a narrow amplicon (~400 kB, ~20 copies) in the DLCL cell line U698 by genomic array studies. U698 cells express high amounts of PIM1 mRNA and pim1 protein, and are resistant to radiation-induced apoptosis and cell cycle arrest. (Unfortunately, no amplica at 6p were detected by genomic array analysis in the B-NHL cases with 6p gain, possibly because of the low sensitivity of the technique.) None of the analyzed genes, including PIM1, showed copy numbers above 5 by FISH in 10 primary tumors with 6p gain by CGH. Also, only low-level amplification of PIM1 was detected in a panel of primary DLCL tumors that expressed high levels of PIM1 mRNA (New Engl J Med, 346:1937, 2002). It appears that the amplica in primary tumors covers large parts of 6p, and that the level of amplification is low. It may be that overexpression of pim1 promotes lymphomagenesis, but our study indicates that neither PIM1, IRF4, CCND3, E2F2, nor BMP6 is the candidate gene affected in the majority of B-NHL cases with the 6p amplification.

96743

VH-GENE USAGE IS OF PROGNOSTIC VALUE IN CLL

Jan Jules Philippé[1], Ann Janssens[2], Kaat Smits[3], Ilse Mollet[1], Fritz Offner[4]

[1]Ghent University, Ghent, Belgium; [2]Ghent University Hospital, Hematology, Ghent, Belgium; [3]Ghent University, Clinical Chemistry, Ghent, Belgium; [4]Ghent University, Hematology, Ghent, Belgium

In chronic lymphocytic leukaemia (CLL) the mutation status of the immunoglobulin variable heavy chain gene (VH) is known as a prognostic factor. We have investigated if specific VH-gene usage is of additional prognostic importance. Peripheral blood samples from 91 CLL patients were analysed for VH usage. Recombinations occurring at least 6 times in VH-genes were V1-69 (n=10), V3-7 (n=9), V3-21 and V3-23 (n=8), V3-33 (n=7), and V3-30 and V4-34 (n=6). The occurrence of these is related to mutation status, cytogenetic abnormalities (available in 36/54 pts) and survival in the table below. Two groups can be made with V3-21, V1-69 and V3-33 as one group and V3-7, V3-23, V3-30 and V4-34 as a second group, with significantly more somatically unmutated cases in the first group (cut-off 98%, p=0.008; cut-off 96%, p=0.014). If the first group is compared to all others we only find a difference for the 96% cut-off (p=0.02). There is no difference in the frequency of cytogenetic abnormalities described above. Most importantly there was a statistically significant difference between the two groups for survival with the worst prognosis for the first group (p=0.01). This holds when the first group is compared to all others (p=0.009). We conclude that the biological background of VH mutated and unmutated CLL was reflected by the characteristic usage of individual VH genes, and that the immunoglobulin specificity reveals specific subgroups with differing prognosis. Legend to the table: M=mutated, U=unmutated, 98% and 96% =cut-off values, CGΔ covers cytogenetic abnormalities for del 11q22-q23, tris 12q13 or del 17p, CG= =no cytogenetic abnormalities detected.

VH-gene usage

	M 98%	U 98%	M 96%	U 96%	CG&δ	CG=	alive	dead
V 3-21	6	2	2	6	1	5	5	3
V 1-69	1	9	1	9	6	1	5	5
V 3-33	4	3	4	3	1	4	4	3
ε	11	14	7	18	8	10	14	11
V 3-7	8	1	5	4	1	5	9	0
V 3-23	7	1	5	3	2	2	7	1
V 3-30	4	2	4	2	2	2	5	1
V 4-34	5	1	5	1	3	1	5	1
others	21	16	19	18	11	13	30	7
ε	45	21	38	28	19	23	56	10

98291

SPONTANEOUS AND CYTOSTATIC-INDUCED APOPTOSIS IN CHRONIC LYMPHOCYTIC LEUKAEMIA

Malgorzata Sieklucka[1], Jacek Rolinski[2], Anna Dmoszynska[3], Piotr Pozarowski[1], Norbert Grzasko[2], Malgorzata Kowal[2]

[1]University School of Medicine, Lublin, Department of Clinical Immunology, Lublin, Poland; [2]University Medical School, Lublin, Poland; [3]University School of Medicine, Lublin, Department of Haematooncology, Lublin, Poland

B-cell chronic lymphocytic leukaemia (B-CLL) is a B-cell disease, characterised by the progressive accumulation of mature lymphocytes in peripheral blood and bone marrow. A high lymphocyte count, observed in B-CLL patients, is a result of failed apoptosis rather than increased proliferation. Purine analogues, such as 2-chloro-2'-deoxyadenosine (2-CdA) and fludarabine (FAMP), used for the treatment of B-CLL, have been shown to trigger the apoptotic cascade. In this study, we examined ex vivo susceptibility of leukaemic cells to enter apoptosis before treatment and after 2-CdA or fludarabine administration. Peripheral blood was obtained from 40 B-CLL patients. The degree of apoptosis was measured by two methods: annexin V technique (AxV+/PI- cells) and chloromethyl-X-rosamine staining (Mito Tracker Red CMXRos; $\Delta\psi_m$low/GlyA- cells), using flow cytometry (Becton Dickinson). We found that the patients receiving 2-CdA in monotherapy showed a higher number of $\Delta\psi_m$low/GlyA- cells 3 hours after cytostatic administration than the patients treated with FAMP. On the contrary, both the percentage of $\Delta\psi_m$low/GlyA- cells and the percentage of AxV+/PI- cells 24 hours after drug administration were higher in fludarabine treated patients compared to 2-CdA treated patients. These results seem to confirm the direct influence of 2-CdA on mitochondria and an indirect mechanism of fludarabine. However, the differences observed between ex vivo and *in vitro* apoptosis after 24 and 48 hours, as it was shown in earlier study, suggest that in human organism there exist some factors influencing the susceptibility of leukaemic cells to enter apoptosis, such as cytokines. Further investigations comparing these two drugs are required in patients representing the same stage of the disease.

96397

SUPERVISED AUTOMATED MICROSCOPY INCREASES SENSITIVITY AND EFFICIENCY OF DETECTION OF SENTINEL NODE MICROMETASTASES IN BREAST CANCER PATIENTS

Hans J. Tanke[1], Wilma Mesker[2], Willem Sloos[2], Hans Vrolijk[2], Rob Tollenaar[3], Paul De Bruin[4], Paul Van Diest[5]

[1]Leiden University Medical Center, Leiden, Netherlands; [2]Leiden University Medical Center, Molecular Cell Biology, Leiden, Netherlands; [3]Leiden University Medical Center, of Surgery, Leiden, Netherlands; [4]St. Antonius Hospital, Pathology, Nieuwegein, Netherlands; [5]University Medical Center Utrecht, Pathology, Utrecht, Netherlands

Background: To test the practicality and sensitivity of supervised automated microscopy (AM) for the detection of micrometastasis in sentinel lymph nodes (SLNs) from patients with breast carcinoma. **Methods:** 440 SLN slides (IHC stained for cytokeratin) from 86 patients were obtained from two hospitals. Samples were selected on the basis of 1. a pathology report mentioning micrometastases (Nx) or 2. reported negative nodes (N0). AM and image analysis in batches of up to 50 slides provided detection of IHC positive cells and digital storage of the images for quick manual review. **Results:** From a test set of 29 slides (12 SLN positive patients: selected positive and negative nodes) 18 slides were scored positive by supervised AM and 11 negative. Routine examination revealed 17 positive slides and 12 negative; AM thus identified one positive slide missed by routine pathology. Subsequently, automated re-analysis of 187 slides (34 patients; institute I) and 216 slides (40 patients; institute II) from reported node negative (N0) patients showed respectively 2 and 7 slides (2 and 5 patients respectively) with micro-metastases, all confirmed by the pathologists, corresponding to 5.9% and 12.5% missed patients, respectively. In 4 out of the 7 cases from institute II, that were missed by manual classification, AM also detected clusters of 4-30 cells (micrometastasis) but all with a size <0.2 mm. **Conclusions:** Supervised AM is more sensitive to detect IHC stained micrometastasis in SLNs than routine pathology. The high degree of automation may allow cost effective implementation of this technology in routine pathology.

Parallel Session 7: Aquatic Sciences

Chair: Philippe Lebaron

96359

RECENT DEVELOPMENTS IN THE FIELD OF MICROBIAL ECOLOGY AND PERSPECTIVES

Philippe Lebaron[1], Philippe Catala[2], Julia Baudart,[3]

[1]Université P & M Curie (Paris VI), Banyuls-sur-Mer, France; [2]Observatoire Oceanologique, Microbiology, Banyuls-sur-Mer, France; [3]University Paris VI, Microbial Ecology, Banyuls-sur-Mer, France

The recent development of cellular and molecular tools in the field of microbial ecology allows new investigations (i) to further understand the role of microbial communities in the functioning of natural ecosystems and (ii) to detect and quantify specific populations including pathogens in the environment. In aquatic systems, flow cytometry allows multiparameter analyses at the single-cell level and offers several advantages in aquatic microbial ecology. When combined with molecular tools, flow cytometry allows investigations on the physiological state of individual cells within natural communities and provides more relevant ecological parameters than traditional methods used in microbial ecology. New applications are also emerging in the field of viral ecology. The combination of molecular techniques with cell sorting of labeled cells by flow cytometry allows the detection and identification of active species in natural waters. By this way, it is possible to investigate the relationships between genetic, taxonomic and functional diversity and to provide further understanding on factors which regulate bacterial activity within microbial food webs. The diversity of species as determined from sorted fractions has sometimes only little overlap with the diversity determined at the community level. The ecological relevance of diversity assessment will be discussed. Population ecology is an emerging theme in the aquatic environment to analyze temporal and spatial variations of specific populations of bacterioplankton. However and although this approach remains essential, cell counts of targeted species are generally below the detection limit of most current instruments. Recent developments in cytometry have improved this sensitivity and seems very promising. We will emphasize these recent investigations, their potential applications in sanitary microbiology. and the remaining instrumentation limits.

96374

TESTS OF A FOUNTAIN FLOW CYTOMETRY SYSTEM FOR REAL-TIME QUANTIFICATION OF RARE MICROORGANISMS IN AN AQUATIC ENVIRONMENT

Paul Johnson[1], Philippe Lebaron[2], Tony Deromedi[1], Julia Baudart[2], Philippe Catala[2]

[1]University of Wyoming & SoftRay Inc., Department of Physics & Astronomy, University of Wyoming, Laramie, Wyoming; [2]Université Pierre & Marie Curie (Paris VI), Banyuls-sur-Mer, France

A self-contained system for detection of pathogenic microorganisms in water, including *Escherichia coli*, Cryptosporidium, and *Naegleria fowleri* is described and method detection limit and detection efficiency measurements summarized. This innovative system is based on laser induced immunofluorescence. The resulting fluorescence is detected with a CCD imager using a novel integration scheme that we call Fountain Flow. The objective is to develop a pathogenic bacteria/protozoa detection technique that can analyze 1 ml of fluid for selected pathogens in less than 5 minutes, with a sensitivity of less than 10 pathogenic microorganisms per ml. Cryptosporidium, *N. fowleri* and *E. coli* are examples of human-pathogenic, environmentally resistant microorganisms found in raw water sources worldwide. Cryptosporidium contamination in drinking water is one of the greatest environmental health risks to the public and *E. coli* contamination is a significant aquatic recreation hazard. Although *N. fowleri* infection is rare, it is becoming more common in warm water and has an extremely high mortality rate. We have tested a novel, low-cost, portable, real-time, biodetection system for the rapid and sensitive analysis of environmental water samples for microorganisms (patent pending). In the Fountain Flow system, the aqueous sample flows up a tube toward a source of on-axis epi-illumination and imaging optics so that sample particles can be imaged continuously onto a CCD camera. A sequence of digitized images is then automatically examined with a detection algorithm that allows enumeration of detected particles in real time. The imaging optics include a filter isolating the wavelength of fluorescent emission. Normally the sample flows upward, vertically. The ideal situation is where a particle flowing up the flow tube is imaged in the same pixel(s). The cross-section of the flow tube that can be conveniently imaged is not dependent on the opacity of the sample fluid and can be very large (in our case a 2 mm diameter hole). It is expected that flow throughputs of greater than 0.2 ml/minute can be achieved in a straightforward way. In this paper we summarize our latest measurements of method detection limit and detection efficiency with *E. coli* and *N. fowleri* spiked into clear buffer and natural water samples. We acknowledge support from Electricité de France, the Wyoming Water Development Commission, and the United States Geological Survey.

94836

EFFECT OF ELEVATED PCO2 ON OPTICAL PROPERTIES OF THE COCCOLITHOPHORID *EMILIANIA HUXLEYI* GROWN UNDER NITRATE LIMITATION

Michel Denis[1], Antoine Sciandra[2], Jérôme Harlay[3], Dominique Lefèvre[1], Rodolphe Lemée[2], Peggy Rimmelin[1], Jean-Pierre Gattuso[2]

[1]CNRS-Université de la Méditerranée, Centre d'Océanologie de Marseille, Marseille cedex 9, France; [2]CNRS UMR 7093, Laboratoire d'Océanographie, Villefranche-sur-Mer cedex, France; [3]Université Libre de Bruxelles, Service d'Océanographie Chimiue et Géochimique des Eaux, Bruxelles, Belgium

Side scatter and red fluorescence properties of the coccolithophore *Emiliania huxleyi* were investigated by flow cytometry when NO3-limited continuous cultures were submitted to a CO2 partial pressure (pCO2) increase from 400 to 700 ppm. Cultures renewed at the rate of 0.5 d-1 and were submitted to saturating light level. pCO2 was controlled by bubbling CO2-rich or CO2- free air in the cultures. Most of the analyses were repeated 5 times and the average SD were < 1.6%, 0.1 and 0.2% for counting, fluorescence and side scatter respectively. Considering the possible decalcification induced by the increase of CO2 in the chemostat atmosphere, the maximum variation that can be expected for side scatter is that provided by the coccolith depletion upon acidification of the cell suspension. The acidification induced a large (36%) decrease of the side scatter signal but had no detectable effect on the red fluorescence. A control was run with a non-calcifying species, Dunaliella tertiolecta, where acidification induced no detectable change, both on fluorescence and side scatter. During the time of the experiment, the decline of side scatter in chemostat 1 never approached the potential 36% change observed when coccoliths are fully dissolved. Interestingly, the specific chl a fluorescence of *E. huxleyi* slightly increased during the period of high CO2 level. At the end of the experiment this increase amounted to a significant 2.8% of the initial signal. Furthermore, it progressed linearly with time over the period of observation. However, the experiment did not last enough to know if the fluorescence increase had already reached its maximum value. The acidification experiment supported the use of side scatter as a relevant parameter to trace potential changes in calcification. Since the estimated 25% decrease in calcification induced by the rise in CO2 atmosphere did not result in dramatic changes in side scatter values, we can conclude that the number of cocoliths and the overall shape and granulosity of cells was not significantly affected by this decrease. Changes must have only affected tiny structure details of the coccoliths which is supported by scanning electron microscopy observations. The small but significant increase of the fluorescence signal can be considered as a physiological response to the CO2 rise. This suggests a more dynamic photosynthetic process that would result in a higher rate of organic matter production providing that the system is not nutrient limited as in the present situation.

96405

REAL TIME ENUMERATION OF *SALMONELLA* AND ENTEROBACTERIACEAE CELLS IN WATERS

Julia Baudart[1], Philippe Catala[2], Philippe Lebaron[2]

[1]Université P&M Curie (Paris VI)-CNRS-INSU-UMR 7621, Microbiology, Banyuls-sur-Mer, France; [2]Microbiology, Banyuls-sur-Mer, France

Water quality assessment involves the specific, sensitive and rapid detection of bacterial indicators and pathogens in water samples, including Viable But Non Culturable (VBNC) cells. This work evaluates the sensitivity of a new emerging laser scanning cytometer (Scan RDI) combining a physiological assay (Direct Viable Count, DVC) with a specific approach (immunofluorescence and fluorescent *in situ* hybridization) for a direct enumeration, at a single-cell level, of highly diluted *Salmonella* spp. and Enterobacteriaceae cells in waters following concentration on membranes. We will demonstrate that the approach combining the DVC assay to specific detection with a fluorescent probe is efficient and allows the detection of a single pathogen after concentration. We will discuss the advantages of this method in comparison to traditional methods and the potentialities of this approach for further applications.

97105

INSTRUMENTAL, METHODOLOGICAL, AND ORGANIZATIONAL NEEDS FOR MICROBIAL CYTOMETRY

Howard Shapiro[1]

[1]The Center for Microbial Cytometry, West Newton, Massachusetts

The pace of development of instruments, reagents, and techniques optimized for cytometry of microorganisms has been glacial. Measurements of bacteria and viruses in conventional cytometers are limited by photoelectron statistics. Although smaller microbes, and microbial constituents present at levels below 1,000 molecules/cell, are undetectable or not measurable with precision in current commercial instruments, manufacturers now appear reluctant to produce suitable apparatus. However, it has been shown that existing technology is adaptable to measure bacteria, viruses, and smaller particles, e.g., DNA fragments, with substantially greater sensitivity. This should make it possible to define subpopulations of microorganisms on the basis of subtler structural and physiologic differences than can now be distinguished, and to sort individual bacteria and viruses, permitting these differences to be related to virulence or response to therapy. Staining of bacteria with dyes that have proven tractable in mammalian cells may be unpredictable; uptake and efflux of dyes, drugs, and other reagents by and from bacterial cells are affected by cell wall structure and by the presence of pores and pumps, some unique. It is inadvisable to conclude that even well-characterized dyes behave in bacteria as in mammalian cells, and unwise to assume that staining procedures developed for mammalian cells can be applied to protists and prokaryotes without further investigation. Relatively few monoclonal antibodies against microbial antigens are commercially available, and the choice of labels for most is limited. Other specific reagents, e.g., rRNA probes, are also difficult to find. Immunologists and hematologists have cooperated for over a generation to define the CD antigens, antibodies to which have become profitable for many companies; a similar cooperative effort will have to be undertaken to make better reagents available for microbiology. The Center for Microbial Cytometry, a nonprofit corporation, was established in 2001. The first mission of the Center is to bring interested parties from academia, government, and industry together, electronically and in person, to define and catalog the principal problems and currently available solutions. In many cases, one group of investigators may have solutions to another group's problems, which should lead to productive collaborations. Ideally, this will increase manufacturers' level of interest in providing needed apparatus and reagents; if not, the exercise should at least create a data base and a clearing house that could facilitate instrument modification and construction and exchange of reagents and techniques by and between researchers.

Parallel Session 7: *In vivo* Imaging

Chair: Deborah R. Shapira

96368

VISUALISING MOLECULAR INTERACTIONS IN LIVING CELLS

Hans J. Tanke[1], Christiaan Molenaar[1], Ilke Krouwels[1], Karien Wiesmeijer[1], Nico Verwoerd[1], Roeland W. Dirks[1]

[1]Leiden University Medical Center, Molecular Cell Biology, Leiden, Netherlands

Immunocytochemistry (IC) and fluorescence *in situ* hybridisation (FISH) are of limited value when applied to living cells. Fortunately, there is the GFP labelling technology that allows for visualisation of proteins in live cells. Specific DNA sequences however, are difficult to detect in live cells, since denaturation is not an option. Single stranded RNA, can be demonstrated using 2'-O-methyl modified oligonucleotides, PNA (peptide nucleic acid) probes or molecular beacons. We obtained optimal hybridisation results by using 2' O methyl oligoribonucleotide probes that are labelled at their 5' end with a fluorophore. Molecular beacon type of probes revealed specific hybridisation signals for the different target sequences though hybridisation signals were less intense while a considerable amount of 'background' signal was present in cell nuclei. Apparently, the molecular beacon probes, as constructed, opened up in the cell nucleus before reaching their target sequences. PNA probes proved to be very suitable for detecting telomere sequences in living cells under non denaturing conditions. This is an important finding because it will allow studying the dynamics of telomere positioning in the cell nucleus under various experimental conditions and during the cell cycle. The labelling technology for RNA was combined with GFP constructs allowing the study the dynamics of proteins (labelled by GFP) involved in transcription, and in processing and transport of RNA. To demonstrate functional association of labelled proteins with RNA, spatial (co)localization studies are insufficient. More reliable information is obtained when functional association is assessed by measurements of fluorescence resonance energy transfer (FRET), either on the basis of spectral analysis or by life-time measurements. As an example, we studied the role of heterochromatin protein 1 (HP 1), considered as a key component of constitutive heterochromatin and a player in gene silencing. GFP-HP-1 protein appeared to accumulate in a number of nuclear subdomains, such as PML bodies. We demonstrated that HP-1 proteins form complexes with SP 100 in PML bodies using CFP and YFP as tags, by measuring their interaction by FRET-FLIM.

97054

PARALLEL-PLATE FLOW CHAMBER AND INTRAVITAL MICROSCOPY: TWO FLUORESCENCE ANALYSIS TOOLS TO QUANTIFY PLATELET INTERACTIONS WITH ENDOTHELIAL CELLS (EC) AFTER IRRADIATION

Valérie Vereycken-Holler[1], Marc Benderitter[2], Marie Hélène Gaugler[2]

[1]IRSN, DRPH/SRBE, Fontenay-aux-Roses cedex, France; [2]IRSN, DRPH/SRBE, Fontenay-aux-Roses cedex, France

Tissue response to ionizing radiation is defined as a pathological tissue repair process. One hypothesis developed in our laboratory is based on the deleterious effects of the initiation and persistence of EC activation after radiation exposure. The purpose of this study is to compare *in vitro* and *in vivo* methods to investigate interactions of platelets with activated endothelial cells. In such a process, changes of platelet-endothelial dynamics are characterized by rolling and/or adhesion of platelets on the activated endothelium. In the *in vitro* model, confluent monolayers of human microvascular EC irradiated or not at 10 Gy were placed in a parallel-plate flow chamber. To simulate physiological shear flow, rhodamine 6G fluorescently-labelled whole blood was perfused over EC. Adhesion of single platelets and platelet aggregates was quantified by image analysis coupled to real-time videomicroscopy and expressed as the surface covered by those platelets. In the *in vivo* model, blood cells were stained by intravenous administration of rhodamine 6G. Blood flow and platelet-endothelium interactions were visualized in mesenteric post-capillary venules from sham or 10 Gy irradiated mice and quantified according to 4 parameters: shear rate, number of rolling platelets, number of adhering platelets and duration of platelet adhesion. Intravital microscopy explores changes of microhemodynamics as well as platelet-endothelial interactions following radiation exposure but observation can be sometimes limited by the diffusion of light through the mesentery. Compared to intravital microscopy, the flow chamber apparatus includes several advantages: i) in visualizing the morphology of EC and platelets during blood flow with a high level of video quality, allowing a more precise quantification of the surface covered by platelets, ii) in allowing experiments on human tissues (blood and EC). These two methods allow us to demonstrate increased interactions of platelets with EC after radiation exposure. In fact, the number of adhering platelets was augmented 2-fold 6 hours after *in vivo* irradiation. Furthermore, a 2.5-fold increased in the surface covered by platelets was obtained 7 days after *in vitro* irradiation. Both techniques are complementary in quantification of platelet interactions with EC in physiological and pathophysiological conditions. Intravital microscopy fits better to blood flow changes and cell quantifications and the flow chamber system seems to be more precise to study cell-cell interactions.

96780

DAUNOMYCIN-INDUCED CONDENSATION OF CHROMATIN IN LIVING CELLS

Jurek W. Dobrucki[1], Krzysztof Wojcik[1], Miroslaw Zarebski[1]

[1]Jagiellonian University, Biophysics, Faculty of Biotechnology, Krakow, Poland

The goal of this study was to investigate the effects of a DNA-intercalating drug, daunomycin, on nuclear and chromatin structure. Daunomycin is an anthracycline antibiotic which intercalates into DNA and causes helix unwinding. Daunomycin is extensively used as an antitumour drug, however, the mechanism of a cytotoxic action of this agent is still not fully understood [1]. It may involve DNA binding and alkylation, DNA-crosslinking, and interference with DNA unwinding and strand separation. The action of daunomycin was studied in transfected human fibroblasts and HeLa cells, with histones tagged with eGFP. Daunomycin at clinically relevant doses (25–1000 nM, 0.5-24h) caused various degrees of condensation of chromatin. Confocal images of viable cells *in vitro* treated with daunomycin revealed penetration of a drug into cells, accumulation in cytoplasm and nucleus, detachment of H1 histone (but not H2B), and an apparent gradual change in nuclear structure leading to a state of chromatin, which resembled a prophase condensation pattern. It has been shown previously (by flow cytometry and confocal microscopy) that sensitivity of DNA *in situ* to denaturation correlates with chromatin condensation and varies during cell cycle and apoptosis [2]. DNA denaturation was detected using a metachromatic dye acridine orange, which differentially stains single stranded and double stranded DNA sections. Using this approach we have demonstrated now that chromatin, which condensed as a result of an exposure to daunomycin, exhibited greater sensitivity to denaturation than chromatin in untreated cells. These preliminary data indicate that daunomycin used at clinically-relevant concentrations disrupts high-order chromatin structure in living cells and renders DNA more sensitive to denaturation. It is postulated that the mechanism of this phenomenon involves drug intercalation, helix unwinding, an increase in DNA torsional stress, and subsequent detachment of linker histones (although no detectable damage to nucleosomes) and eventually a polymer collapse. Funded by The Wellcome Trust and Polish State Committee for Scientific Research.

98300

NANOMEDICINE- NANOPARTICLES, MOLECULAR BIOSENSORS, AND TARGETED GENE/DRUG DELIVERY

Tarl Prow[1], Jose Salazar[2], William Rose[3], Jacob N. Smith[4], Lisa Reece[2], Andrea Fontenot[3], Nan Wang[2], James F. Leary[2]

[1]University of Texas Medical Branch at Galveston, Pathology, Galveston, Texas; [2]University of Texas Medical Branch at Galveston, Internal Medicine, Galveston, Texas; [3]University of Texas Medical Branch at Galveston, Galveston, Texas; [4]University of Texas Medical Branch at Galveston, Internal Medicine, Infectious Diseases, Galveston, Texas

A joint NCI-NASA research program in nanomedicine is being performed to develop "sentinel nanoparticles" which will seek out diseased (cancerous, virally infected) cells, enter those living cells, and either perform repairs or induce those cells to die through apoptosis. These nanoparticles are envisioned as multifunctional "smart drug delivery systems". They are being developed as multilayered nanoparticles (nanocrystals, nanocapsules) containing cell targeting molecules, intracellular re-targeting molecules, molecular biosensor molecules, and drugs/enzymes/gene therapy. These "nanomedicine systems" are being constructed to be autonomous, much like present-day vaccines, but will have sophisticated targeting, sensing, and feedback control systems—much more sophisticated than conventional antibody-based therapies. The fundamental concept of nanomedicine is to not to just kill all aberrant cells by surgery, radiation therapy, or chemotherapy. Rather it is to fix cells, when appropriate, one cell-at-a-time, to preserve and re-build organ systems. When cells should not be fixed, such as in cases where an improperly repaired cell might give rise to cancer cells, the nanomedical therapy would be to induce apoptosis in those cells to eliminate them without the damaging bystander effects of the inflammatory immune response system reacting to necrotic cells or those which have died from trauma or injury. The thrust of nanomedicine is to combine diagnostics and therapeutics into "real-time medicine", using where possible *in vivo* cytometry techniques for diagnostics and therapeutics. A number of individual components of these multicomponent nanoparticles are already working in *in vitro* and *ex vivo* cell and tissue systems. Work has begun on construction of integrated nanomedical systems which are being tested in animals.

96714

AUTOMATED *IN VIVO* IMAGING OF CELL INTERIOR USING FLUORESCENT PROTEINS

Miroslav Varecha[1], Jana Amrichova[1], Vladan Ondrej[2], Emílie Lukasova[2], Stanislav Kozubek[2], Michal Kozubek[1]

[1]Faculty of Informatics, Masaryk University, Laboratory of Optical Microscopy, Brno, Czech Republic; [2]Institute of Biophysics AS CR, Department of Cytology and Cytometry, Brno, Czech Republic

Techniques with fluorescent proteins have become very valuable tools for the study of cellular processes in living cells. These proteins enable the non-invasive quantitative visualization *in vivo* as molecular tags on natively non-fluorescent molecules of interest. Fluorescent proteins are welcome innovation in the field of cell biology, because *in vivo* experiments bring new interesting results and different point of view than *in vitro* and *in situ* experiments. This presentation will address automated 2D/3D high-resolution confocal image acquisition and analysis of cells stained with fluorescent proteins. While the approaches to automated *in situ* imaging of cell interior have been previously described by our group (Cytometry 45, 1-12, 2001), this contribution will concentrate on the modifications (both hardware and software ones) of our high-resolution image cytometers made for the purpose of automated *in vivo* imaging. This work is supported by the Grant Agency of the Czech Republic (grant number 204/03/D031) and by The Ministry of Education, Youth and Sports of the Czech Republic (project number MSM-143300002).

Parallel Session 7: Host Defense

Chair: TBD

96963

SURVIVAL RATE (SR) AND GROWTH RATE (GR): FLOW CYTOMETRY INDICATORS FOR FURTHER CHARACTERIZATION OF APOPTOTIC AND MITOTIC RESPONSES OF T LYMPHOCYTES

Alfredo Prieto[1], David Diaz[1], Hugo Barcenilla[2], Guillermo Revilla[1], Jorge Monserrat[1], Paz Prieto[1], Antonio De La Hera[1], Alberto Orfao[3], Melchor Álvarez-Mon[4]

[1]Alcala University, Immune System Diseases and Oncology Laboratory, CNB-CSIC R&D Associated Unit, Alcala de Henares, Madrid, Spain; [2]Alcala University, Alcala de Henares, Madrid, Spain; [3]Universidad de Salamanca, Salamanca, Spain; [4]University Hospital "Principe de Asturias", Immune System Diseases and Oncology Service, Alcalá de Henares, Madrid, Spain

Background: The study of *in vitro* T cell responses presents difficulties because the responses of individual T cells are neither homogeneous nor synchronic and also because the role of apoptosis has been underestimated for long time. **Objective:** To study both apoptosis and growth of mitogen stimulated T cells we applied ratiometric methods of T cell enumeration by flow cytometry **Materials and Methods:** T cells were enumerated by a ratiometric method based on the addition of a known quantity of fluorescent microbeads. This technology has been developed in our laboratory and has an extraordinary potential for the *in vitro* study of relationships between processes of cell proliferation and differentiation. To study the changes of the absolute numbes of cells in culture we developed two indicators: one to measure the proportion of cells which survived to the apoptotic phase and another to measure the net growth of the surviving cells. These indicators are Survival rate (SR) and the growth rate (GR). The SR measures the fraction of original cells that survive after the initial phase of predominant apoptosis. GR measure the relative increase in cell number (net growth) with respect to the original number of surviving cells after apoptotic phase. These measurements were performed after polyclonal stimulation with either lectin phytohemmaglutin or with antiCD3 and antiCD28 antibodies bound to polystiren microbeads. **Results:** SR and GR allow to compare responses of different subsets to policlonal stimulation. We found that SR and GR were markedly different for the several subsets studied. In experiments with sorted cells we found that the SR of CD45RA+ T cell was significantly higher than of CD45RO+ cells but GR of CD45RO+ was significantly higher than of CD45RA+ cells. **Conclusions:** Thanks to this flow cytometry ratiometric method of cell enumeration we can measure the exact number of cells in each moment, and how many cells have suffered apoptosis.

96362

POLYMORPHONUCLEAR NEUTROPHILS APOPTOSIS DURING PRIMARY SIV INFECTION, INVOLVEMENT IN DISEASE PROGRESSION

Stéphanie François[1], Valérie Monceaux[2], Bruno Hurtrel[2], Marie-Anne Gougerot-Pocidalo[3], Jérome Estaquier[2], Carole Elbim[3]

[1]Unité INSERM U479, Paris, France; [2]Institut Pasteur, Unité de physiopathologie des infections lentivirales, Paris, France; [3]Hôpital Bichat, Laboratoire d'Immunologie-Hématologie, Paris, France

The primary acute phase of HIV and SIV infection is characterized by an early burst in viral replication, an exponential rise in plasma viral load, the dissemination and seeding of the virus in all the peripheral lymphoid organs, and the induction of the host immune response to the virus. Accumulating evidence suggests

that this early phase dictates further progression towards AIDS. In particular, extensive apoptosis induction in peripheral lymphoid organs is an early and predictive event. Furthermore, recent data reported the presence of neutropenia during primary SIV infection. As polymorphonuclear neutrophils play a key role in innate immunity, neutropenia observed during primary infection could have major implications in the virus dissemination and disease progression. As experimental infection of macaques with SIV is the most useful model for studying the pathogenesis of SIV-induced AIDS, we performed a longitudinal study of 8 rhesus macaques experimentally infected with SIVmac-251 isolate (4 infected with pathogene isolate, 4 infected with non pathogene δnef isolate); 7 healthy controls non infected were included in parallel. We used flow cytometry to study, in whole blood, CD11b expression at the PMN surface, PMN oxidative burst by using dihydroethidin oxidation and spontaneous apoptosis by using staining with annexin-V and 7-actinomycin D. PMN chemotaxis induced by chemoattractant was evaluated using Transwell plates and the total number of neutrophils that migrated into the lower well was counted by flow cytometry. PMN functions were analysed at different times following infection (J0, J15, J28, J45, J60). We observed normal PMN oxidative burst and normal CD11b expression at PMN surface in SIV-infected macaques suggesting that PMN were not activated during primary SIV infection. However, during the first two weeks of infection, percentage of apoptotic PMN was significantly higher in macaques infected with pathogene isolate as compared with macaques infected with δnef non pathogene isolate; among the 4 macaques infected with SIVmac251 pathogene isolate this percentage was higher in the future rapid progressor than in the 3 futur low progressors. Furthermore, PMN apoptosis correlated with plasma viral load as well as with PMN count; this last result suggest that neutropenia observed during primary SIV infection could be related at least in part to increased PMN apoptosis. In conclusion, our results identified increased PMN apoptosis during primary SIV infection as an early and predictive event that may play a crucial role in impairing the capacity of the immune system to control viral replication and progression towards disease.

96552

FLOW CYTOMETRIC QUANTITATION OF OPSONOPHAGOCYTOSIS AND INTRACELLULAR KILLING ACTIVITY OF HUMAN NEUTROPHILS REQUIRING ONLY SMALL AMOUNT OF BLOOD VOLUME

Kovit Pattanapanyasat[1], Kalaya Tachavanich[2], Kasama Sukapirom[3], Egarit Noulsri[3], Sakorn Kaewmoon[3]

[1]Siriraj Hospital, Mahidol University, Bangkok, Thailand; [2]Siriraj Hospital, Mahidol University, Department of Pediatrics, Bangkok, Thailand; [3]Siriraj Hospital, Mahidol University, Office for Research and Development, Bangkok, Thailand

Neutrophils, also called polymorphonuclear leukocytes (PMNs) are the major phagocytic cells in the circulation and play a crucial role in the host defence against invading microorganisms. Various flow cytometric (FCM) methods have been developed to assess different PMN functions. However, the relative large number of PMNs required makes these assays from pediatrics blood samples impractical. Besides, when a high proportion of non-leukocytes contaminated in the blood from thalassemia patients, often results in problem encountered in obtaining the pure PMNs. In this study, we describe a rapid, simple and reliable FCM technique for measuring PMN function using small amount of whole blood. The method was based on the original assay of Lehrer (Lehrer,1970), and later modified by Martin and Bhakdi (1991) that exploit the use of a vital fluorescent marker staining on bacteria or yeast cells which are ingested by PMNs obtained from sedimentation identified by fluorescent labelled monoclonal antibody. Phagocytosis is assessed by double labelling of PMNs and phagocytosed yeast cells, whereas killing activity is quantitated by viable fluorescence retaining yeast cells liberated from the PMNs. The labelled yeast cells were satisfactorily homogeneous with respect to their FCM forward and side light scatter. Viable and non-viable cells killed by whole blood PMNs were distinguishable by their separation in determined side scatter and fluorescence. When the stained whole blood PMNs were incubated with the labelled yeast cells, the nonphagocytosed yeast cells, phagocytosed yeast cells by PMNs, and PMNs without yeast cells can be easily distiguished using two-color dot plot. Intracelluar killing and opsonophagocytosis of whole blood PMNs showed a significant increase in their activities with time. These activities were also comparable with that obtained from fractionated PMNs. The use of a small volume of unfractionated whole blood and FCM provide an assessment of PMN function in pediatric patients. Our method is simple, reliable and may offer alternative approach to study neutrophil function in small experimental animals without sacrifice. *This work was partially supported by Becton Dickinson Biosciences.

98338

PROGRESS IN UNDERSTANDING THE SKIN IMMUNE SYSTEM

Adelheid Elbe-Burger[1]

[1]Department of Dermatology, University of Vienna Medical School, Vienna, Austria

For higher organisms, the first barrier against injurious agents is the skin that for many years was considered only to be a passive form of protection. However, it is now clear that bone marrow-derived leukocytes including epidermal Langerhans cells, and dermal dendritic cells, in combination with other immunoregulatory resident cells initiate and regulate immune responses that protect the integrity of this organ. Such responses in the skin are directly connected to, and indeed constitute a part of, the systemic immune system. Previous studies have suggested that reduced immune responsiveness in early life may be related to the immaturity of neonatal antigen presenting cells. When investigating the ontogeny of the skin immune system, acquisition of immunofluorescence data and image cytometry was done using an automated confocal laser scanning microscope and the analysis software TissueQuest, which permitted recognition of individual cells by a specific identification strategy—a methodology also referred to as microscopy-based multicolor tissue cytometry (MMTC). Results showed that Langerhans cell precursors in the fetal epidermis are phenotypically immature and that endogenous IL-10 partly inhibits their differentiation into immunocompetent Langerhans cells. These findings have important implications for our understanding of mechanisms underlying reduced neonatal immune responses and neonatal tolerance. Nowadays, we have many topically applicable compounds (e.g. glucocorticosteroids, calcineurin inhibitors) which are used in the clinic for their immunosuppressive properties, as well as the technology to measure their functions on the single cell level by means of tissue cytometry without the need to mechanically isolate the target cells. Using MMTC we have shown that glucocorticosteroids but not the calcineurin inhibitor pimecrolimus induce apoptosis in Langerhans cells and keratinocytes *in situ*, implying that the prolonged use of glucocorticosteroids could have adverse effects on the skin immune system.

95852

RAPID DETECTION OF NEONATAL SEPSIS BY SIMULTANEOUS MEASURMENT OF MULTIPLE CYTOKINES USING 100μL SAMPLE VOLUMES

Greg L. Hodge[1], Sandy Hodge[2], Ross Haslam[3], Andrew McPhee[3], Homero Sepulveda[4], Ed Morgan[4], Ian Cameron Nicholson[5], Heddy Zola[6]

[1]Women's and Children's Hospital, Adelaide, Australia; [2]Royal Adelaide Hospital, Thoracic Department, Adelaide, South Australia, Australia; [3]Women's and Children's Hospital, Neonatal Medicine Department, North Adelaide, South Australia, Australia; [4]PharMingen, San Diego, California; [5]Child Health Research Institute, Leucocyte Biology Laboratory, North Adelaide, South Australia, Australia; [6]Child Health Research Institute, North Adelaide, South Australia, Australia

Early diagnosis of neonatal infection has proven problematic due to the inadequacy of currently available laboratory tests. Neonatal sepsis is associated with an increase in plasma-derived cytokine levels but an increase of a single cytokine cannot specifically identify neonatal sepsis and multiple cytokine levels are required. The time constraints and relatively large volume of plasma required to measure multiple cytokines from newborn infants by conventional ELISA techniques is prohibitive. We therefore applied Cytometric Bead Array technology for simultaneous measurement of multiple cytokines from a group of 18 term neonates with infection confirmed by culture and a control group. "Normal" ranges were established for each cytokine from 1-7, 8-14 and 15-21 day old newborns. There was no significant change in the levels of cytokines from infants in different control age groups suggesting basal cytokine levels are unchanged in the first 3 weeks of life. In the patient groups however, there was a significant difference in several cytokines between the different age groups. IL-6, IL-10 and IL-12 were significantly increased in the 1-7 day old patient group compared to either the 8-14 and 15-21 age group, suggesting infection in utero is associated with increased levels of these cytokines compared to infection acquired following birth. When individual patient cytokine levels were compared to normal control reference ranges, 2 patients failed to show significant elevation of any cytokine tested. All other patients showed elevated levels of between 1 and 9 cytokines tested (mean of 4.6). There was no correlation between elevated cytokine levels and types of infective organism or patient age.

Plenary Session 4: 1045–1230

Clinical Issues

115012

HIV

Brigitte Autran[1]

[1]Tissulaire INSERM U[453], Laboratoire d'Immunologie Cellulaire et, Hopital Pitie-Salpetriere, Paris, France

Abstract not available.

99049

CLINICAL APPLICATIONS OF FLOW CYTOMETRY OUTSIDE HIV MONITORING

Marie Christine Bene[1]

[1]Faculty of Medicine & CHU de Nancy, Immunology Dept., Vandoeuvre Les Nancy, France

Flow cytometry initially replaced UV-light microscopy in cell immunophenotyping, and thus mostly for the immunological characterization of leukemic blasts. Recent developments both in flow cytometry and in pathophysiological knowledge have considerably extended the field of application of this technology. Multi-colour fluorescence allows to develop new immunophenotyping strategies and to define immunophenotypic patterns of both normal and abnormal cell types. Fluorescence quantitation moreover makes possible the detection of subtle alterations of such cell functions as adhesion or signalling. Flow cytometry, applicable to nearly all biological fluids, therefore is becoming a pivotal technique in the exploration of haematological and immunological disorders, and in the growing field of immunomonitoring.

115006

HARNESSING HYBRID FLOW CYTOMETRY ASSAY PLATFORM (HYFAP): THE RENAISSANCE OF CLINICAL FLOW CYTOMETRY

Francis F. Mandy[1]

[1]National Laboratory for HIV Immunology, Health Canada, Ottawa, Ontario, Canada

The AIDS pandemic during the 1980s enabled the clinical immunology laboratories of wealthy nations to acquire flow cytometers. Nearly a quarter century later the time is long overdue for cellular immunology to make a significant contribution to the fight against AIDS in the southern hemisphere. Globally, HIV continues to devastate vast segments of populations, robbing developing countries of the valuable human resource needed to strengthen them. Fortunately, in some parts of the world the annual cost of drug cocktails to combat HIV disease has now been reduced from $15,000 to $150 per patient, thanks to generic drugs and concentrated efforts in this area However this paradigm shift in drug cost is just a small part of the global anti-AIDS revolution that must occur. To dramatically reduce further loss of life, essential diagnostic and monitoring tests must also become affordable. In the US, a massive CDC study uses dried blood spots (DBS) from infants to search for markers of inherited metabolic diseases and complex pathobiologies. Samples are obtained form a heel prick and shipped dehydrated. HyFAP amalgamates multiplexed suspension array technology with cell analysis on a flow cytometer based platform. DBS can be integrated with HyFAP to support large scale implementation of antiretroviral adminstration. Synchronization of a simple sample collection with advanced compact flow cytometry may well offer an affordable diagnostic platform to reach marginalized rural populations who would otherwise be continually denied access to life saving treatment.

115008

T CELL MONITORING DURING VACCINATION AGAINST TUMOR-ASSOCIATED ANTIGENS

Anne Letsch[1]

[1]Charite Universitats, Med Clinik III, Berlin, Germany

T cells play an important role for the immune surveillance of solid tumors and leukemias. For the development of effective vaccination strategies against tumor-associated antigens the monitoring of vaccine-induced T cell responses is an essential tool. The novel generation of sensitive flow based T cell assays enables a direct *ex vivo* quantitation and characterization of vaccine-induced T cell responses. Furthermore a detailed functional characterization is possible using flow cytometry based assays for detection of apoptosis, proliferation and chemokine receptor function. Results from T cell monitoring of various vaccination trials are shown.

1230–1400
Poster Presentations
(See abstracts beginning on page 111)

1615–1715
Janis Giorgi Memorial Lecture

Abstract not available

1715–1815
Robert Hooke Distinguished Lecture

99056

PROGRAMMING OF THE AUTOPOIETIC DEVELOPMENT OF COMPLEX ORGANISMS: THE HIDDEN LAYER OF NONCODING RNA

John S. Mattick[1]

[1]University of Queensland, Biochemistry, Brisbane, Queensland, Australia

The amount of genomic programming required to direct the complex trajectories of eukaryotic differentiation and development has been seriously underestimated. Although proteins are the fundamental components and effectors of cellular structure and function, the vast majority of the genomic output of the higher organisms is in fact noncoding RNA. A wide range of evidence suggests that these noncoding RNAs comprise a highly parallel system of trans-acting signals that relay state information required for the coordination and modulation of gene expression via RNA-DNA, RNA-RNA and RNA-protein interactions, which control chromatin architecture and epigenetic memory, transcription, alternative splicing, RNA turnover, translation and other cellular processes. This system has considerable similarities to other sophisticated information processing systems, and appears to underpin the ontogeny of multicellular organisms and their phenotypic diversity.